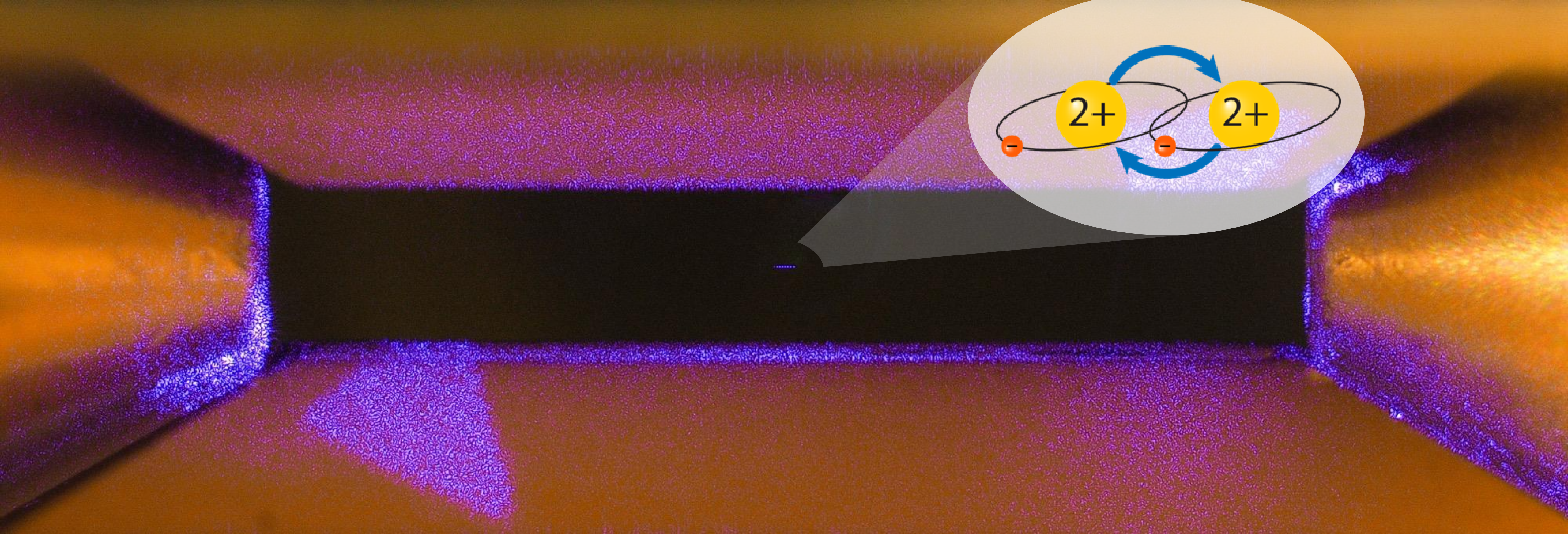

Trapped ions and Rydberg excitation:

From precision qubits to strong interaction

Markus Hennrich

2nd September 2025

Stockholm University

http://qtech.fysik.su.se/

The electronic state of an ion can store a quantum bit (qubit).

Quantum states: $|0\rangle$ and $|1\rangle$

e.g. electronic states of an atom/ion

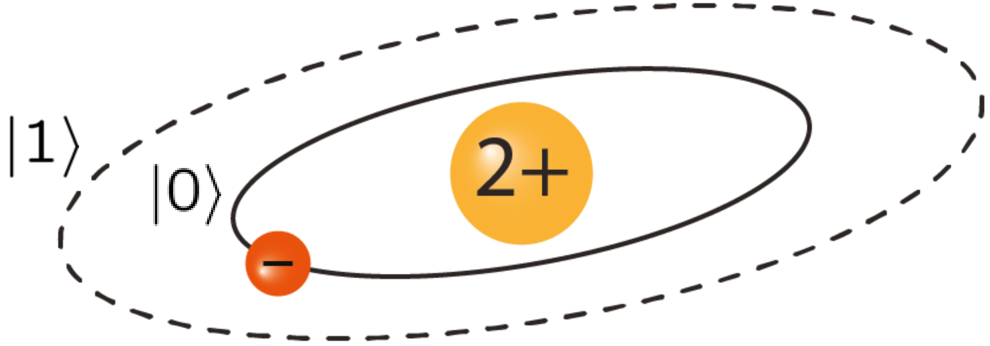

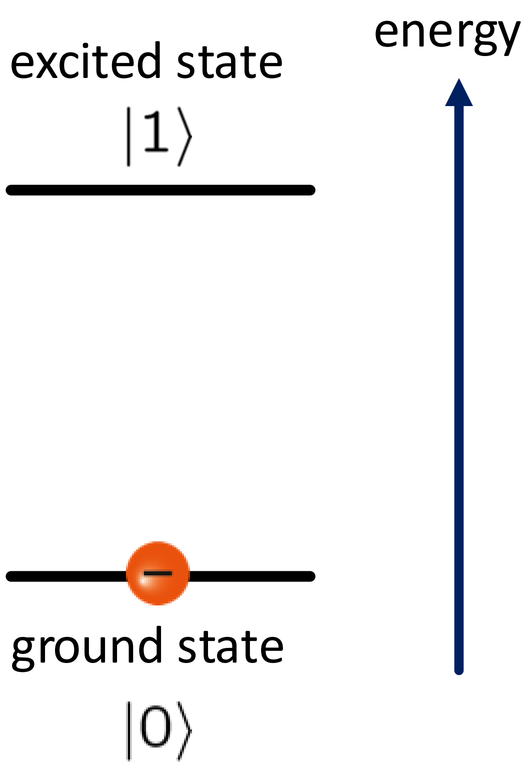

DiVincenzo criteria for quantum computation with trapped ions

1. Scalable system of qubits → up to ≈50 ions in a linear trap → microtraps...
2. Preparation of initial qubit states → laser cooling, optical pumping (>99%)
3. Decoherence time ≫ gate time → up to 100ms (1h) > 100μs (1μs)
4. Universal set of gate operations → addressed & global laser pulses (>99.9%)
5. Detection of final qubit state → electron shelving (>99.9%)

D.P. DiVincenzo Fortschr. Phys., 48, 771 (2000).

Ion species

Ions in use:

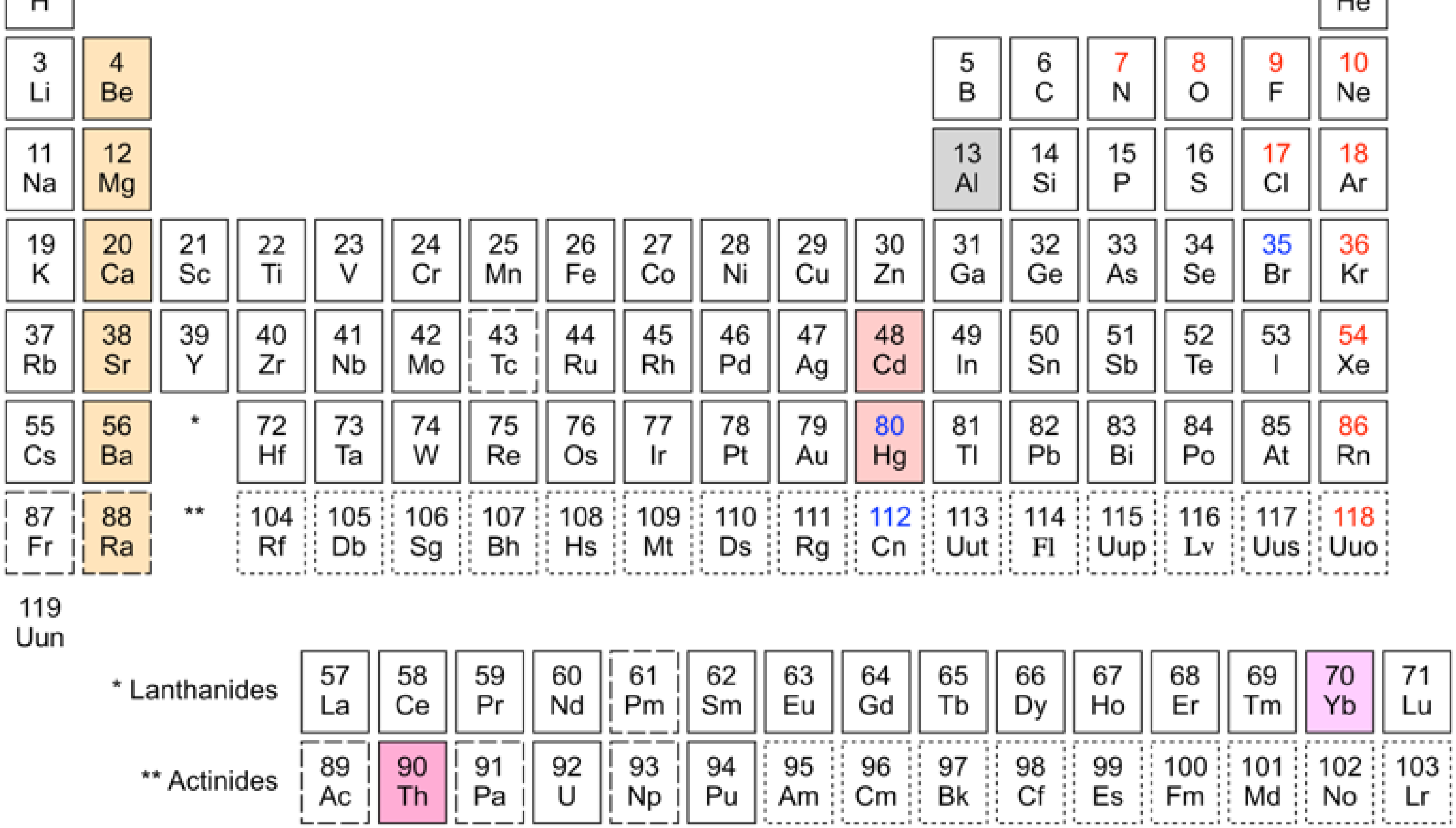

from QC group C. Monroe, Univ. of Michigan

Choosing the right ion species:

- strong cooling transition
- availability of suitable laser sources
- …

https://mivade.github.io/ionptable/

https://iontrap.duke.edu/resources/ion-periodic-table/

Qubits with trapped ions

Storing quantum information requires ***long-lived electronic states***:

Optical transitions on metastable states
S ⇔ D transitions in alkaline earths:
Ca^+, Sr^+, Ba^+, (Yb^+, Hg^+)

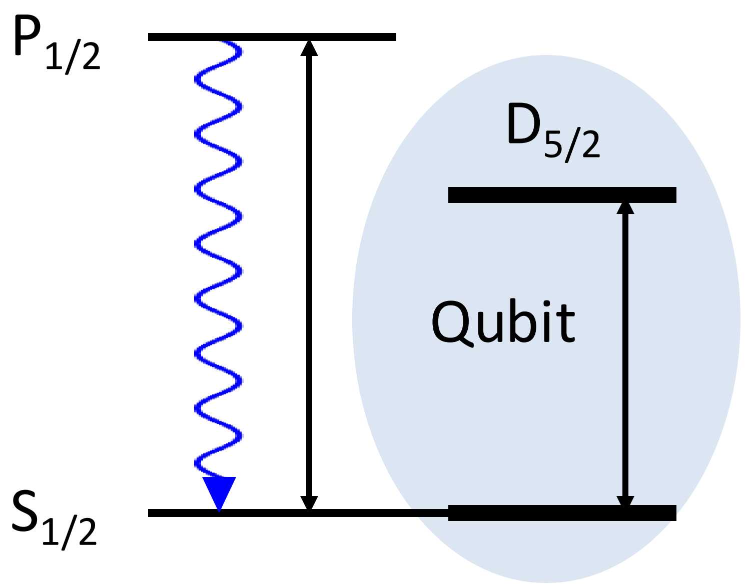

Innsbruck $^{40}Ca^+$; Stockholm $^{88}Sr^+$

Microwave transitions on hyperfine or
Zeeman states alkaline earths:
$^{9}Be^+$, $^{25}Mg^+$, $^{43}Ca^+$, $^{87}Sr^+$, $^{137}Ba^+$, $^{115}Cd^+$, $^{171}Yb^+$

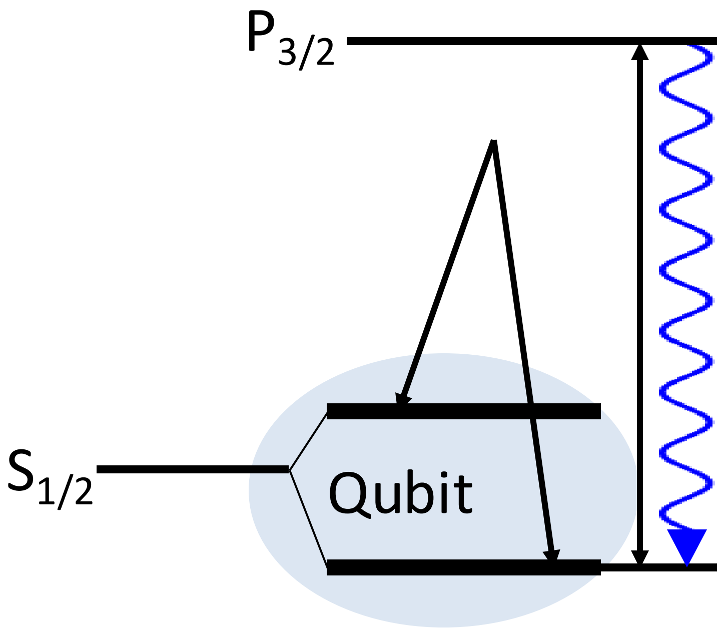

Boulder $^{9}Be^+$; Duke $^{171}Yb^+$;
Mainz $^{40}Ca^+$, Oxford $^{43}Ca^+$

Level scheme of Sr+

e.g. qubit on narrow S ⇔ D quadrupole transition

$$\tau(D_{5/2}) \approx 0.39s$$

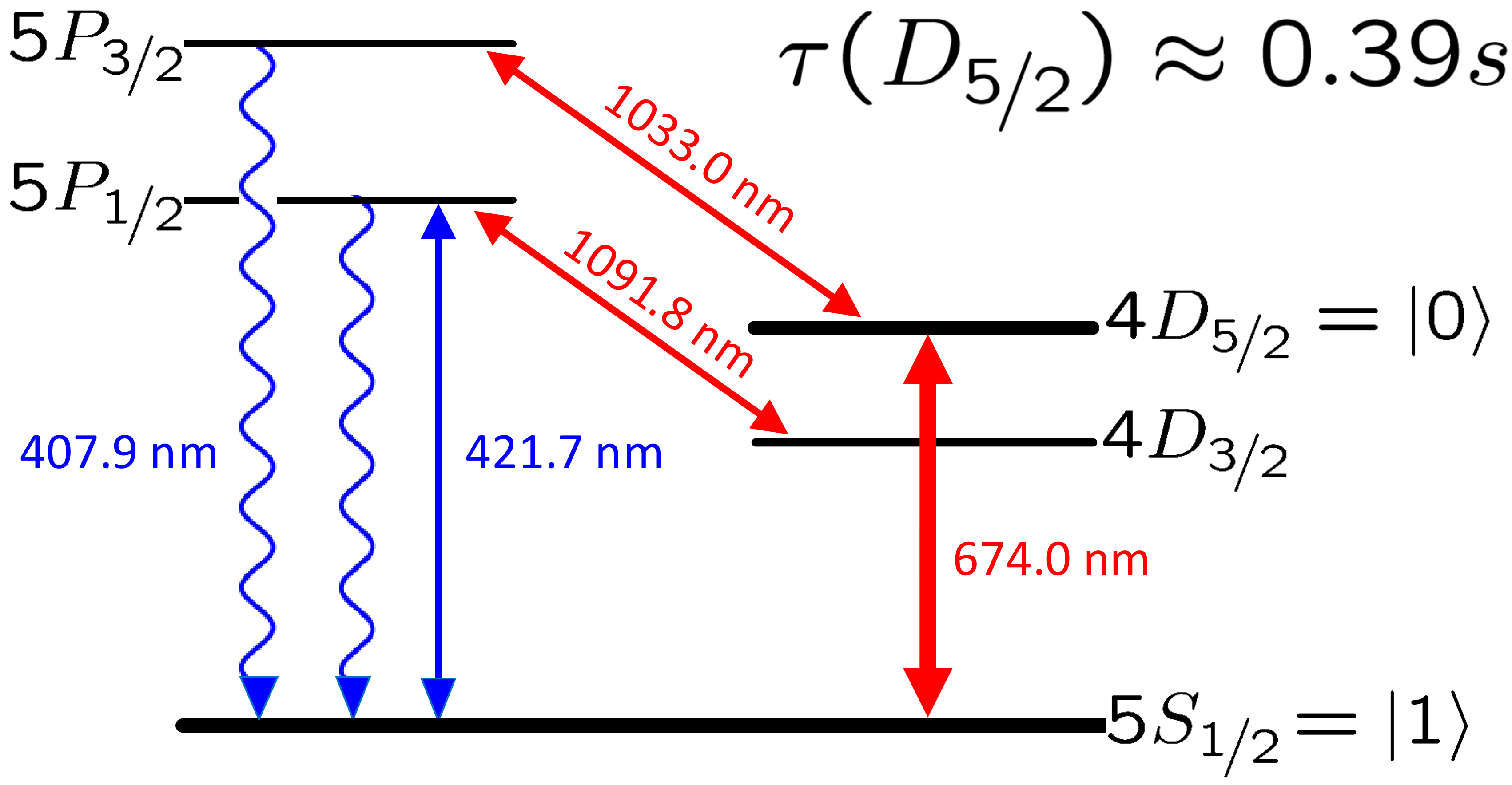

Level scheme of Ca^+

qubit on narrow S ⇔ D
quadrupole transition

$$\tau(D_{5/2}) \approx 1s$$

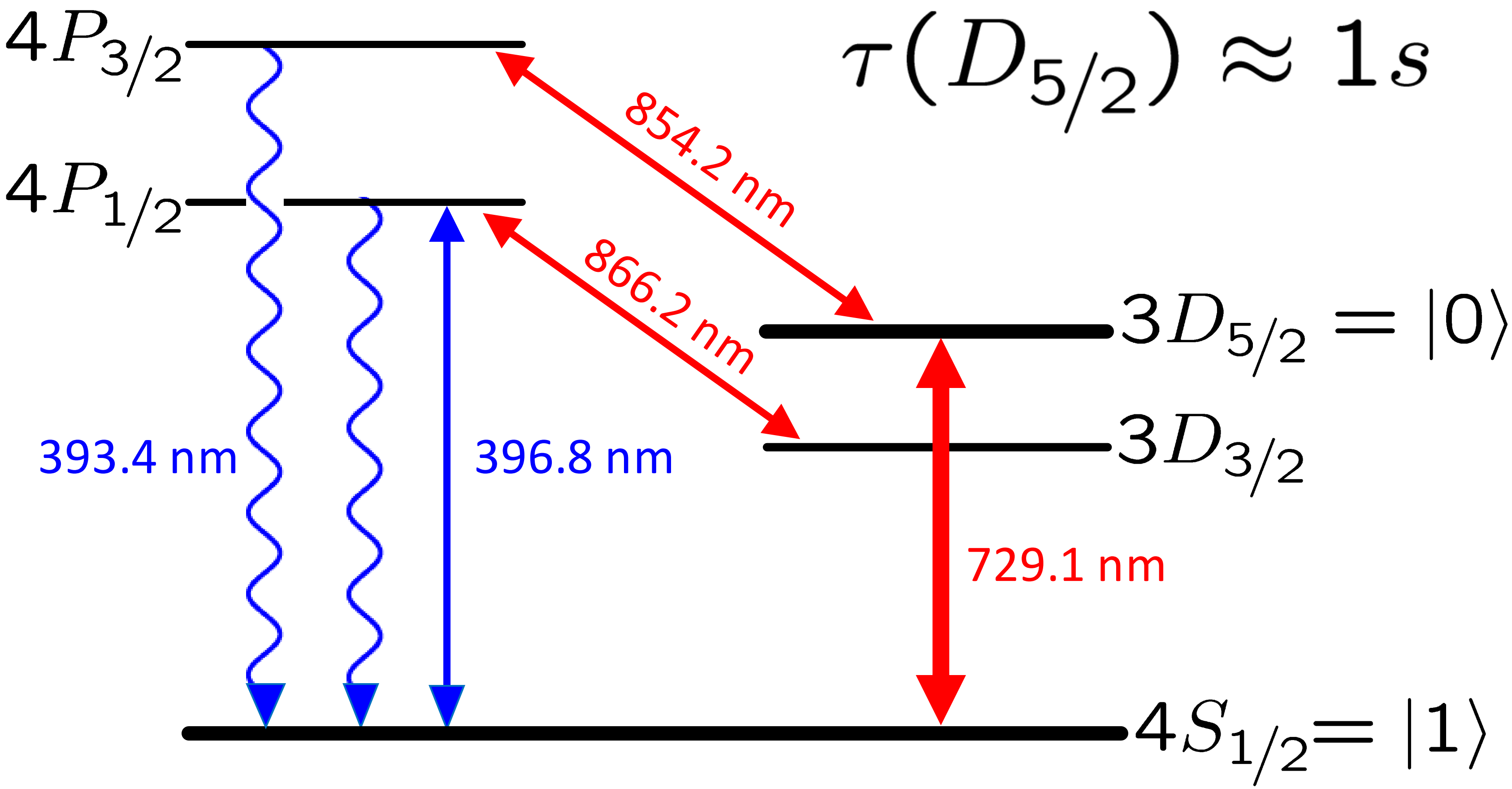

Level scheme of Ba^+

e.g. qubit on narrow S ⇔ D quadrupole transition

$$\tau(D_{5/2}) \approx 32s$$

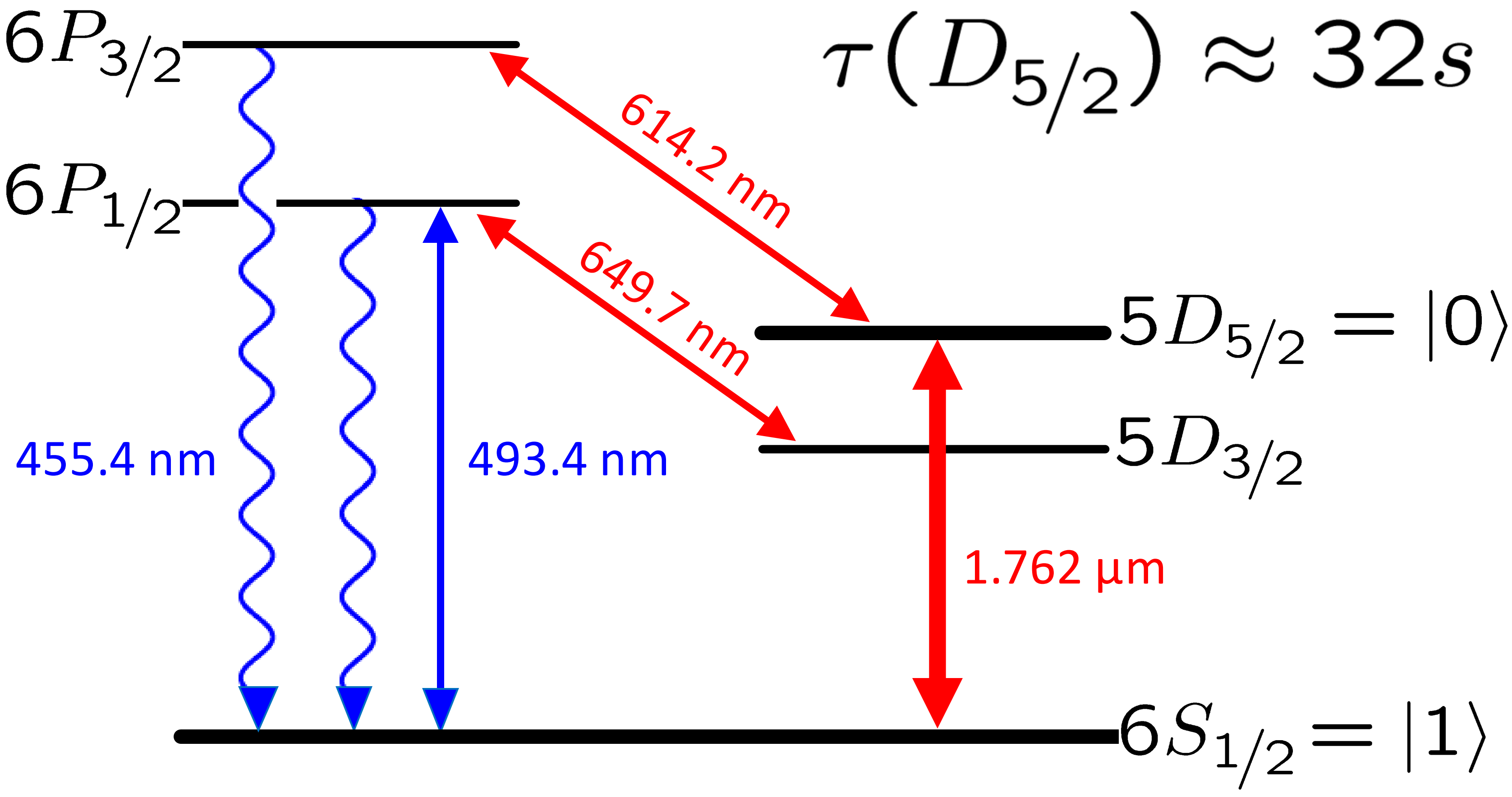

Spectroscopy of the $S_{1/2} \Leftrightarrow D_{5/2}$ transition

Zeeman structure in non-zero magnetic field:

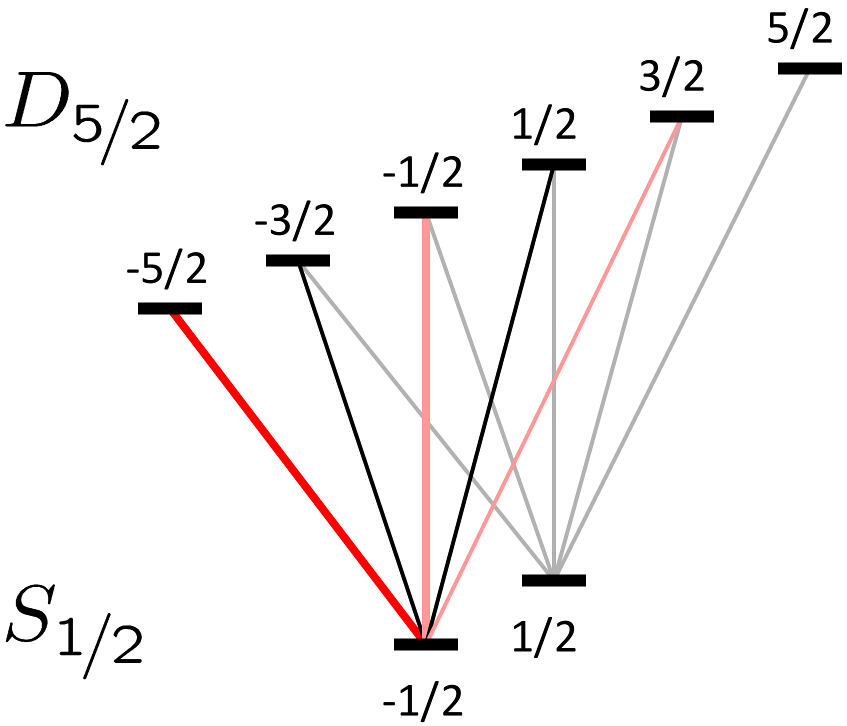

+ vibrational degrees of freedom

2-level-system:

$-1/2 \longrightarrow -5/2(-1/2)$

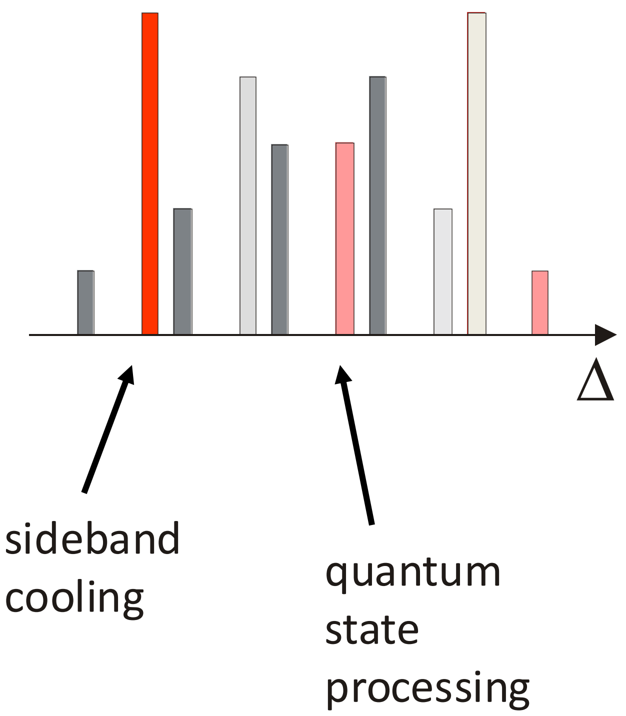

How to trap an ion?

Ion trap

Goal: To trap a single charged particle.

An electric field results in
a force on a charged particle:

Use positively charged
electrodes on all sides?

Laplace-equation:

$$\frac{\partial^2 \Phi}{\partial x^2} + \frac{\partial^2 \Phi}{\partial y^2} + \frac{\partial^2 \Phi}{\partial z^2} = 0$$

Positive curvature in x and y → Negative curvature in z.
Trapped in 2 directions → Anti-trapped in 3rd direction.

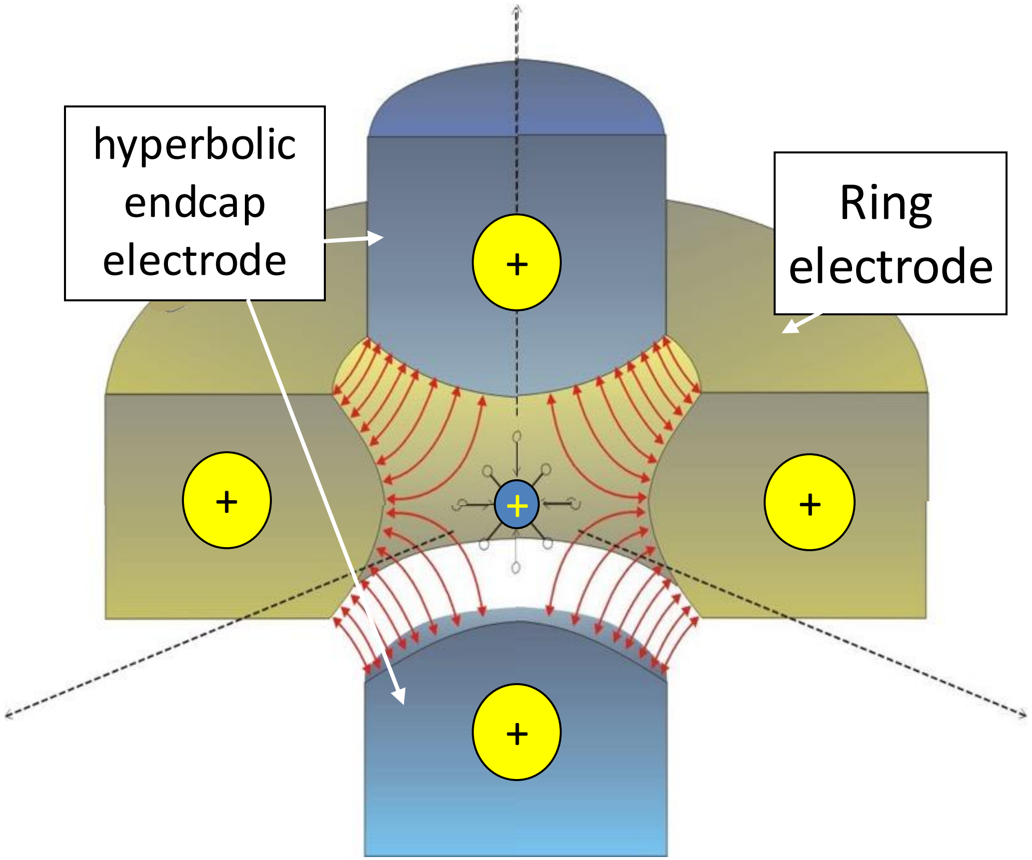

Paul trap: Oscillating electric fields

Solution: Oscillating electric fields.

The force on the ion alternates between attractive and repulsive,

At a certain frequency the effective force is repulsive.

→ Ion stays trapped

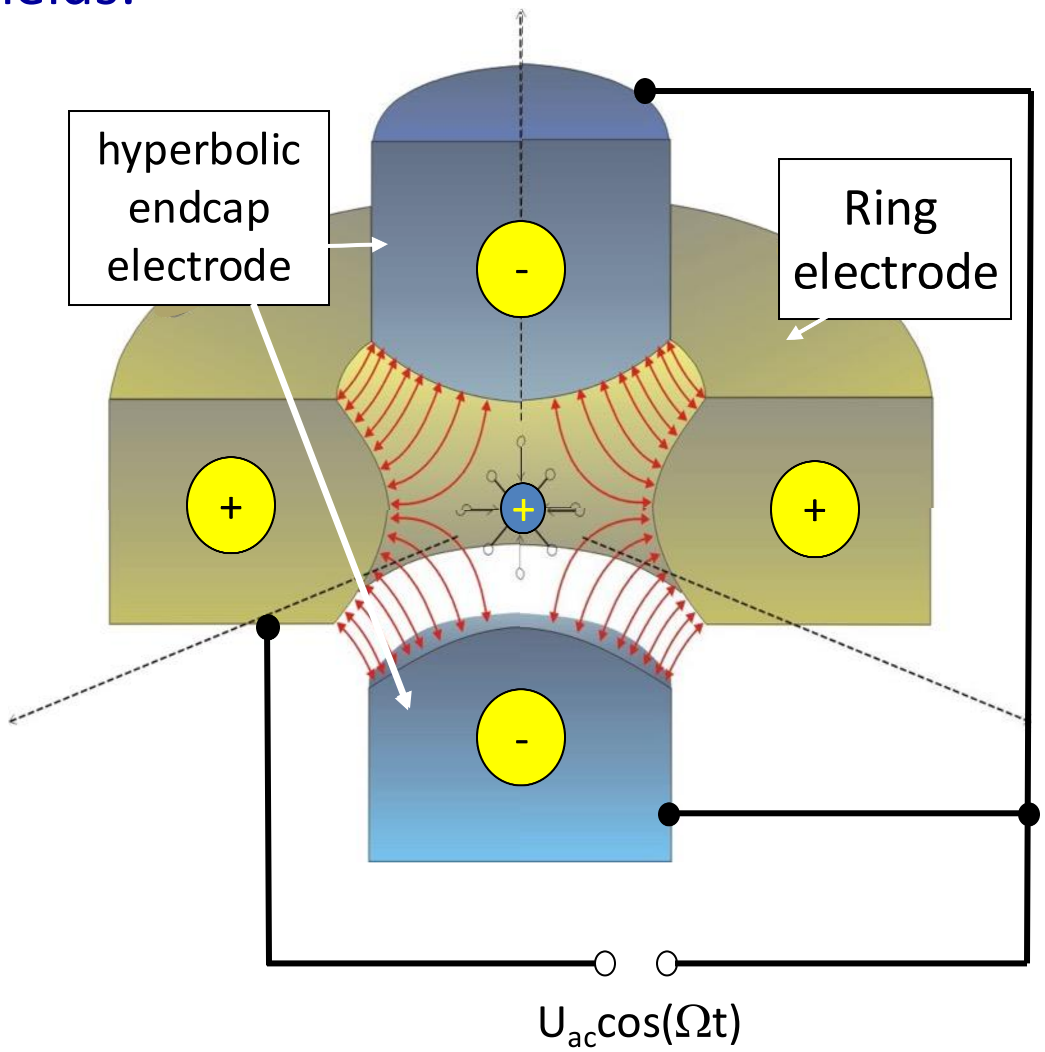

Modell for a trap: A rotating saddle

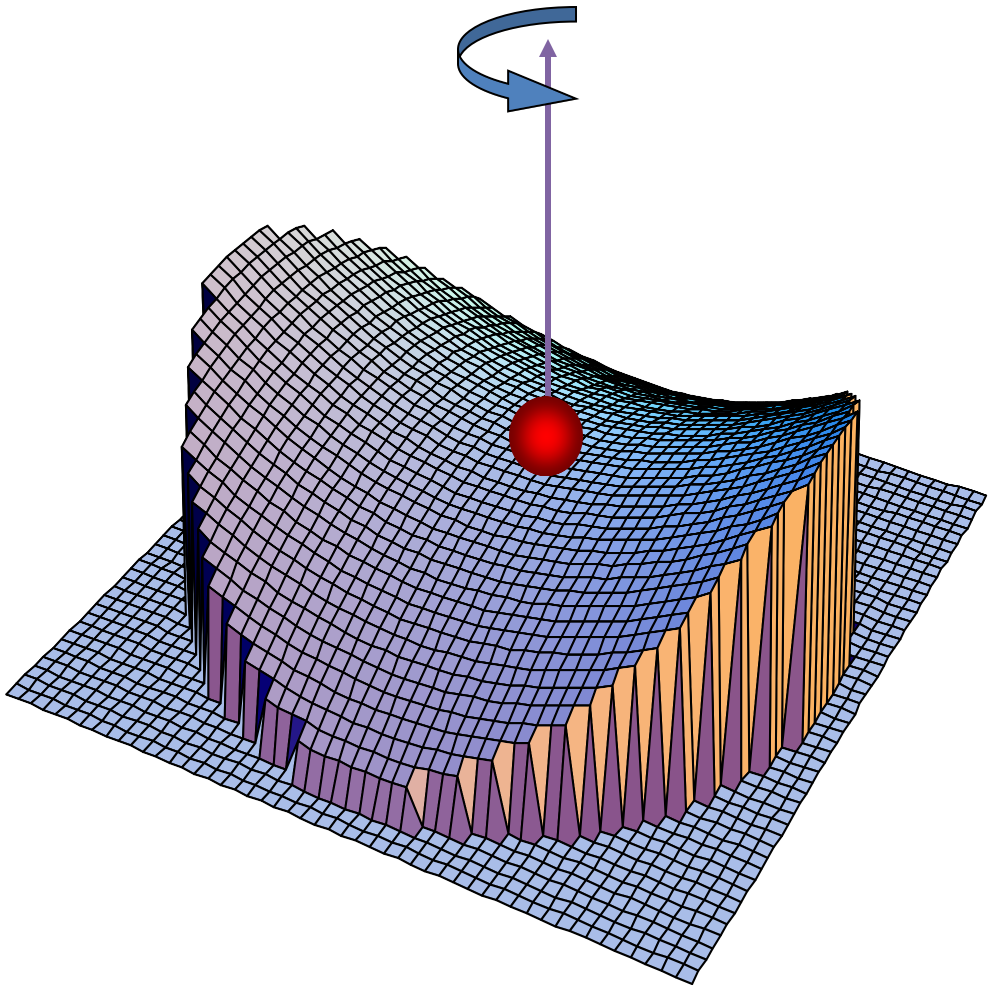

Ion trap - schematic

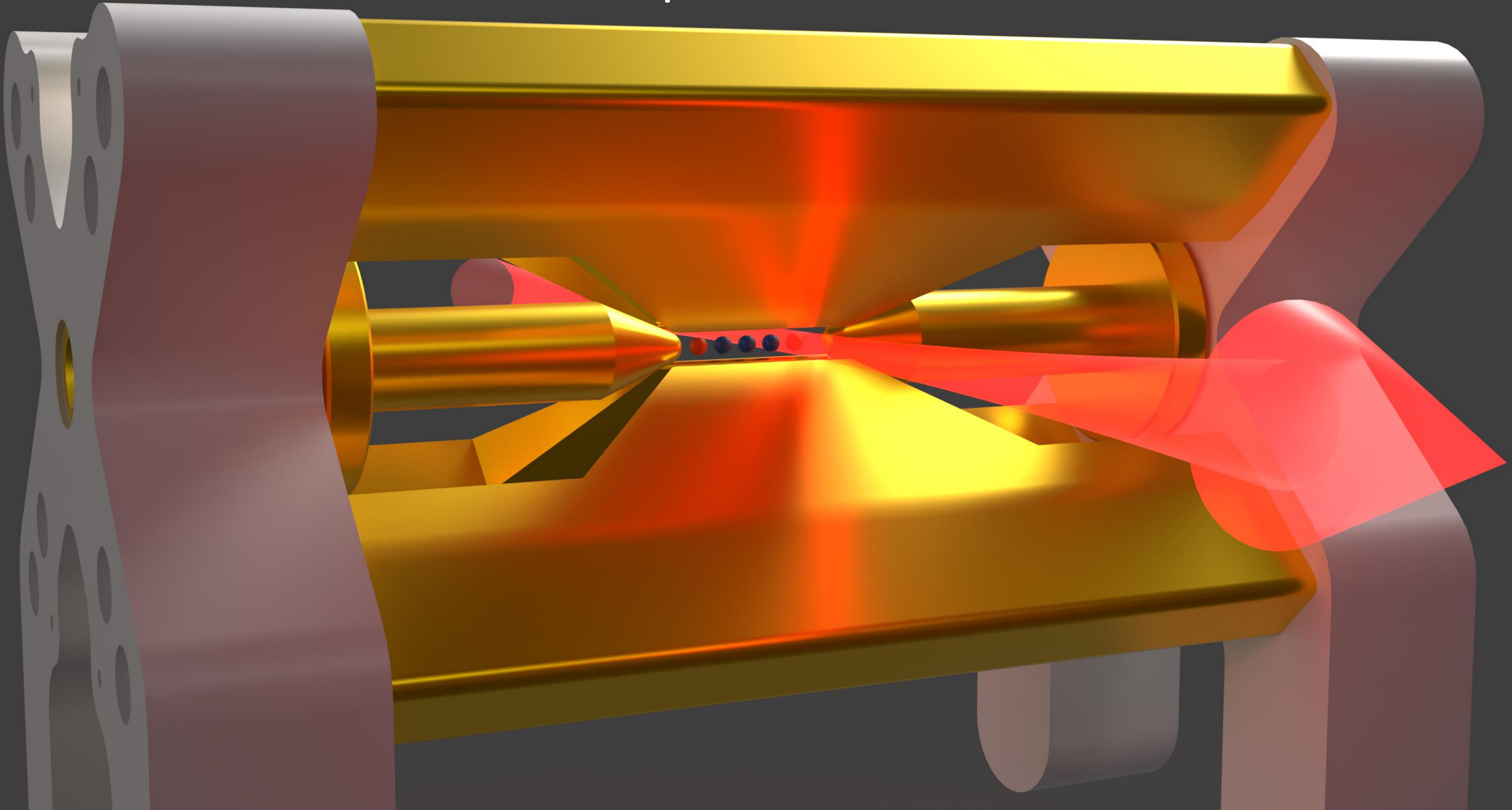

Ion trap - in reality...

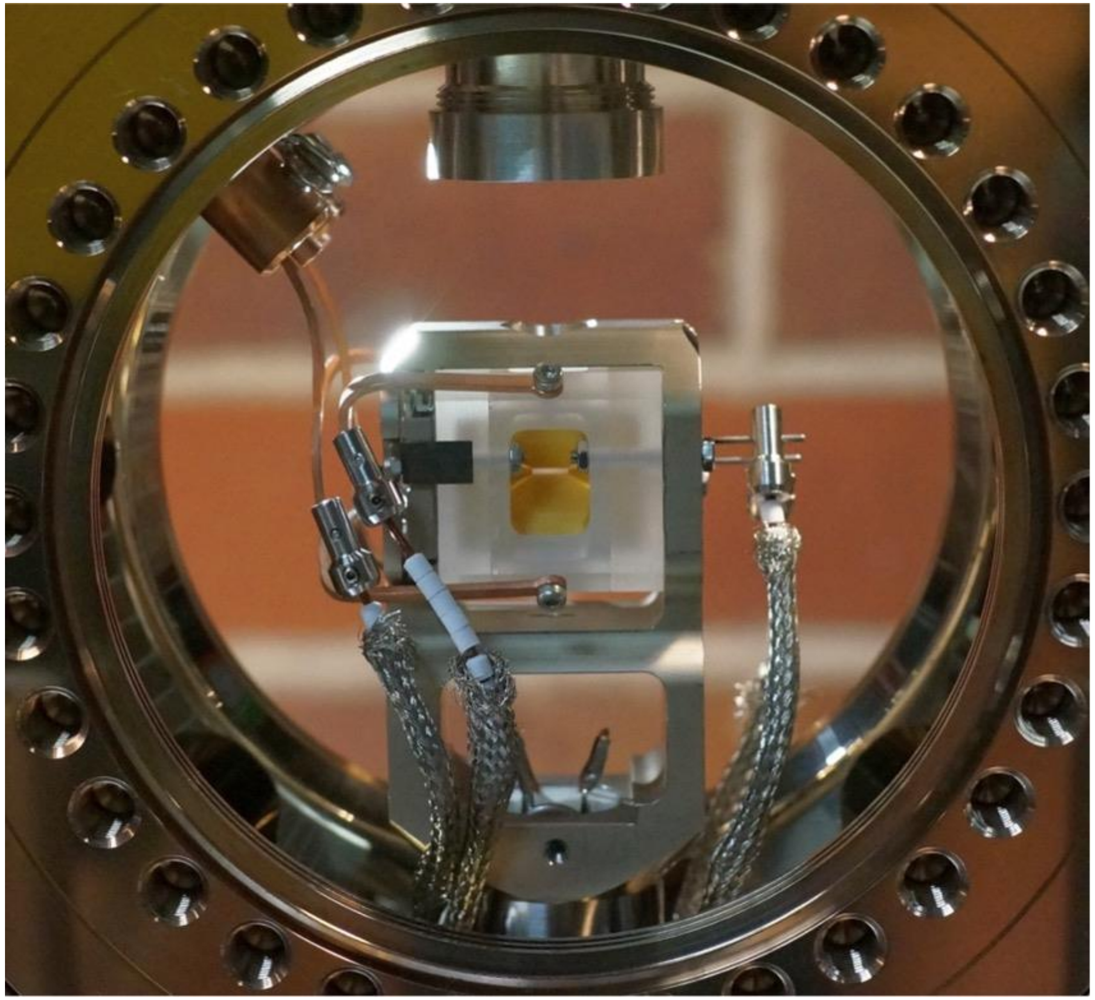

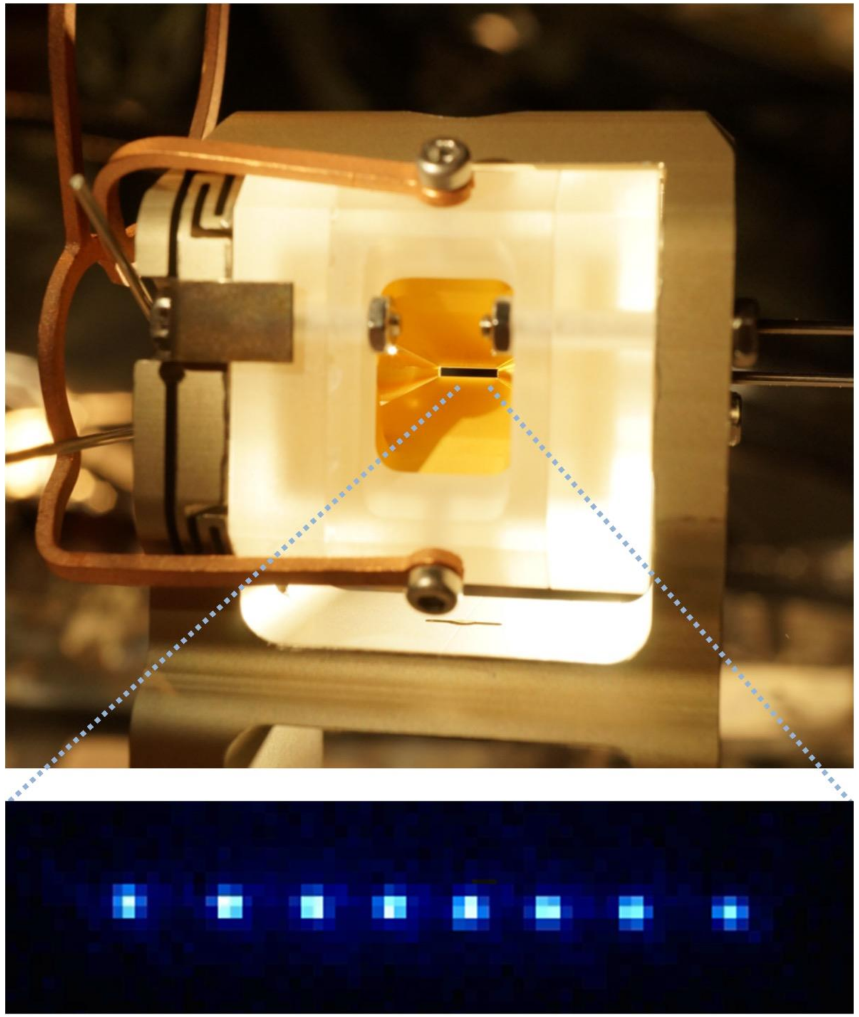

Source for strontium atoms

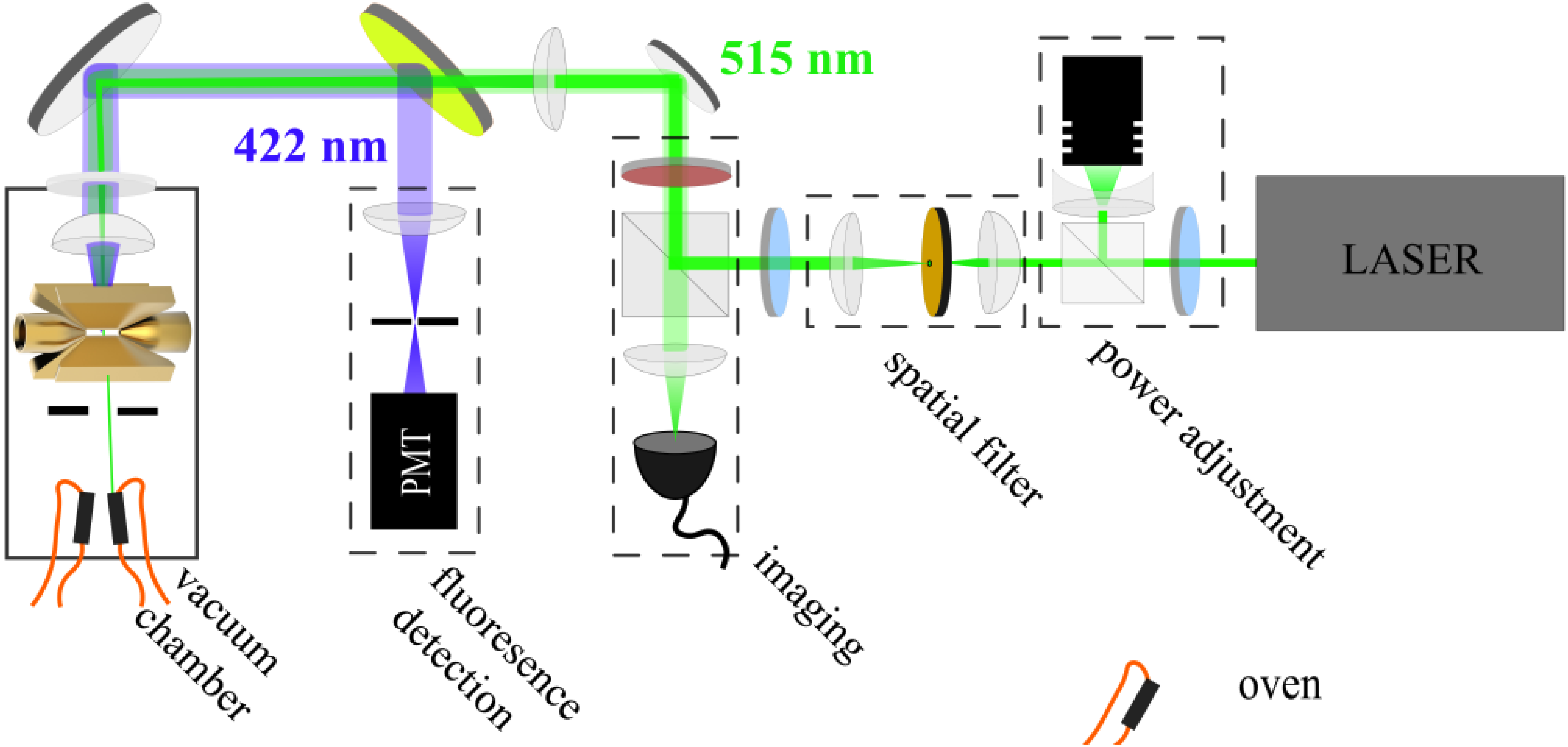

Photo-ionisation of strontium atoms

Sr energy levels

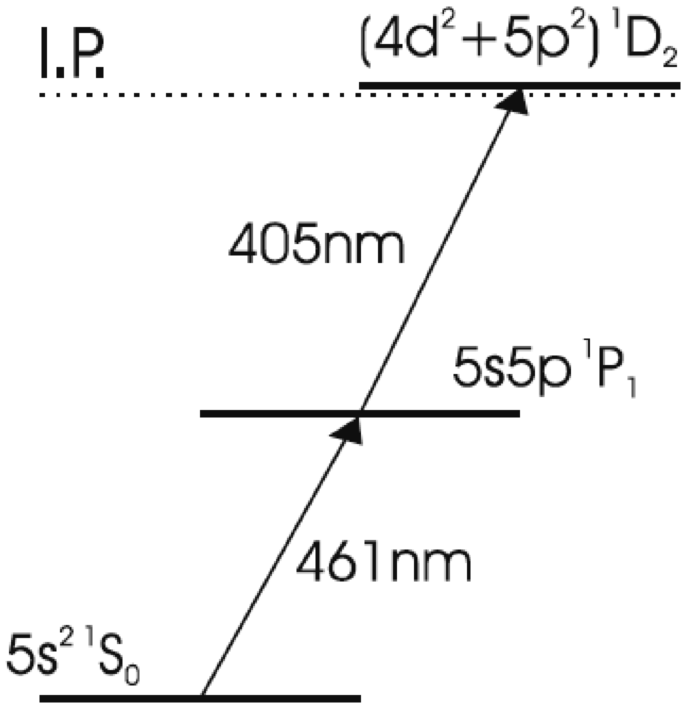

Auto-ionizing state

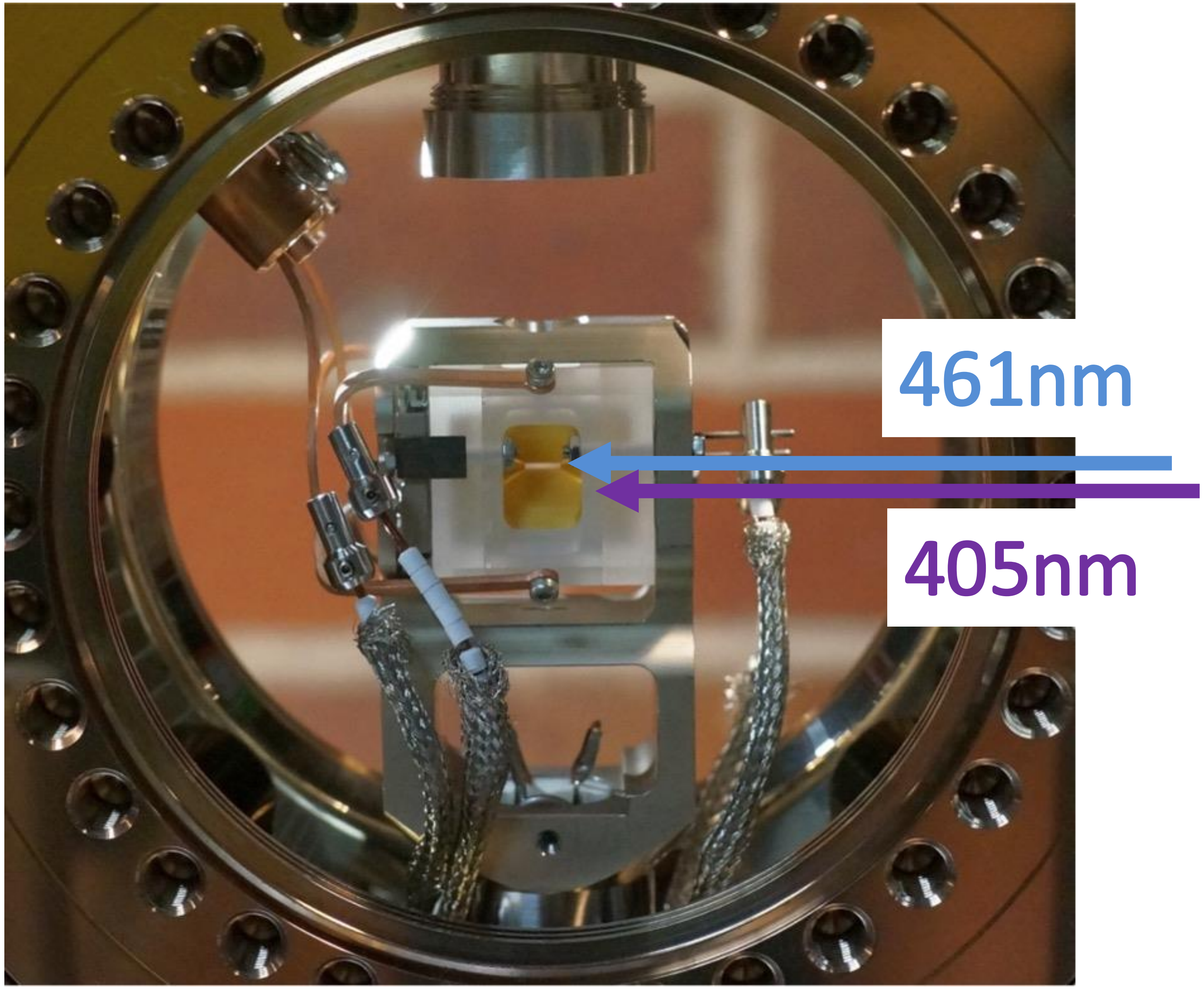

See e.g.: M. Brownnutt, et al. *Appl. Phys. B* **87**, 411 (2007).

At low temperatures: Ion crystals

Laser cooling: Cooling the atoms close to the absolute zero point

Ion temperature	after Doppler cooling	$T \approx 500\mu\text{K}$
	after sideband cooling	$T \approx 70\mu\text{K}$

1 Ion

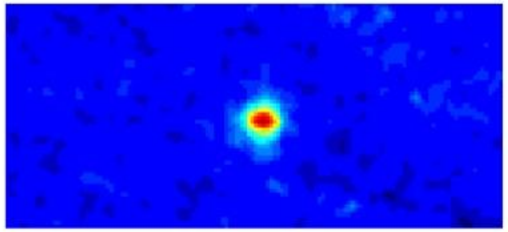

2 Ions

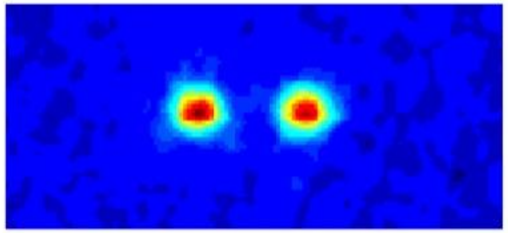

3 Ions

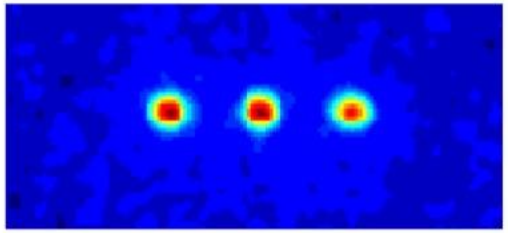

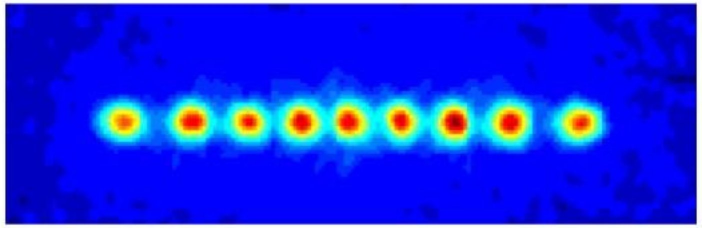

9 Ions

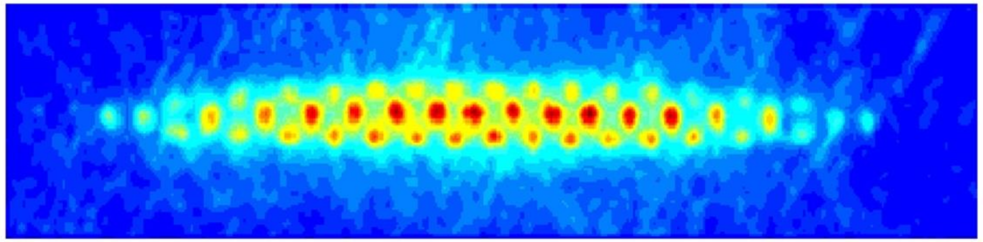

approx. 70 Ions

Oscillation modes of ions crystals

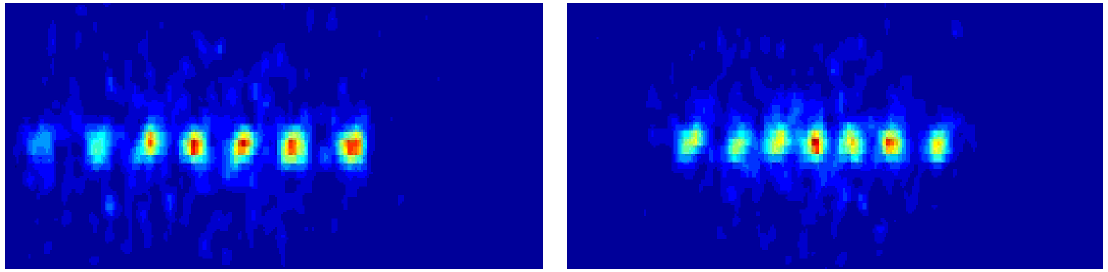

How to use trapped ions for quantum computation and simulation.

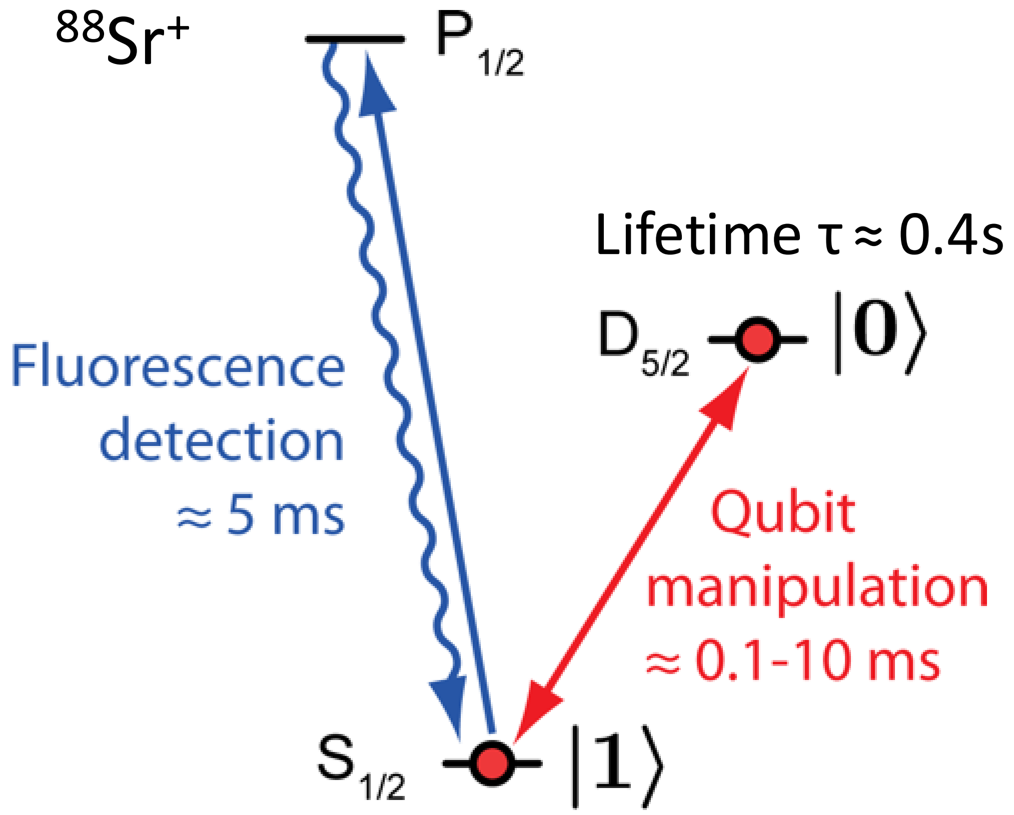

Quantum jumps

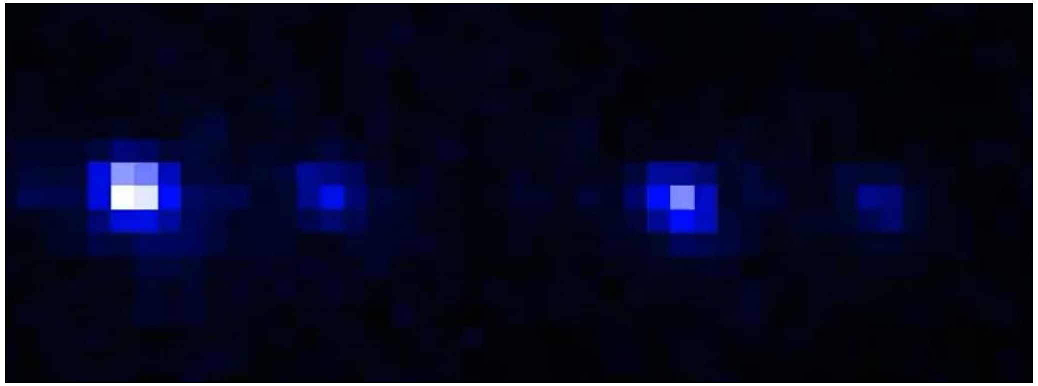

How to control the ion motion?

Common mode excitation

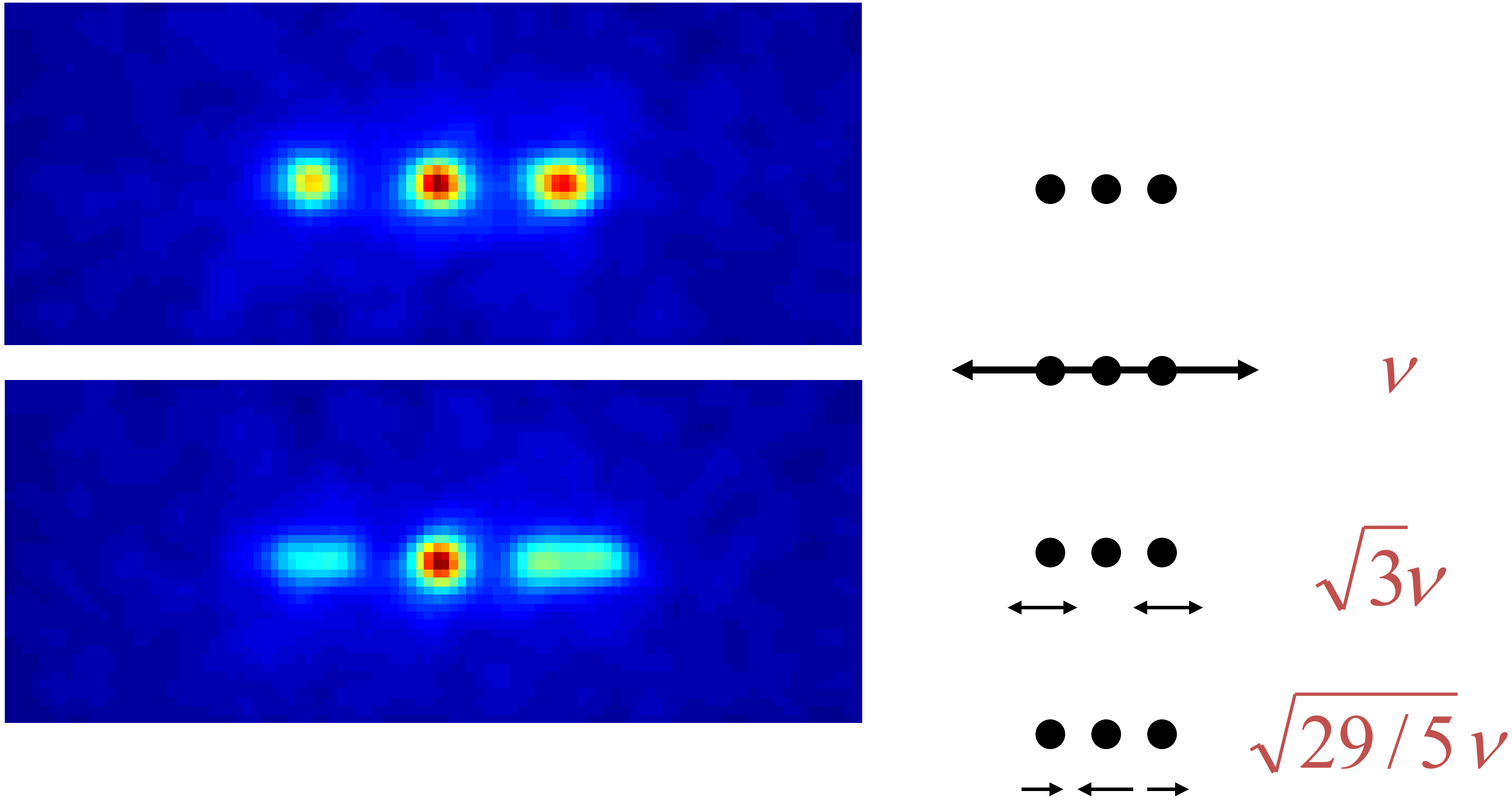

Common mode excitations

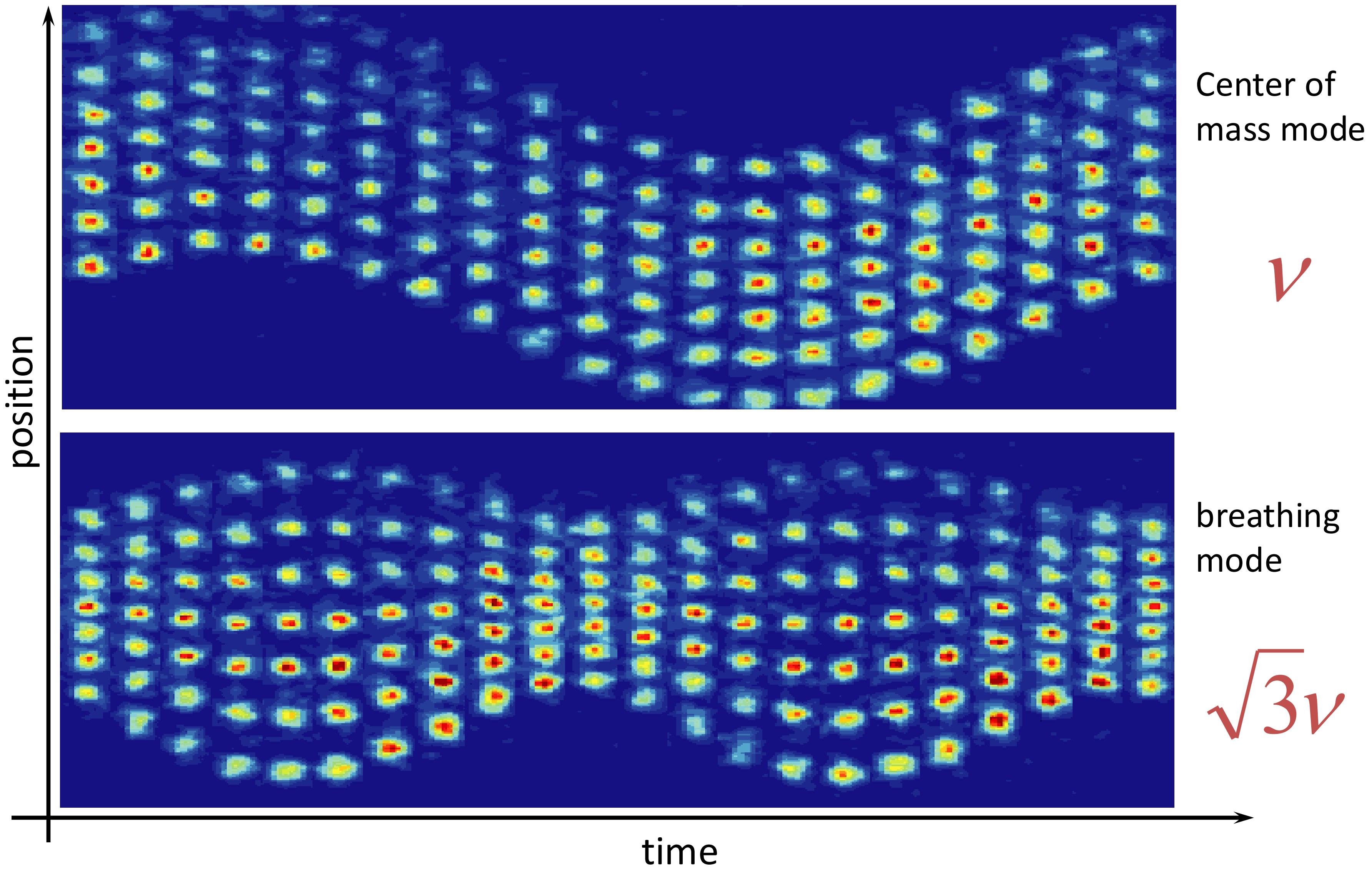

A String of Trapped Ions Coupled to the Motion

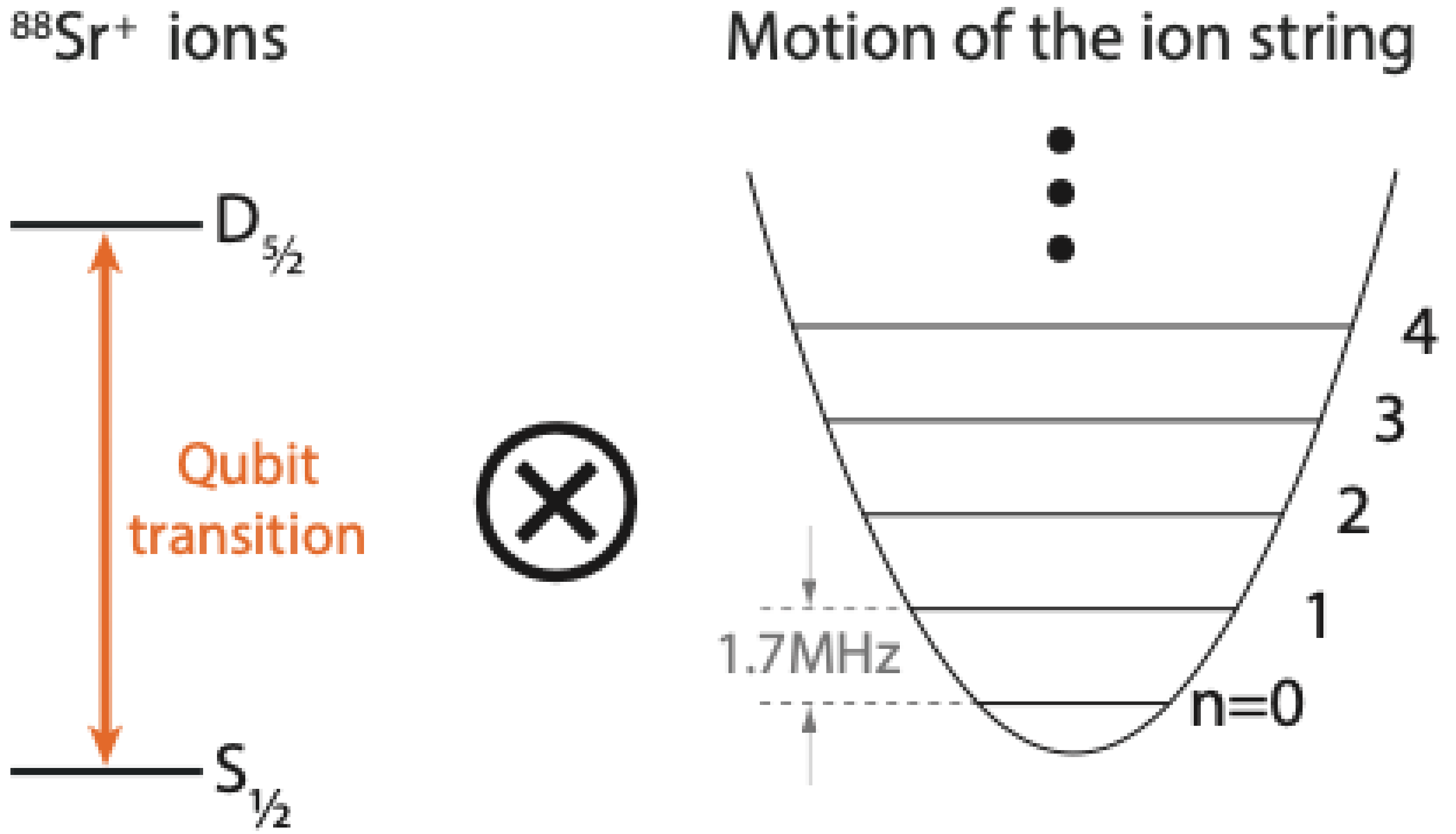

A String of Trapped Ions Coupled to the Motion

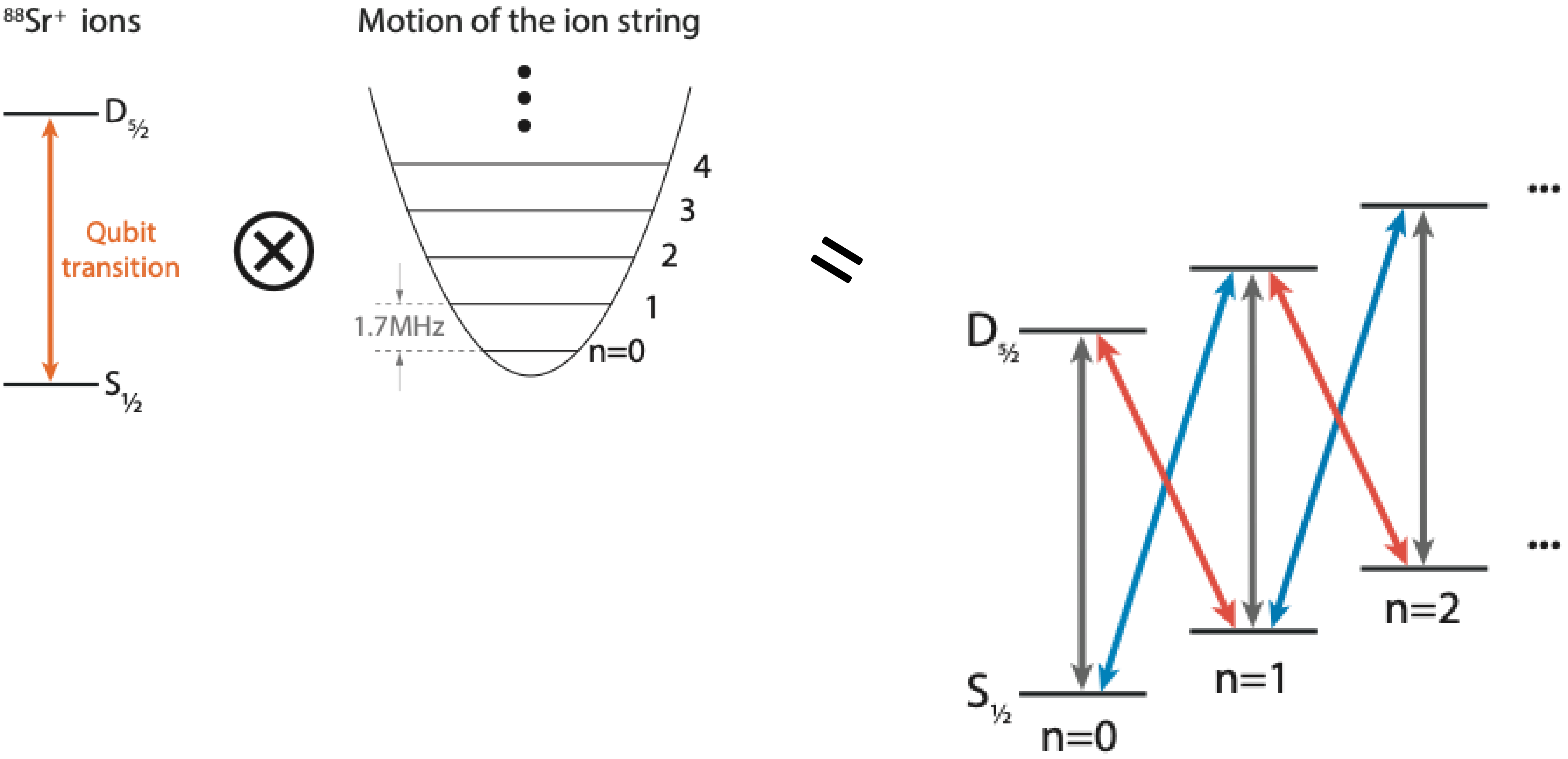

Laser-ion interaction

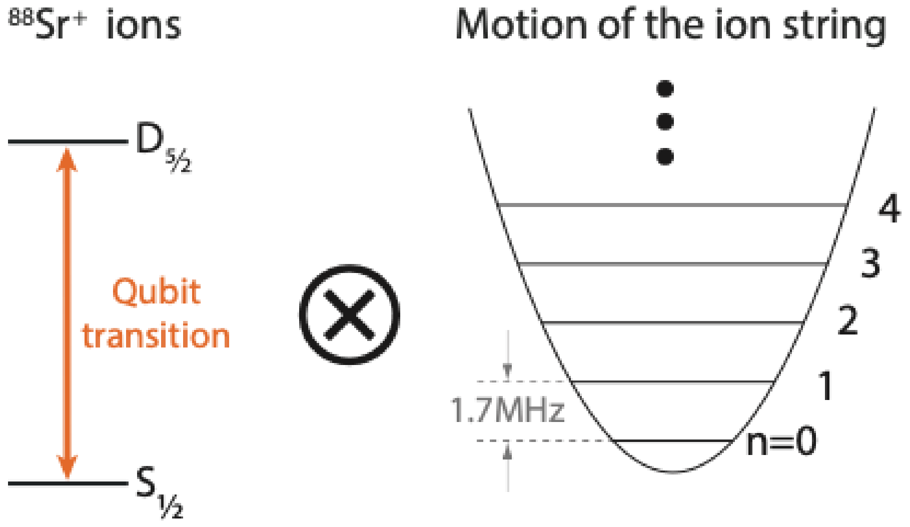

$$\hat{H}_e = \frac{1}{2}\hbar\omega_{eg}(|e\rangle\langle e| - |g\rangle\langle g|)$$

$$\hat{H}_m = \frac{p^2}{2m} + \frac{1}{2}m\omega_t^2 x^2 = \hbar\omega_t(\hat{a}^\dagger\hat{a} + \frac{1}{2})$$

$$\hat{H}_{int} = \frac{1}{2}\hbar\Omega_l(|e\rangle\langle g| + |g\rangle\langle e|)(e^{i(\omega_l t - k_l x)} + e^{-i(\omega_l t - k_l x)})$$

Lamb-Dicke limit

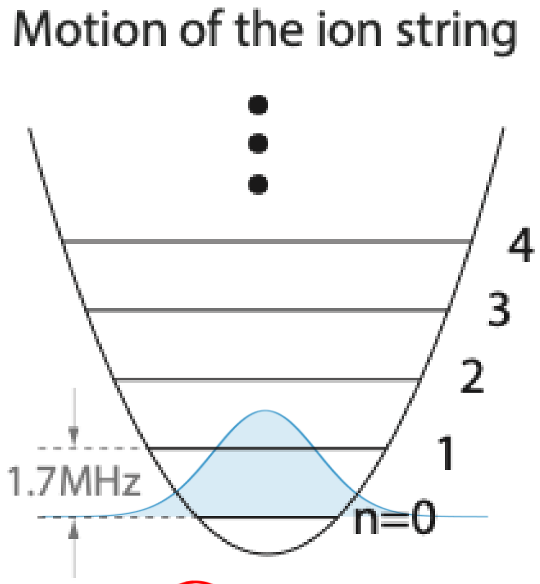

$$\langle x^2 \rangle = (2n+1)\frac{\hbar}{2m\omega_t}$$

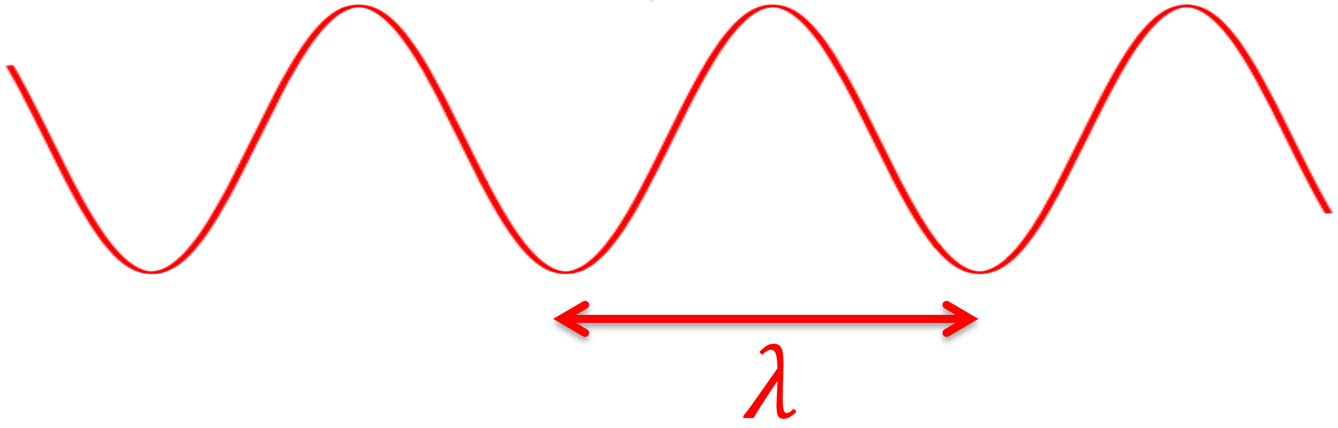

Lamb-Dicke parameter

$$\eta = \frac{2\pi}{\lambda_l} x_0 = k_l \sqrt{\frac{\hbar}{2m\omega_t}}$$

Lamb-Dicke parameter specifies how well the ion is localized compared to the wavelength of the laser.

Small Lamb-Dicke parameter = ion sees a fixed laser phase (=no Doppler effect due to motion).

Position-dependent laser phase expressed in terms of Lamb-Dicke parameter and creation and annihilation operators

$$kx = k_l \sqrt{\frac{\hbar}{2m\omega_j}} (\hat{a}^\dagger + \hat{a}) = \eta(\hat{a}^\dagger + \hat{a})$$

Laser-ion interaction

Taylor expansion of interaction Hamiltonian in η:

$$\hat{H}_{int}^{\text{RWA}} = \frac{1}{2}\hbar\Omega_l\ \hat{\sigma}^+\ e^{i(\Delta t - \eta(\hat{a}^\dagger e^{i\omega_t t} + \hat{a}e^{-i\omega_t t}))} + h.c.$$
$$\approx \frac{1}{2}\hbar\Omega_l\ \hat{\sigma}^+\ e^{i\Delta t}(1 - i\eta(\hat{a}^\dagger e^{i\omega_t t} + \hat{a}e^{-i\omega_t t}) + \mathcal{O}(\eta^2)) + h.c.$$

Carrier transition (on resonance $\Delta = 0$): $|g,n\rangle \leftrightarrow |e,n\rangle$

$$\hat{H}_{int} = \frac{1}{2}\hbar\Omega_l(\hat{\sigma}^+ + \hat{\sigma}^-)$$

Red sideband transition ($\Delta = -\omega_t$): $|g,n\rangle \leftrightarrow |e,n-1\rangle$

$$\hat{H}_{int} = -\frac{1}{2}\hbar\Omega_l\ i\eta(\hat{\sigma}^+\hat{a} - \hat{\sigma}^-\hat{a}^\dagger)$$

Blue sideband transition ($\Delta = \omega_t$): $|g,n\rangle \leftrightarrow |e,n+1\rangle$

$$\hat{H}_{int} = -\frac{1}{2}\hbar\Omega_l\ i\eta(\hat{\sigma}^+\hat{a}^\dagger - \hat{\sigma}^-\hat{a})$$

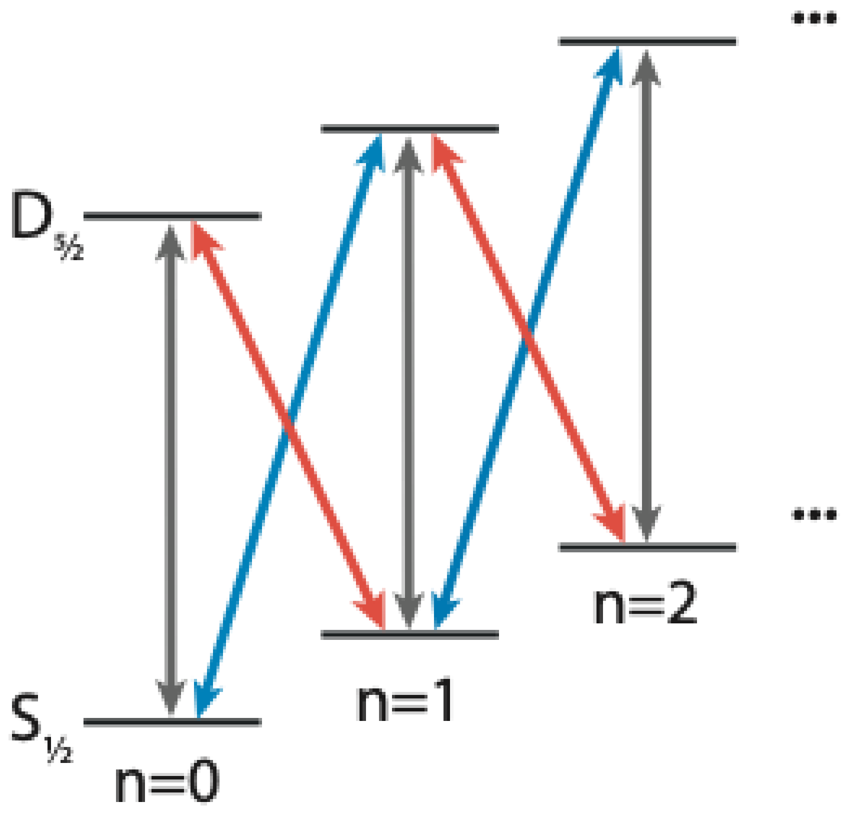

Excitation spectrum of single ion in linear trap

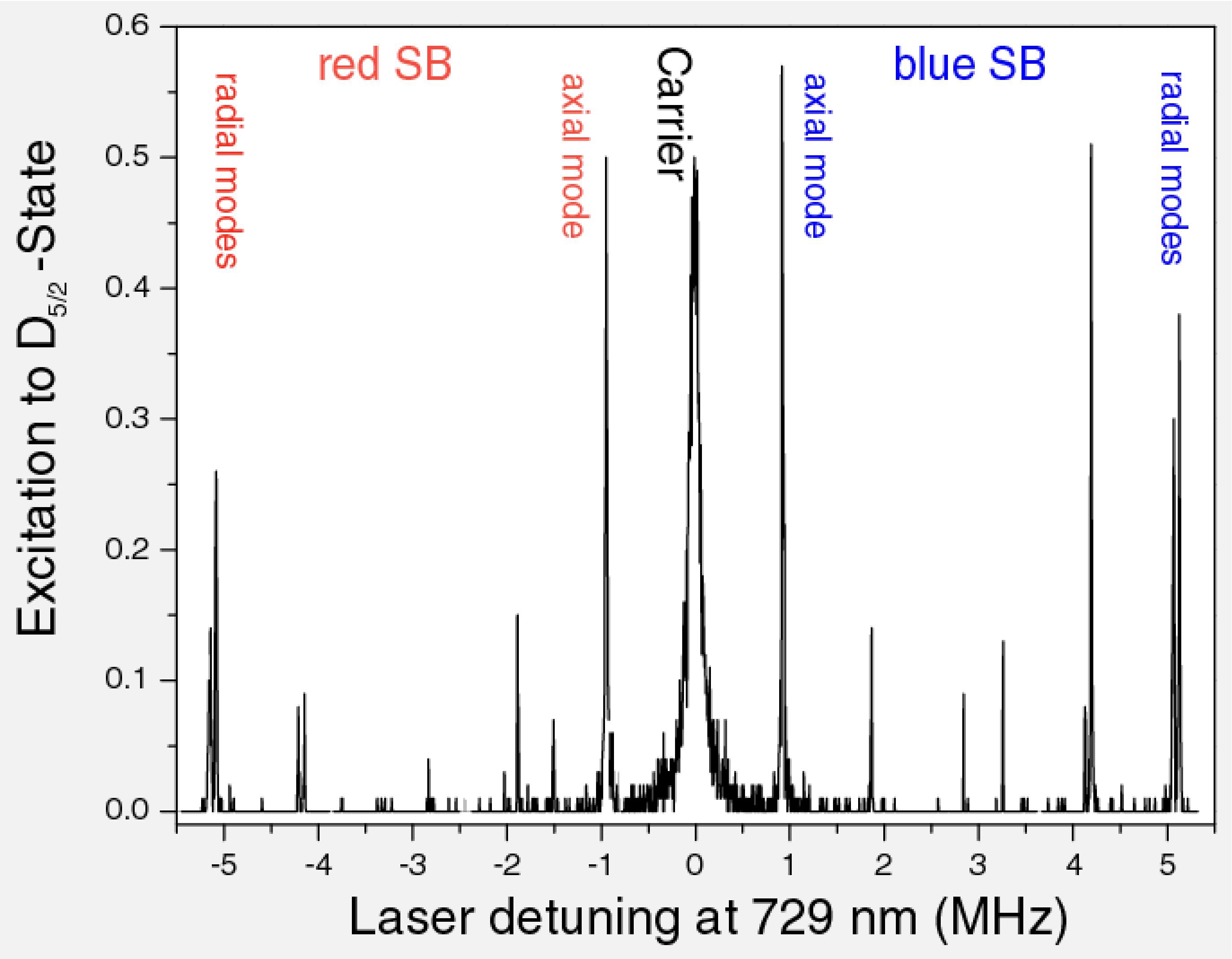

ω_{ax} = 1.0 MHz

ω_{rad} = 5.0 MHz

Coherent state manipulation

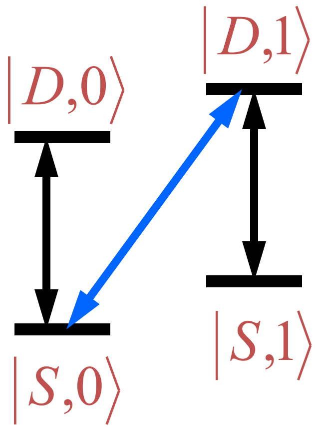

carrier and sideband
Rabi oscillations
with Rabi frequencies

$\Omega, \quad \eta\Omega\sqrt{n+1}$

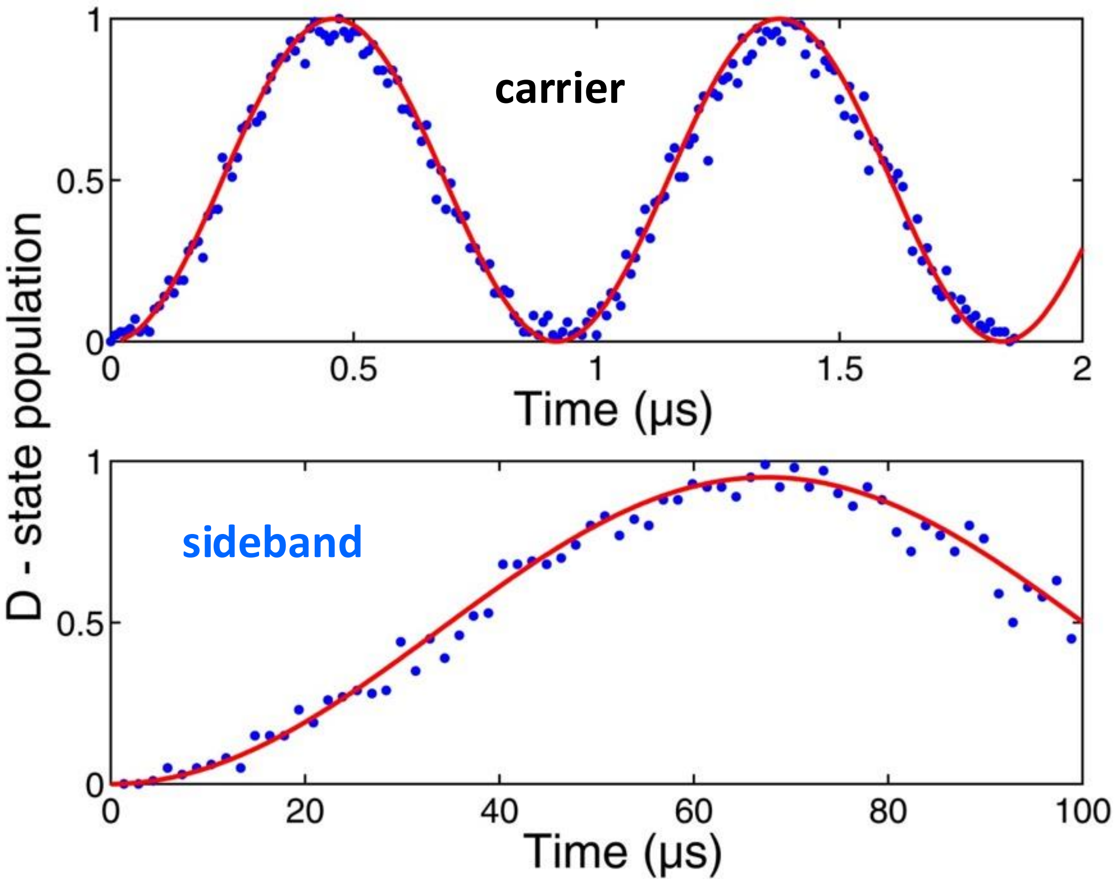

$\eta = kx_0$ Lamb-Dicke parameter

Doppler cooling

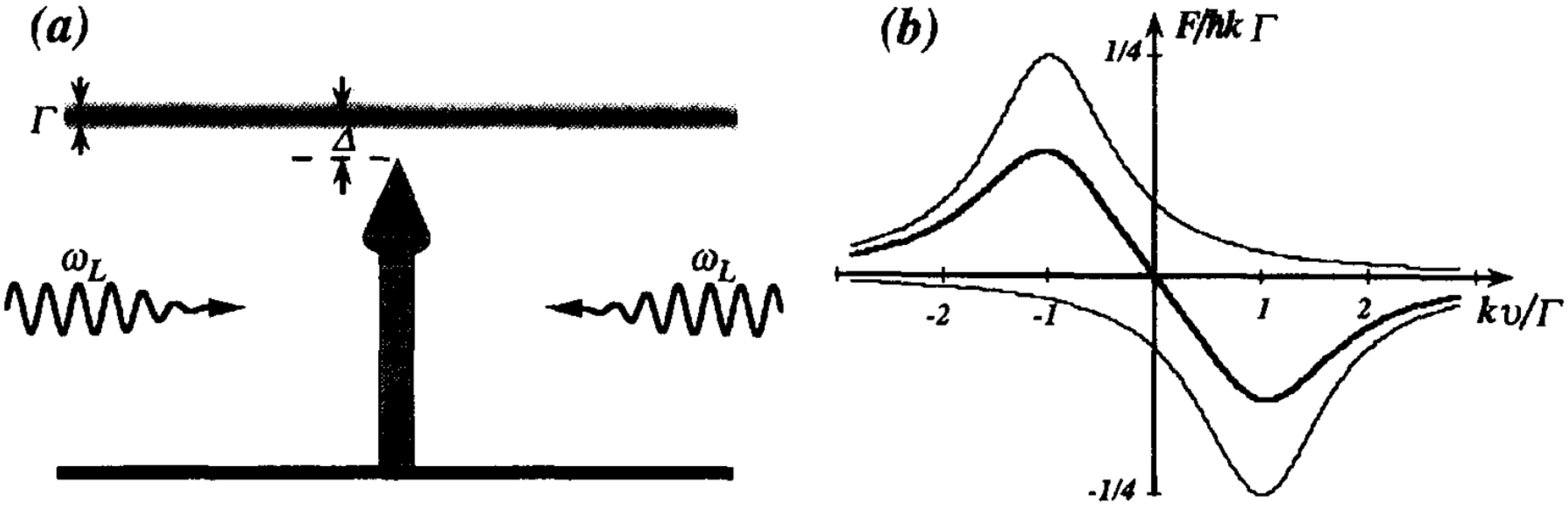

→ Brings the ion into the Lamb-Dicke regime

Sideband cooling

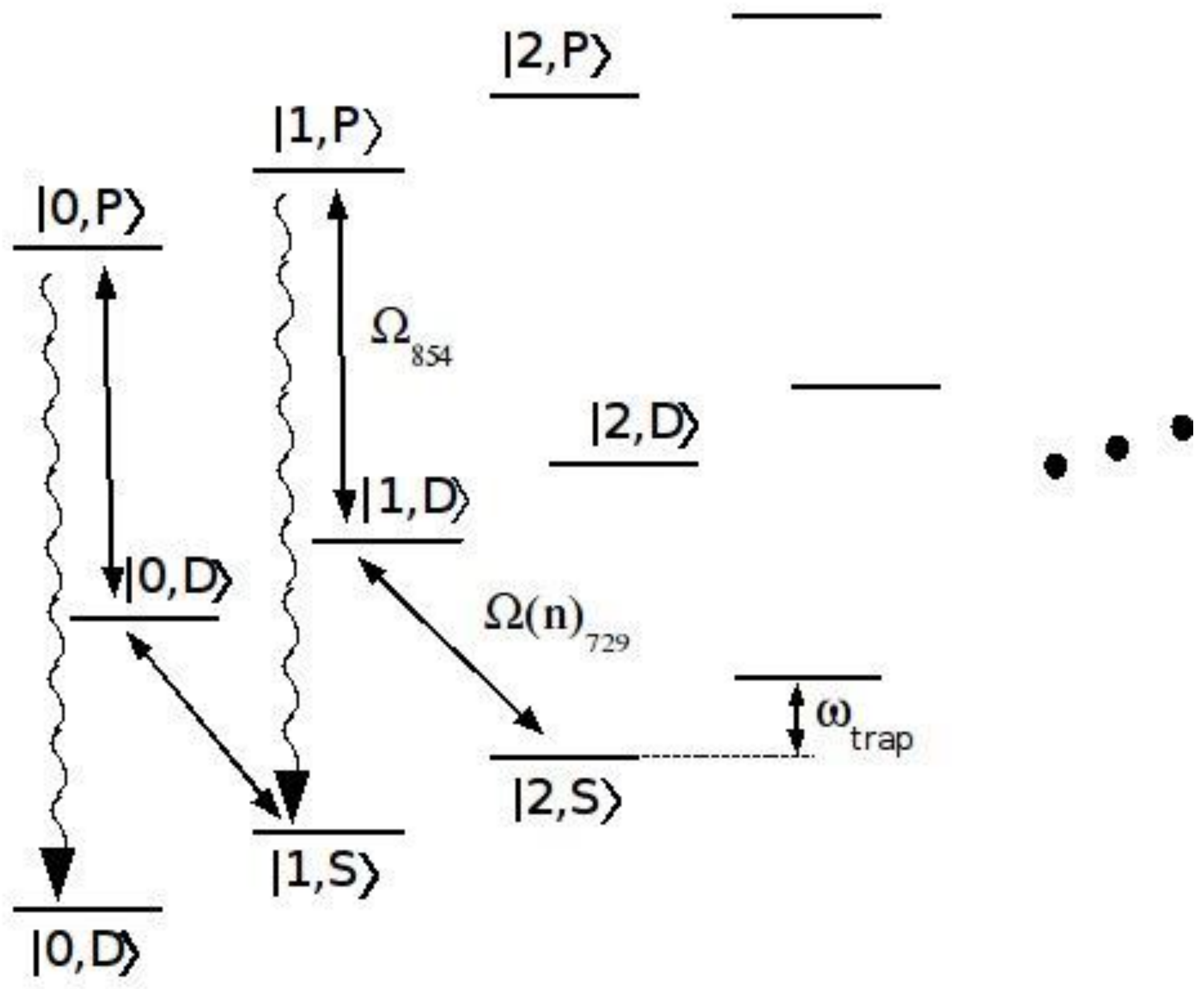

A typical experimental sequence.

The experimental sequence

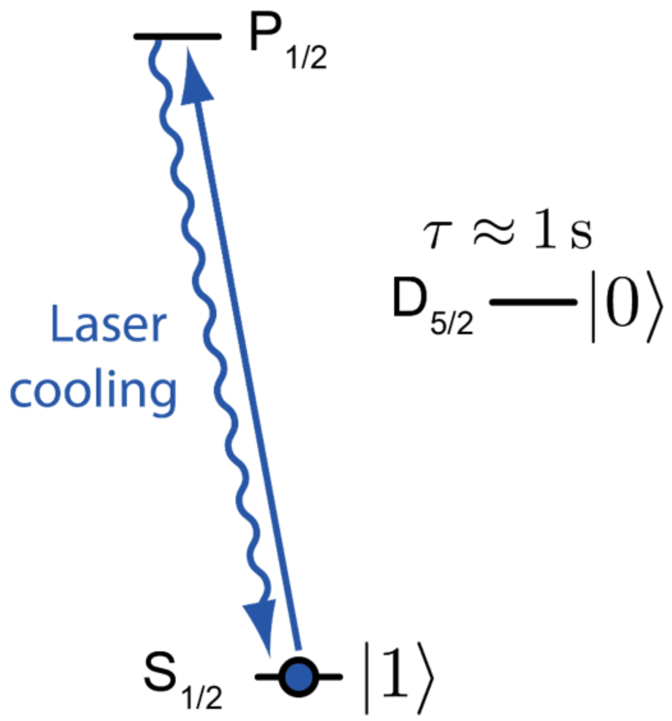

1. Initialisation

The experimental sequence

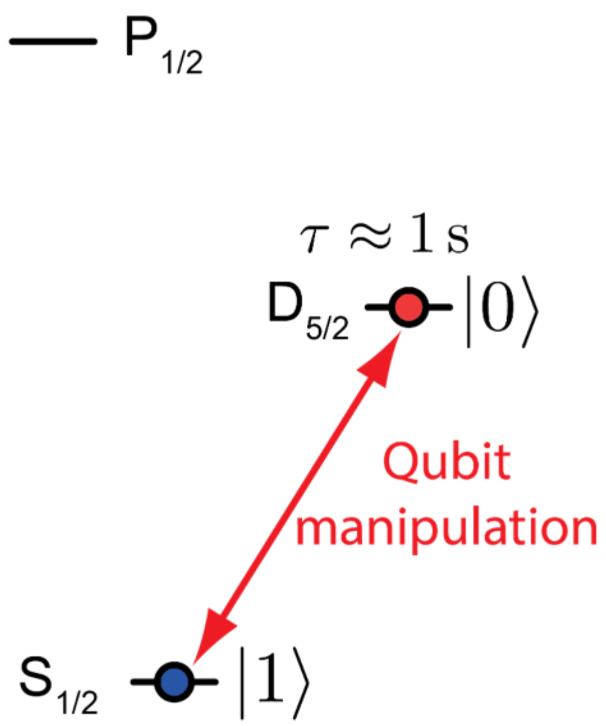

1. Initialisation

2. Laser excitation of the $S_{1/2}$ – $D_{5/2}$ qubit transition

The experimental sequence

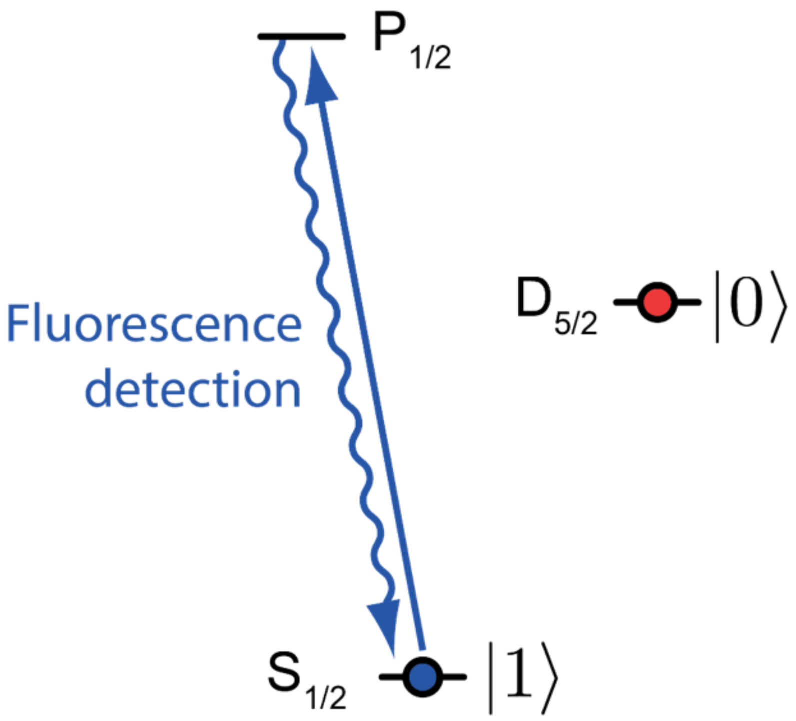

1. Initialisation
2. Laser excitation of the $S_{1/2} – D_{5/2}$ qubit transition
3. Quantum state measurement by fluorescence detection

The experimental sequence

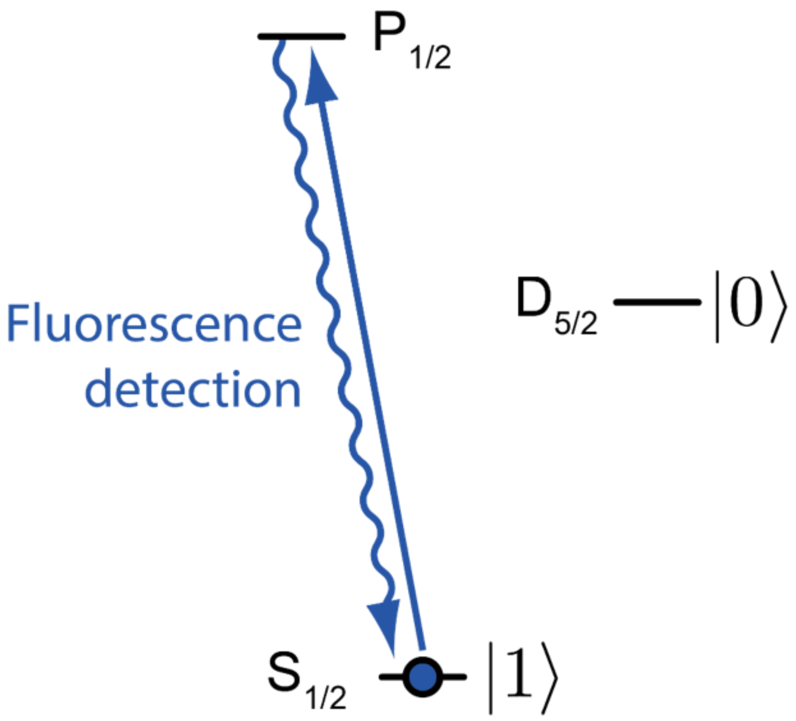

1. Initialisation
2. Laser excitation of the $S_{1/2} - D_{5/2}$ qubit transition
3. Quantum state measurement by fluorescence detection

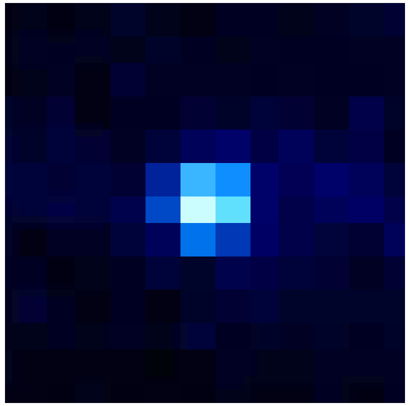

bright picture = ion is in state $|1\rangle$

The experimental sequence

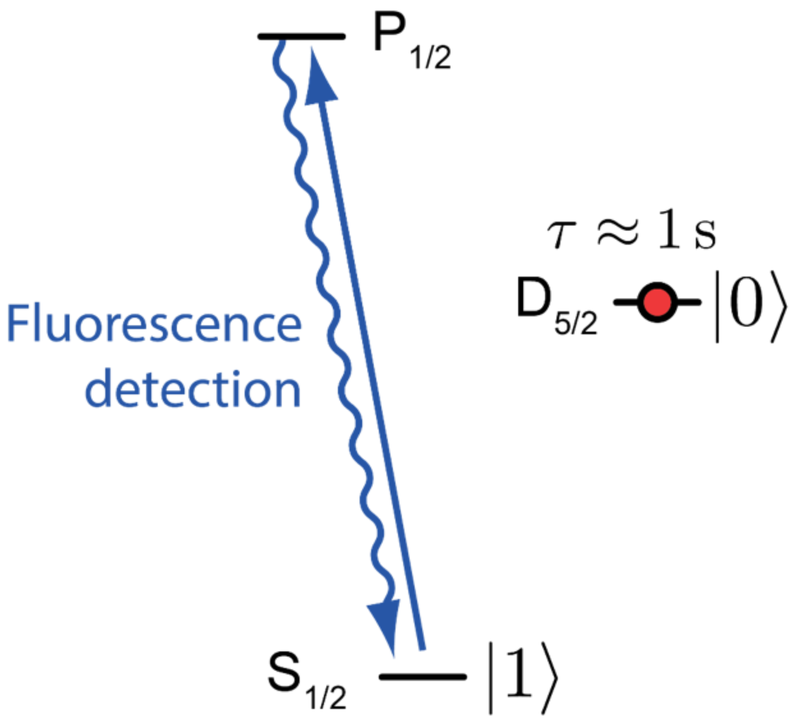

1. Initialisation

2. Laser excitation of the $S_{1/2}$ – $D_{5/2}$ qubit transition

3. Quantum state measurement by fluorescence detection

$$\text{dark picture} = \text{ion is in state } |0\rangle$$

The experimental sequence

<u>Two ions:</u>

Spatially resolved detection with CCD camera

$|SS\rangle$

$|SD\rangle$

$|DS\rangle$

$|DD\rangle$

50 Experiments / s

Repeat experiment 50-1000 times

Measurement process

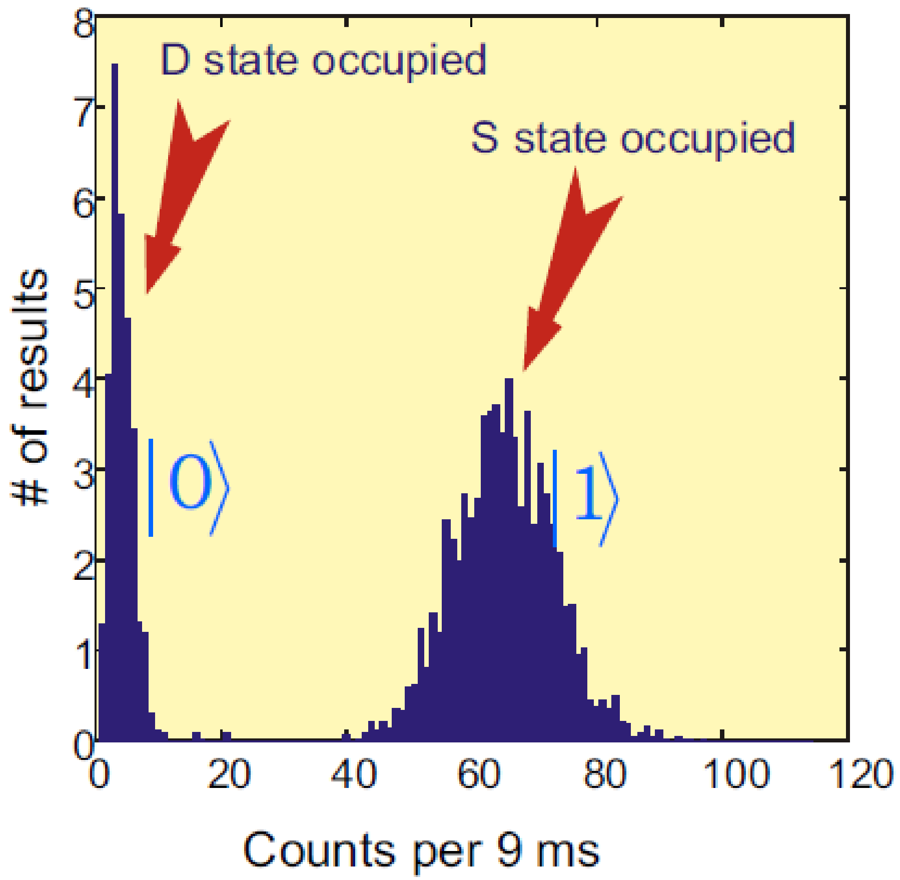

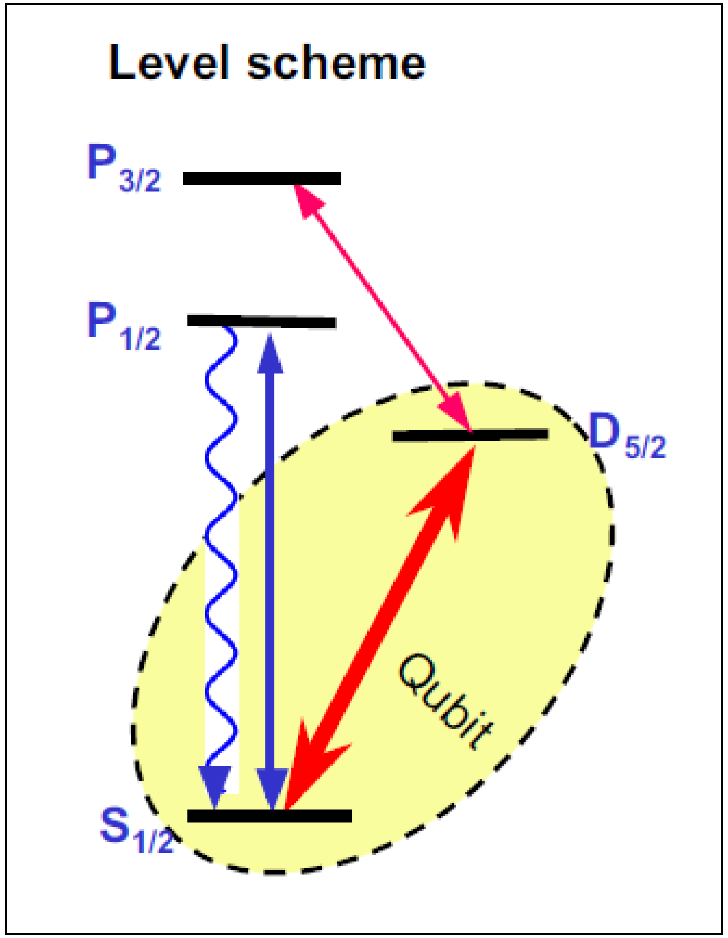

→ The measurement process is equivalent to a projection of the Bloch sphere onto |0> and |1>.

SPAM error

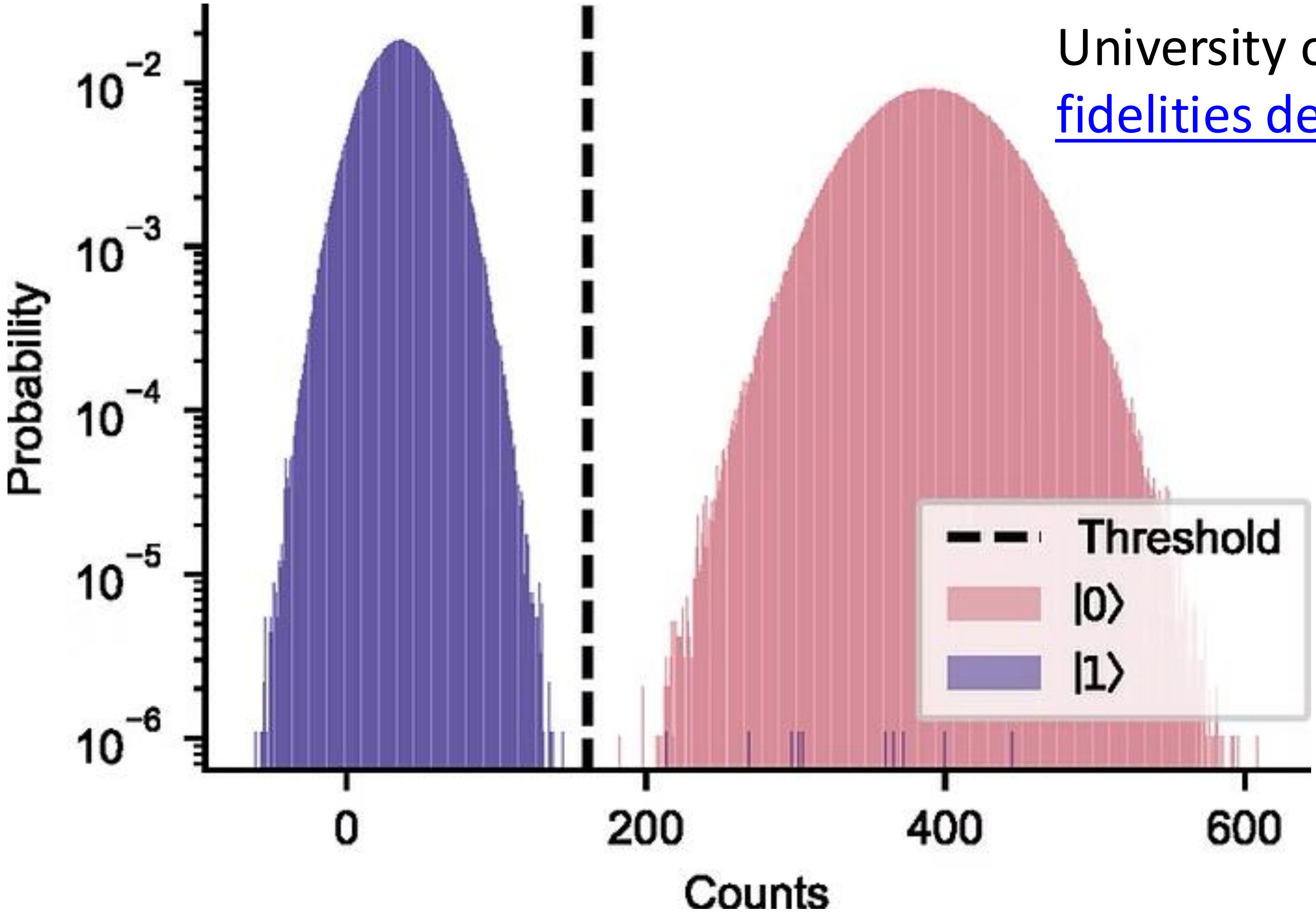

University of Oxford: highest recorded SPAM fidelities demonstrated at 99.9993%.

A. Sotirova, arXiv:2409.05805

Addressing of individual ions

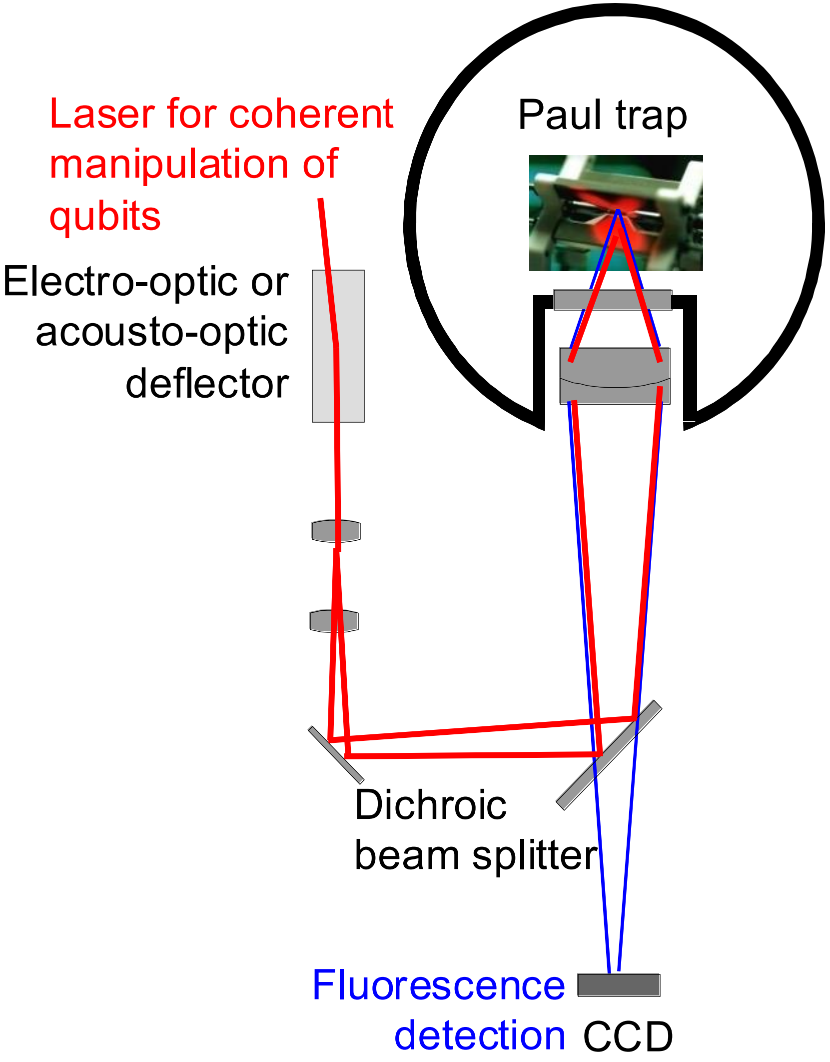

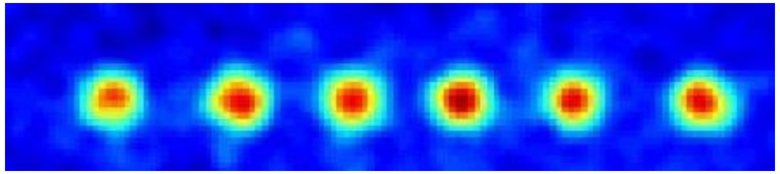

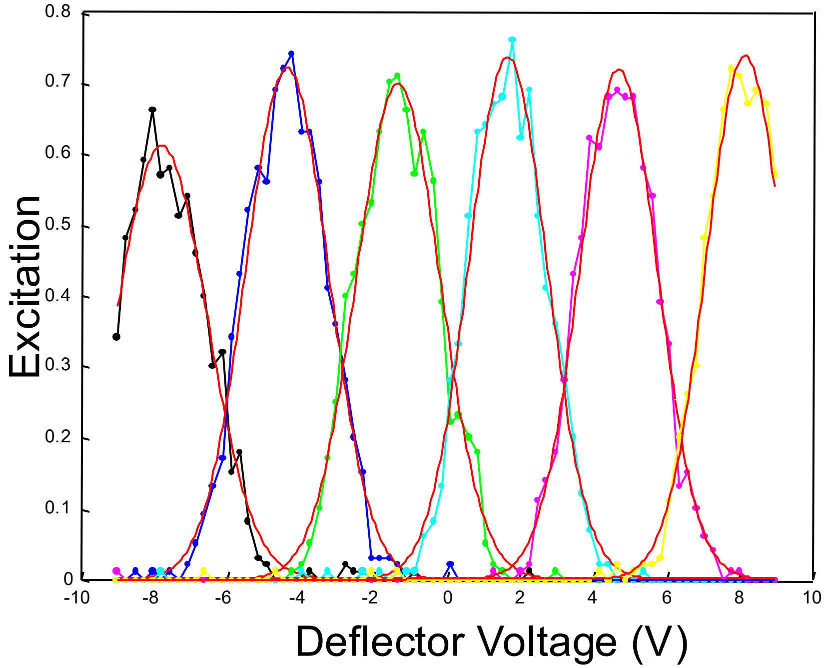

- inter ion distance: ~ 4 μm
- addressing waist: ~ 2 μm

< 0.1% intensity on neighbouring ions

Parallel qubit addressing and readout (Monroe group / IonQ)

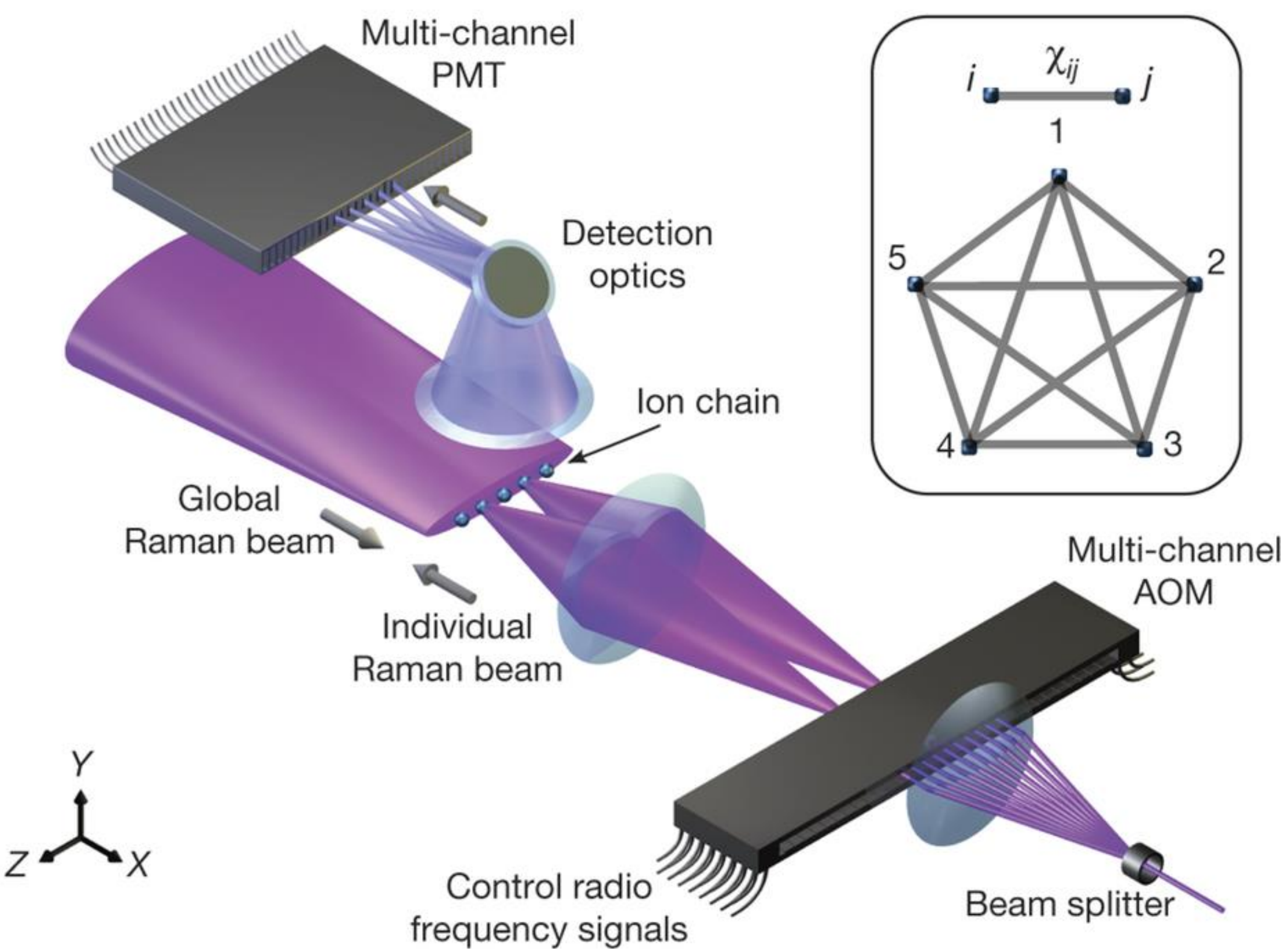

S Debnath *et al.* *Nature* **536,** 63–66 (2016).

Entanglement operations

Ions interact pairwise in the Mølmer-Sørensen entangling operation.

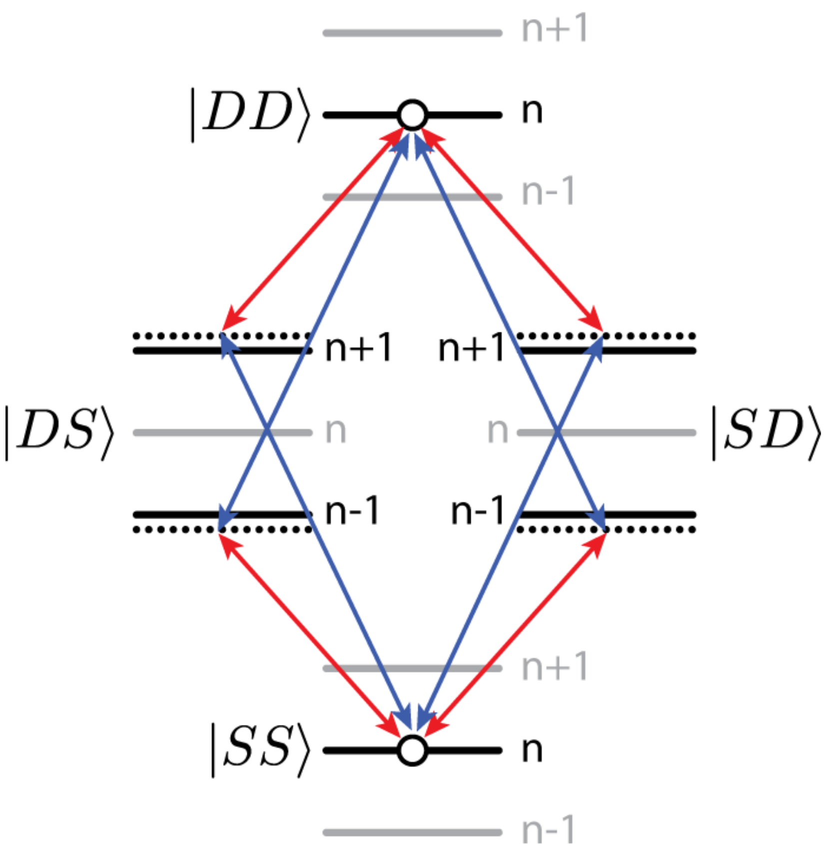

Bichromatic laser field, e.g.

flips ion 1 and adds a phonon

flips ion 2 and removes a phonon

= ions exchange a phonon.

Gate action: correlated spin flips

$$|SS\rangle \leftrightarrow |DD\rangle$$

Directly generates entangled states of N ions

$$|GHZ\rangle = \frac{1}{\sqrt{2}}(|SS \ldots S\rangle + |DD \ldots D\rangle)$$

Deterministic Bell states with the Mølmer-Sørensen gate

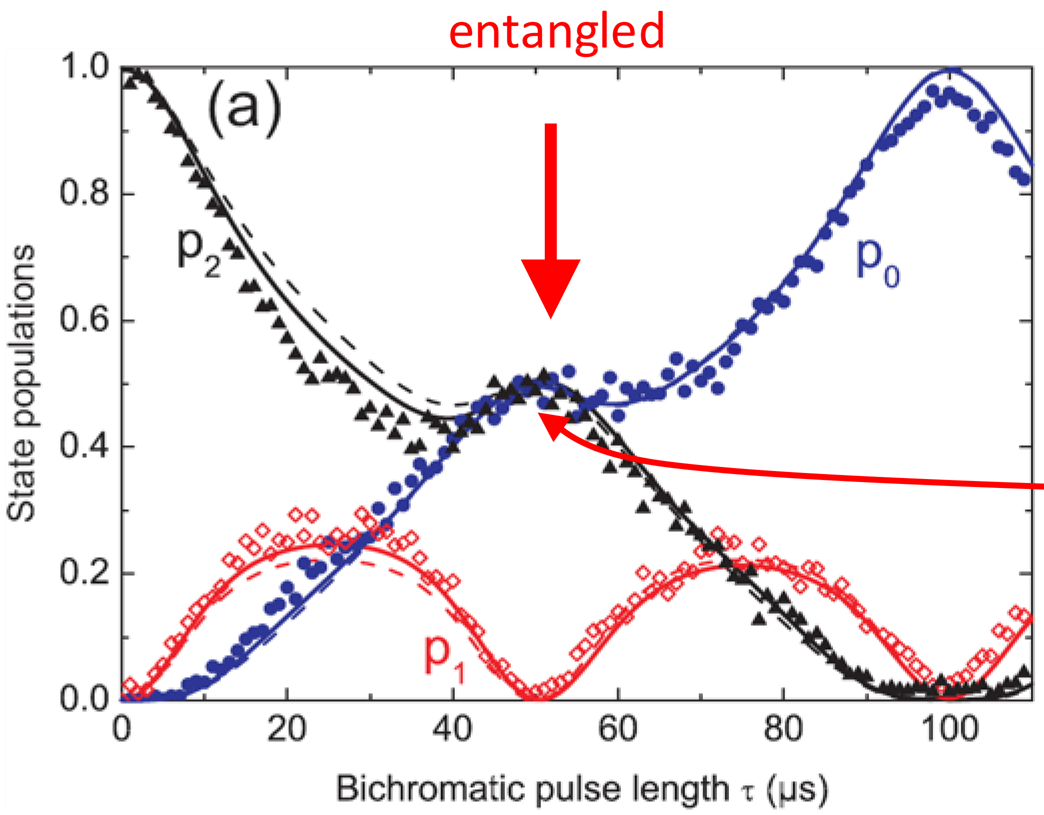

J. Benhelm et al.
Nature Physics ***4****, 463 (2008)*
Theory:
C. Roos, NJP 10 (2008)

measure entanglement
via parity oscillations

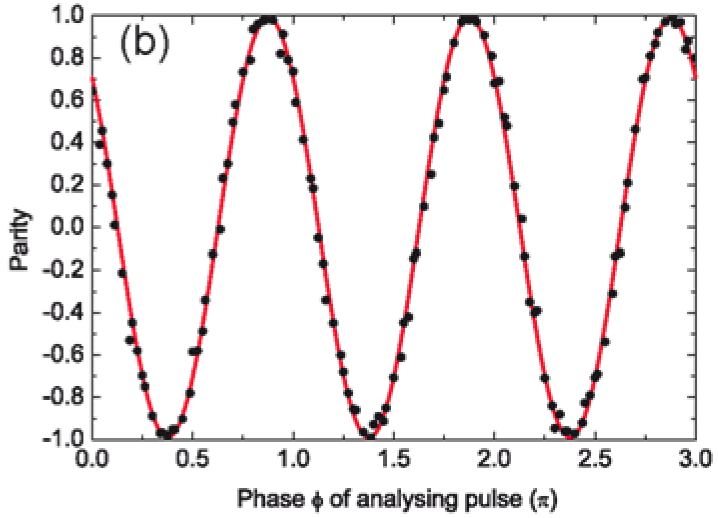

gate duration $51\mu s$

average fidelity

$$F_{\rm MS} = 99.3(0.2)\%$$

The MS-interaction for more ions is equivalent to a large multi-path interferometer.

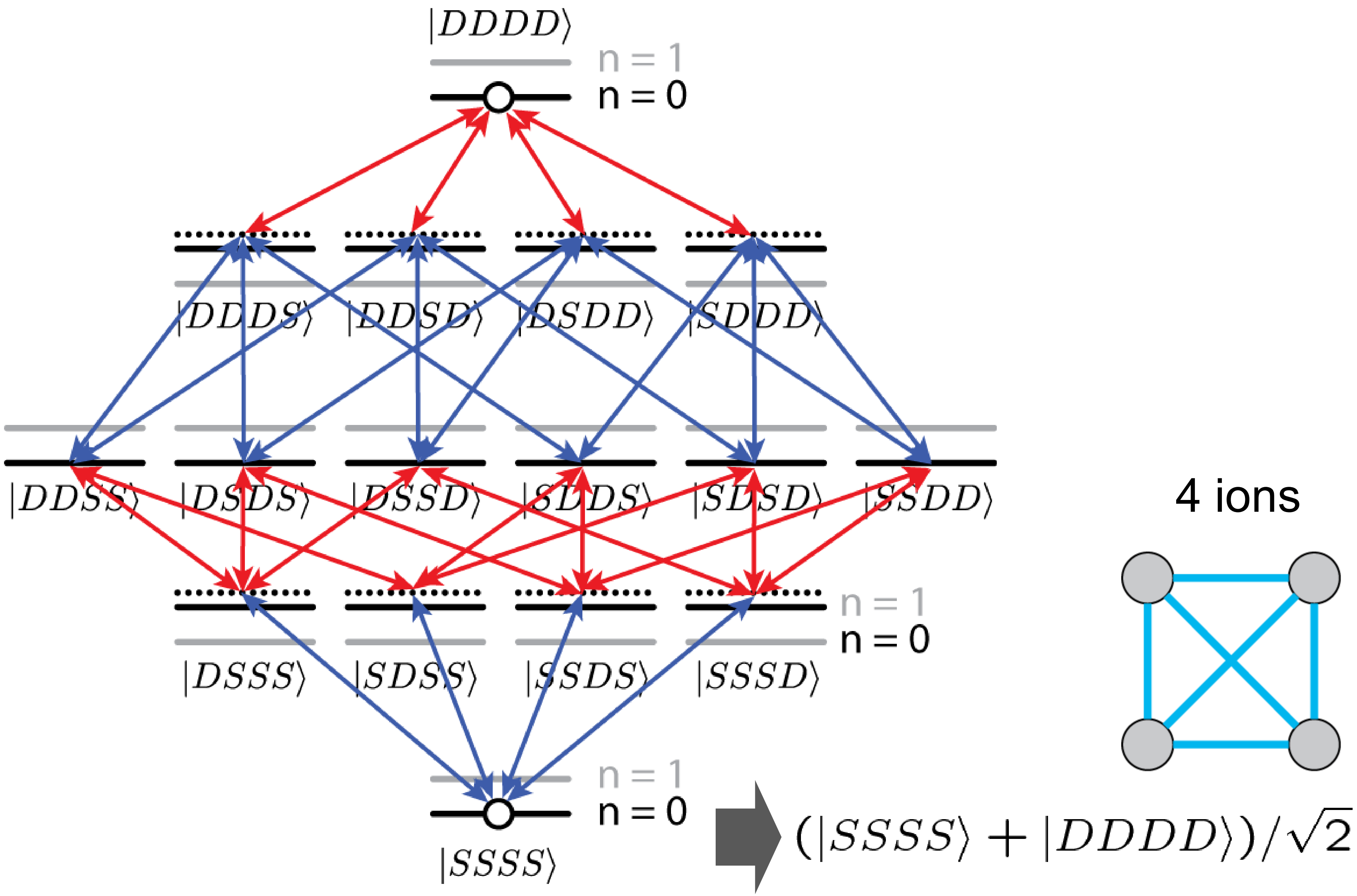

14 ion entanglement (demonstrated with up to 24 ions)

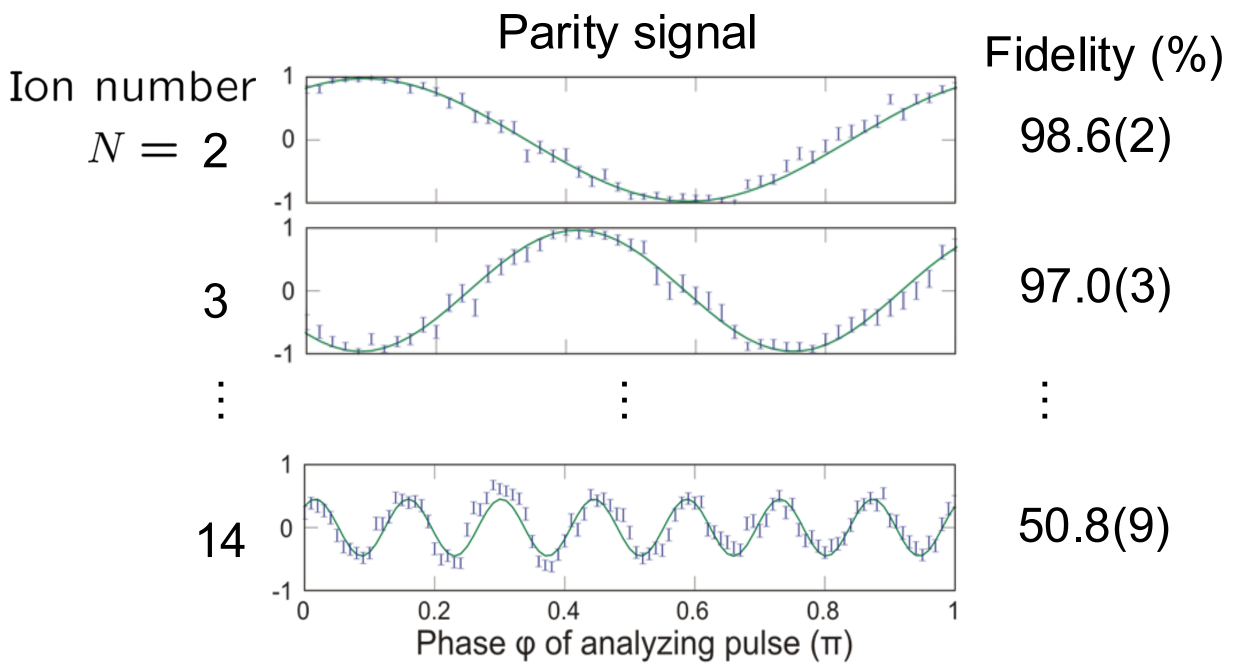

Typical gate operation time ≈ 50μs

14-qubit entangled state (GHZ):

$$|GHZ\rangle = \frac{1}{\sqrt{2}}(|11111111111111\rangle + |00000000000000\rangle)$$

14-qubit Hilbert space has 2^{14} dimensions → Full characterization of density matrix (state tomography) would require 55 days continuous measurement time. (at 1 measurement setting per second).

T. Monz et al., *Phys. Rev. Lett.* **106**, 130506 (2011); I. Pogorelov, et al., *PRX Quantum* 2, 020343 (2021).

Largest genuine Entanglement: Qubits in GHZ state

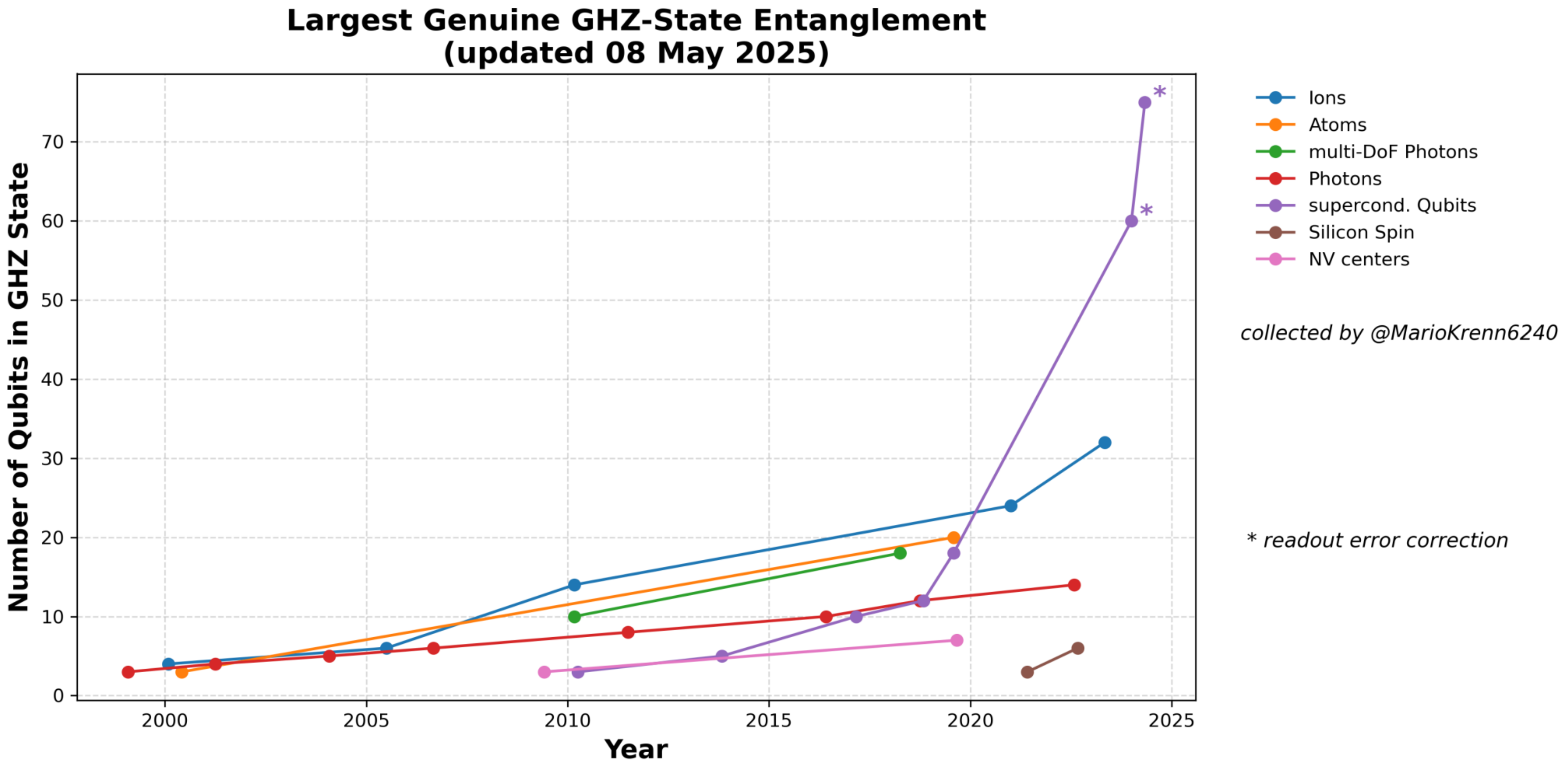

https://mariokrenn.wordpress.com/2021/01/29/reference-list-for-records-in-large-entanglement-generation-number-of-qubits-in-ghz-states/

Largest genuine Entanglement: Qubits in GHZ state

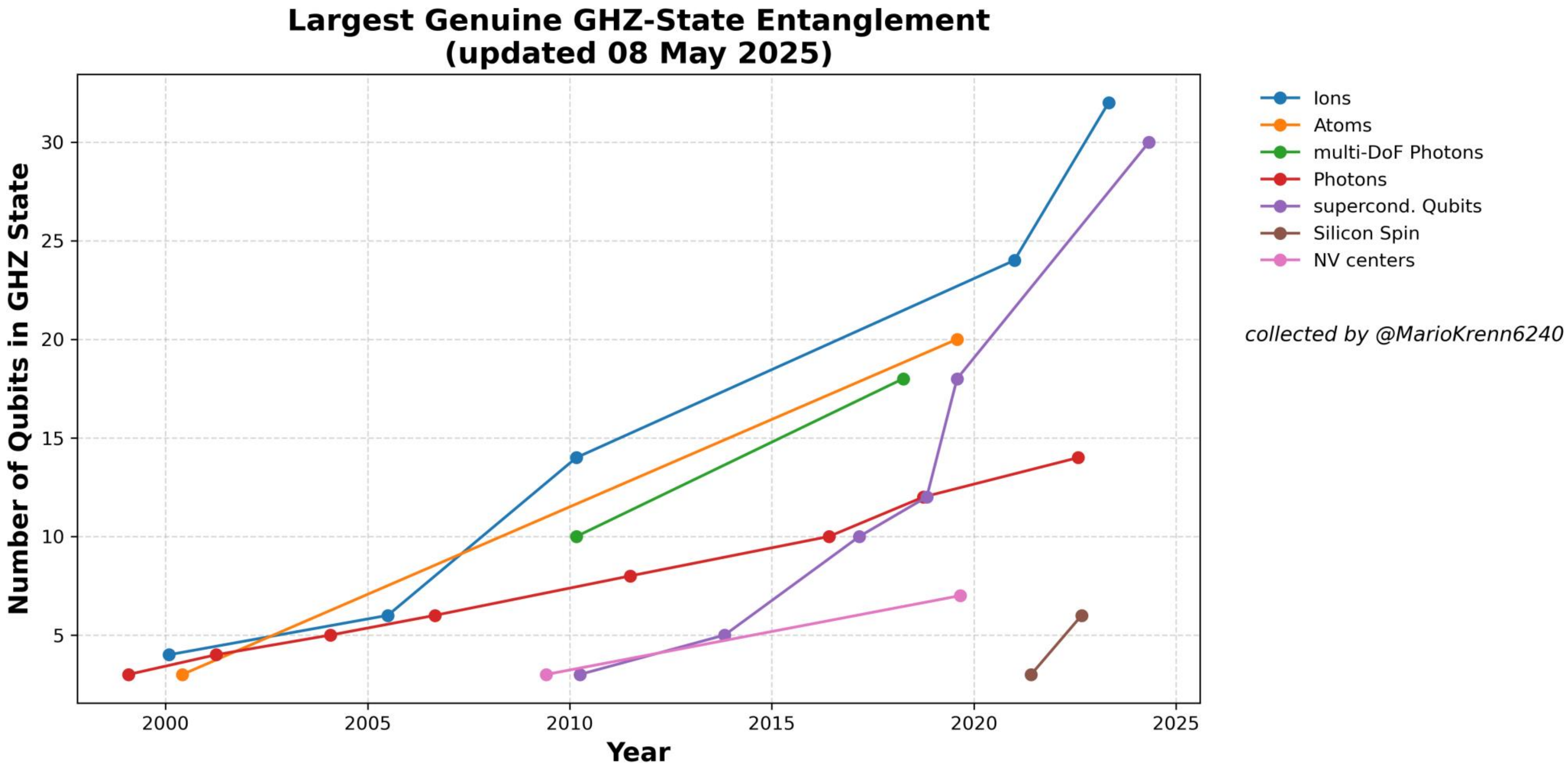

https://mariokrenn.wordpress.com/2021/01/29/reference-list-for-records-in-large-entanglement-generation-number-of-qubits-in-ghz-states/

Full set of gate operations.

It is possible to realize arbitrary unitary operations (=arbitrary calculations) with the following laser pulses…

Basic set of operations:

individual light shift gates	$\sigma_z^{(0)}, \sigma_z^{(1)}, \sigma_z^{(2)}$
collective spin flips	S_x, S_y
Mølmer-Sørensen gate	S_x^2

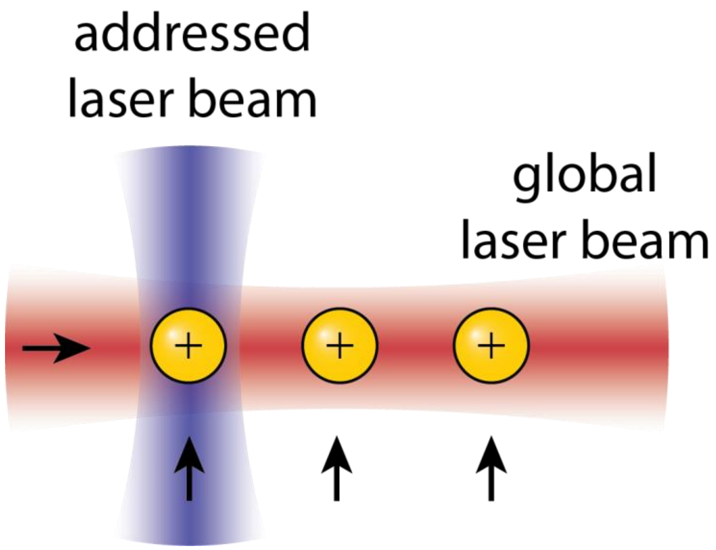

= Full set of quantum operations.

Toolbox of quantum operations

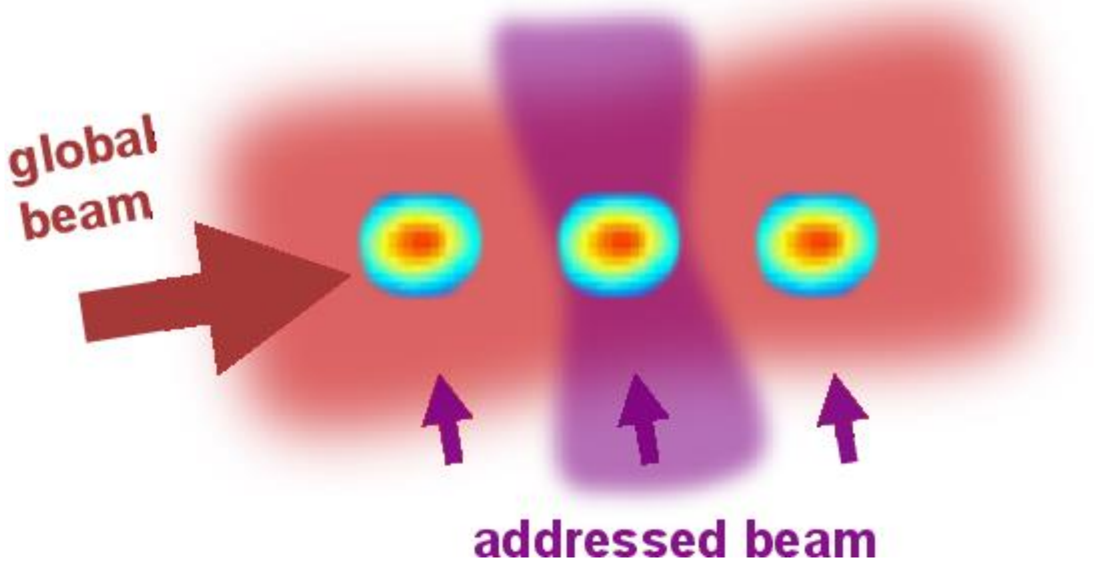

Toolbox: The global laser beam rotates all ions simultaneously around x or y.

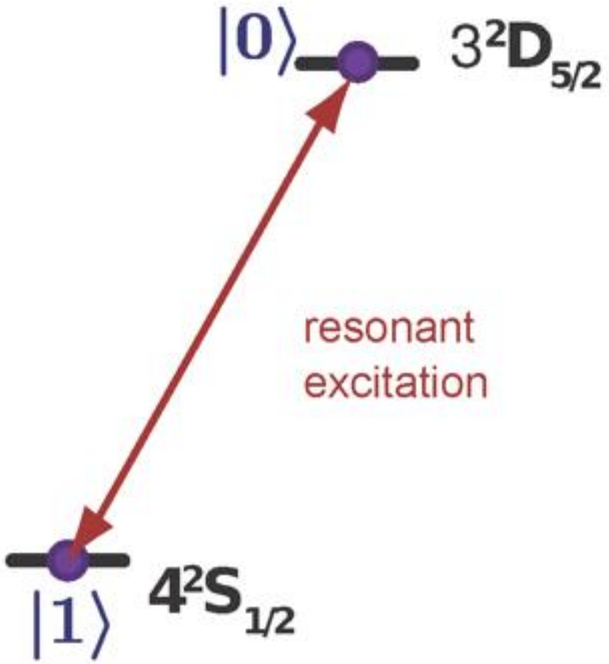

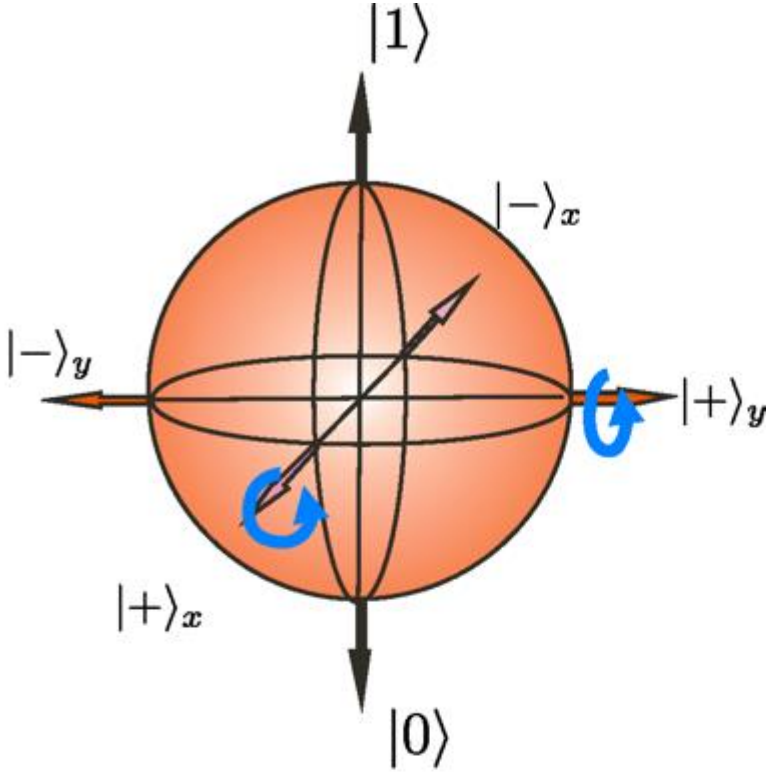

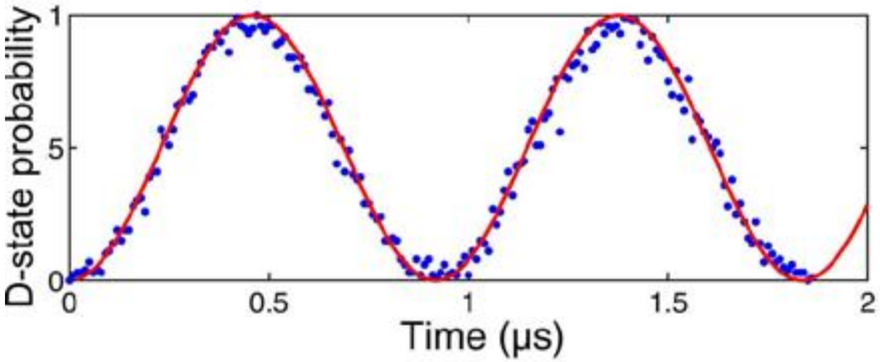

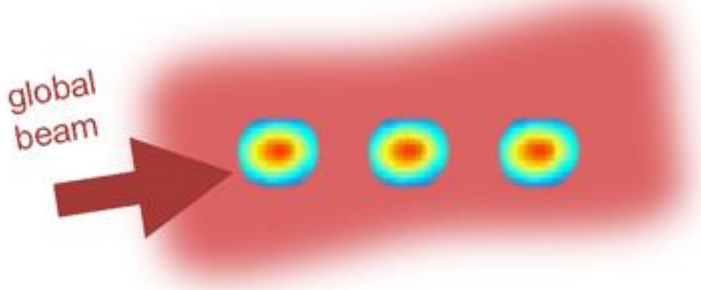

Toolbox: The addressed laser beam rotates this ion around z.

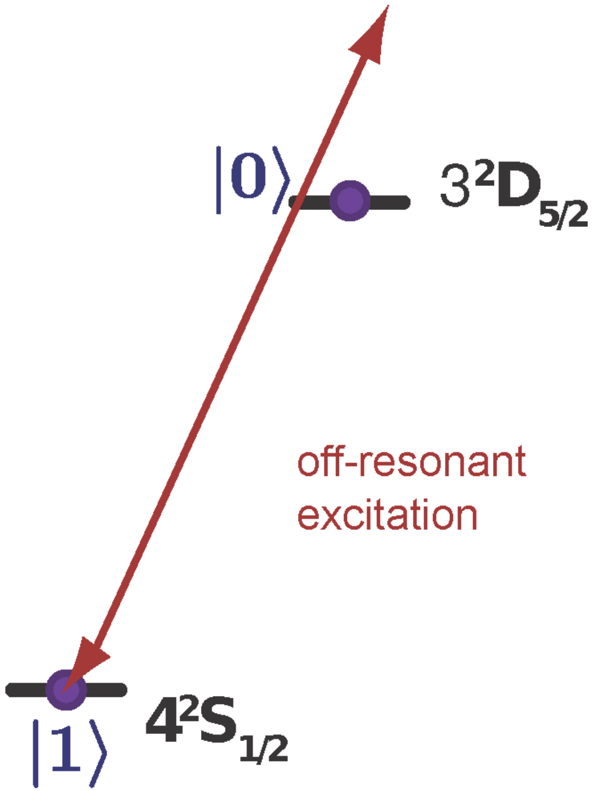

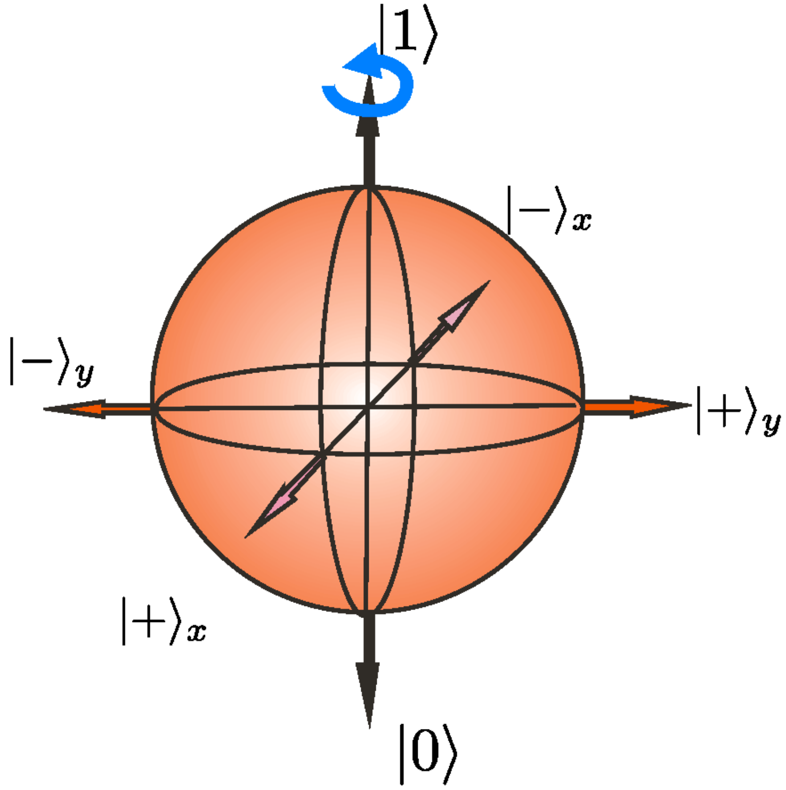

AC-Stark shift causes detuning

Causes rotation around z-axis

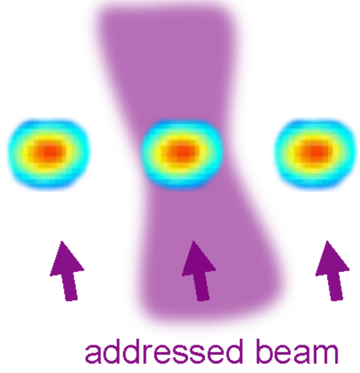

The global Mølmer-Sørensen operation couples ions pairwise.

Mølmer Sørensen entangling gate

Can be interpreted as rotations
on a "super-Bloch sphere“

Works for any number of qubits

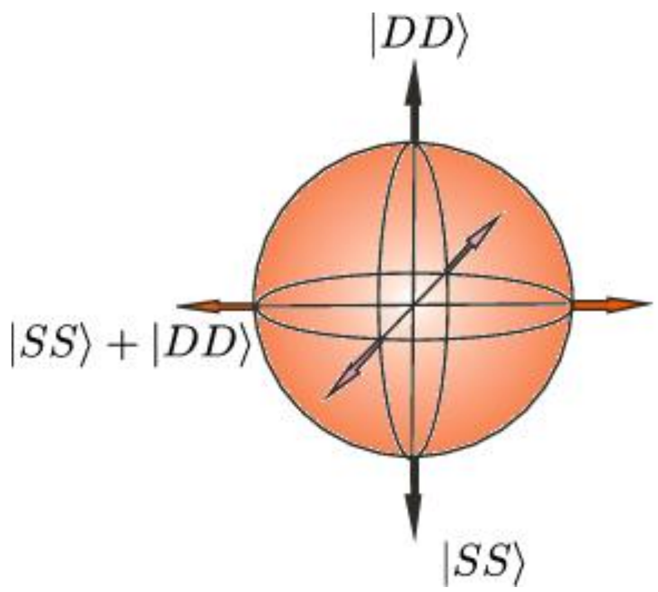

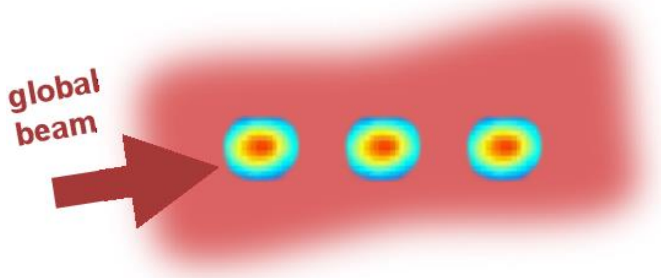

K. Mølmer and A. Sørensen, PRL 82, 1835 (1999).

Together a toolbox for arbitrary unitary operations

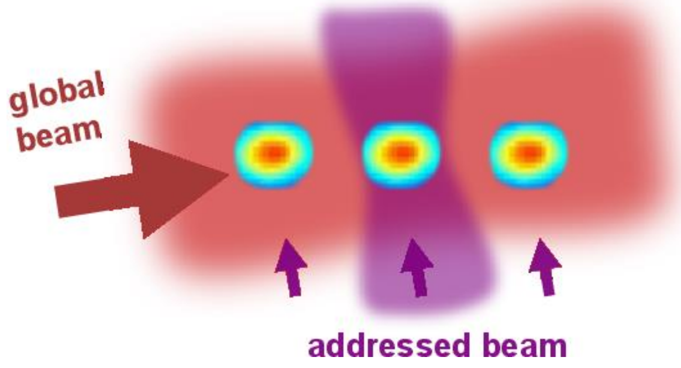

Basic set of operations:

collective spin flips S_x, S_y

individual light shift gates $\sigma_z^{(0)}, \sigma_z^{(1)}, \sigma_z^{(2)}$

Mølmer-Sørensen gate S_x^2

Arbitrary unitary operations can be achieved !

Application examples

What is Quantum Simulation?

- Classical computers struggle with exponential complexity of quantum systems

  Schödinger equation:

$$i\hbar\frac{d}{dt}|\Psi(t)\rangle = \hat{H}|\Psi(t)\rangle$$

  Or formally unitary transformation:

$$|\Psi(t)\rangle = e^{-i\hat{H}t/\hbar}|\Psi(0)\rangle$$

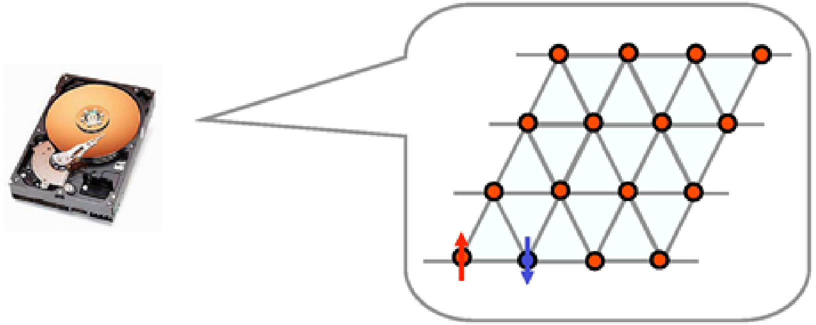

- Feynman: Simulating quantum systems using other controllable quantum devices.

Quantum simulations of magnetism

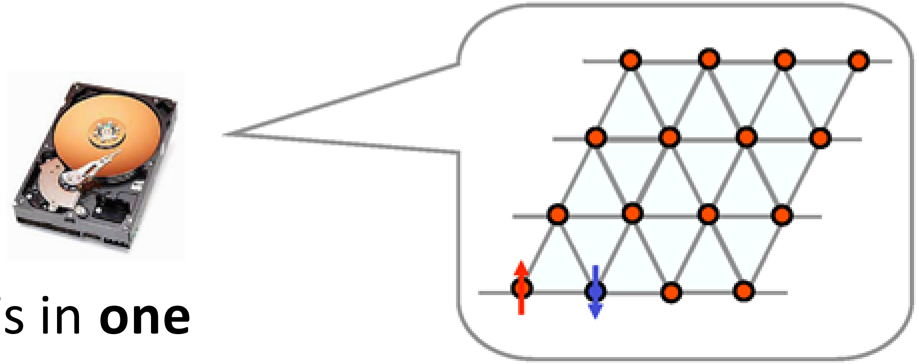

Classical physics: system is in **one** of many possible configurations

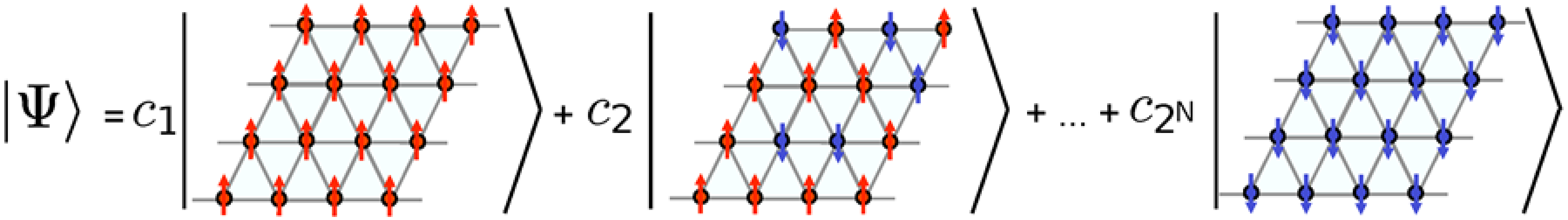

Quantum physics: system can be in a **superposition** of configurations

How to model the Hamiltonian of the simulated system?

Analog vs Digital Quantum Simulations

- Analog: Continuous evolution

$$i\hbar \frac{d}{dt}|\Psi(t)\rangle = \hat{H}|\Psi(t)\rangle$$

- Digital: Gate-based, discrete steps

$$|\Psi(t)\rangle = e^{-i\hat{H}t/\hbar}|\Psi(0)\rangle = U_n \cdots U_2 U_1 |\Psi(0)\rangle$$

An analogue quantum simulator imitates the system.

NMR (Somaroo et al.)

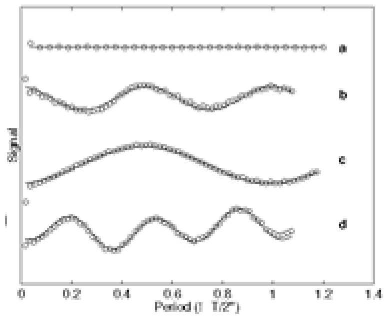

Trapped ions
(Schaetz, Monroe, …)

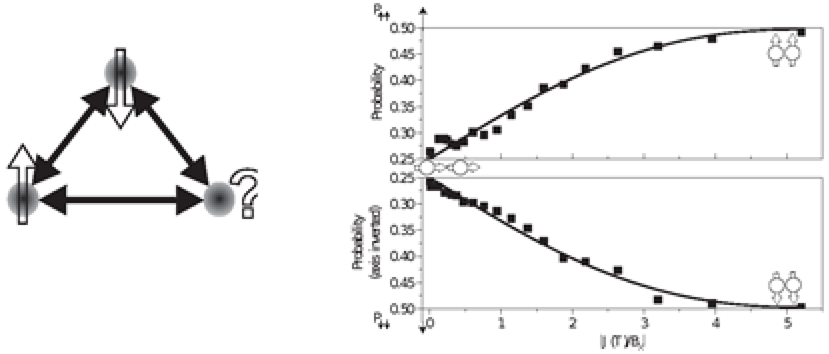

Cold atoms
(Bloch, Greiner, …)

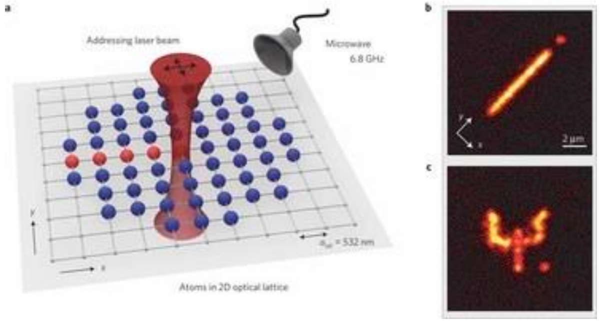

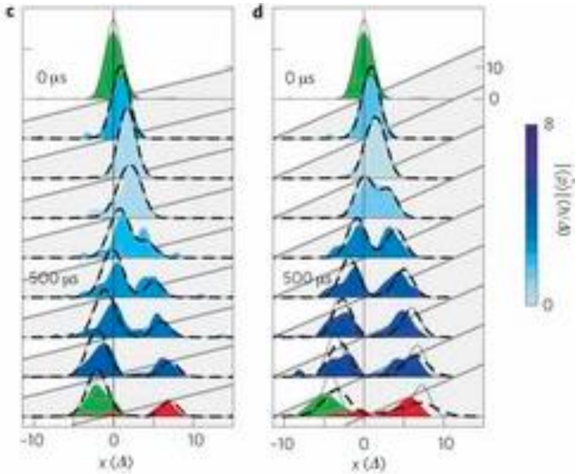

Simulator has same Hamiltonian as system of interest.

A calculation on a quantum computer usually consists of a sequence of unitary, reversible operations.

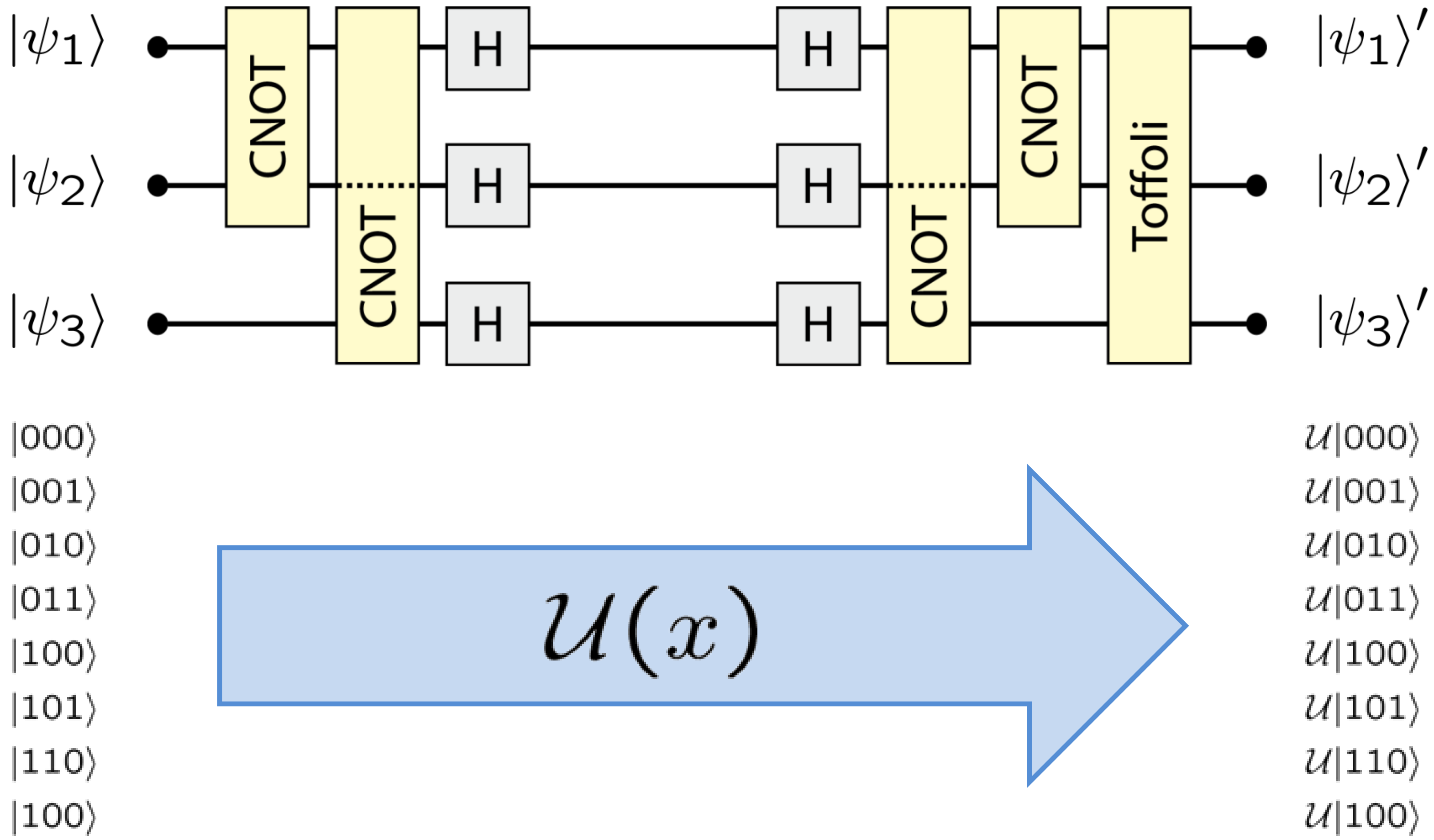

Digital quantum simulation = sequence of gates: $|\Psi(t)\rangle = e^{-i\hat{H}t/\hbar}|\Psi(0)\rangle = U_n \cdots U_2 U_1 |\Psi(0)\rangle$

A digital quantum simulator can perform universal simulations.

Main idea: Approximate a complex unitary time evolution $U(t)$ by a stroboscopic sequence of gates

$$U(t) = e^{iHt/\hbar} = e^{iH\Delta t_n/\hbar} \dots e^{iH\Delta t_1/\hbar}$$

with $H = H_1 + H_2$

$$e^{iH\Delta t/\hbar} \approx e^{iH_1\Delta t/\hbar} \cdot e^{iH_2\Delta t/\hbar} \cdot e^{(\Delta t/\hbar)^2[H_1,H_2]/2}$$

Neglect non-commuting term

Baker–Campbell–Hausdorff formula

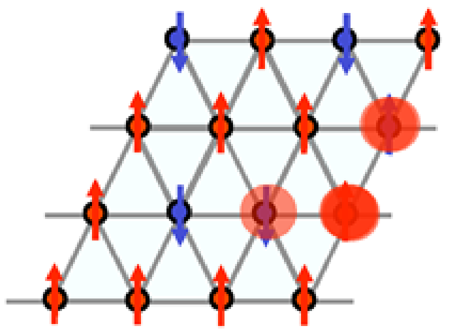

S. Loyd (1996)

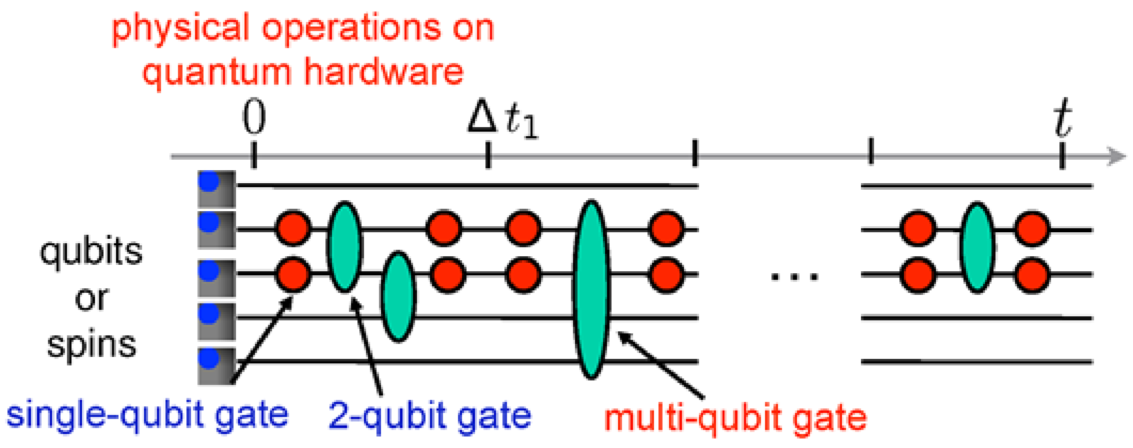

Digital quantum simulator: The Trotterization error can be suppressed by small time steps.

Ising model with two spins

Magnetic field (z)

$$H_1 = B\left(\sigma_z^{(1)} + \sigma_z^{(2)}\right)$$

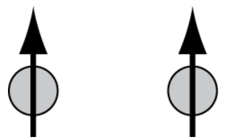

Ising interaction (x)

$$H_2 = J\ \sigma_x^{(1)}\sigma_x^{(2)}$$

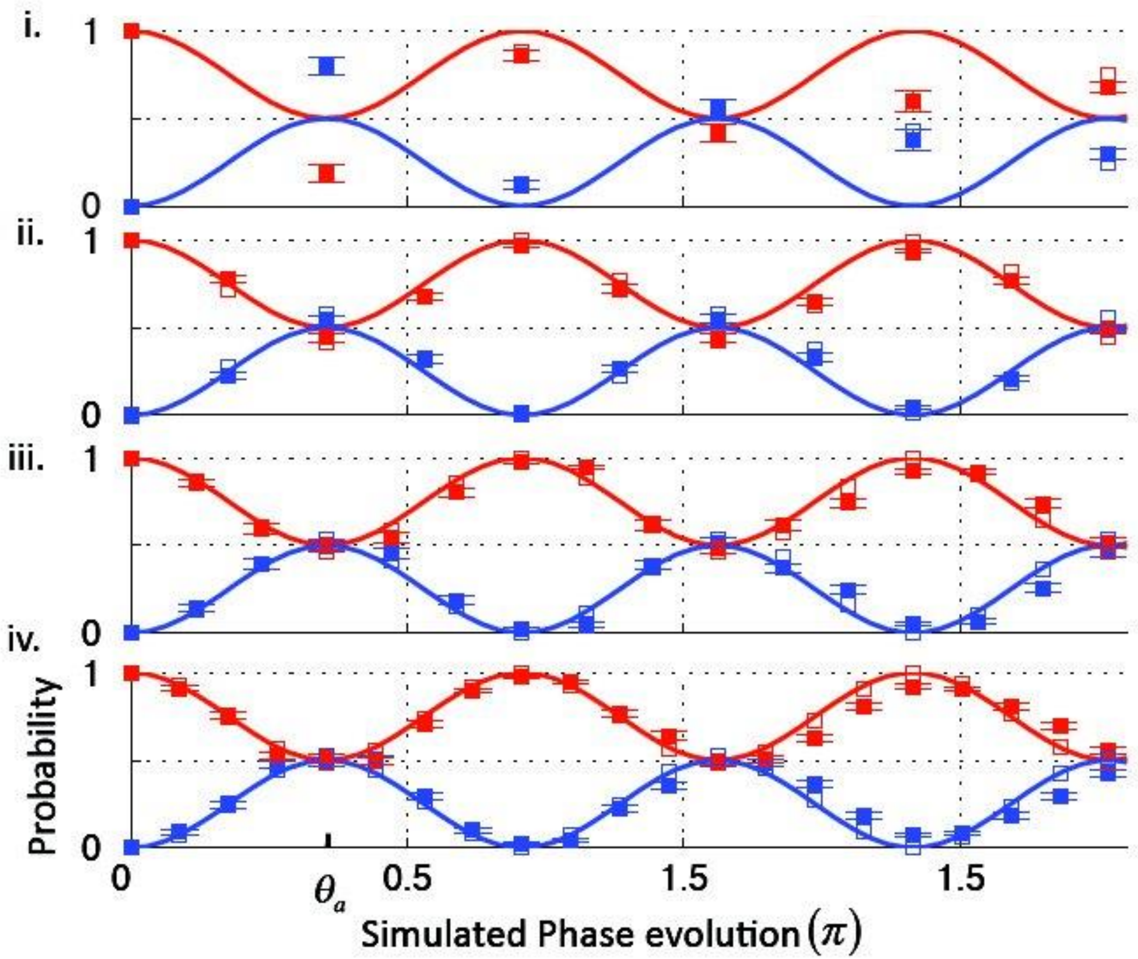

B. Lanyon et al., *Science* **334**, 57 (2011)

More complex systems

- Great flexibility with respect to interactions

- Building block of Heisenberg model

$$H = B\left(\sigma_z^1 + \sigma_z^2\right) + J_{xx}\sigma_x^1\sigma_x^2 + J_{yy}\sigma_y^1\sigma_y^2 + J_{zz}\sigma_z^1\sigma_z^2$$

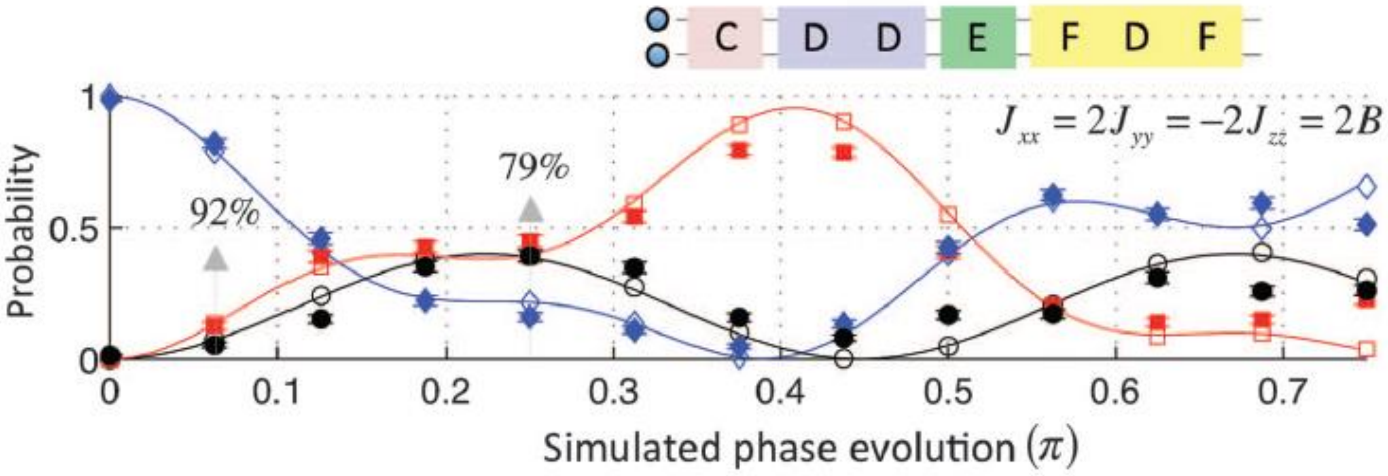

… up to 84 gates.

- Experiments with
  - up to 6 ions/spins
  - time-dependent and inhomogeneous couplings
  - many-body interactions

B. Lanyon et al., *Science* **334**, 57 (2011)

The dynamics of an open quantum system is described by the Master equation.

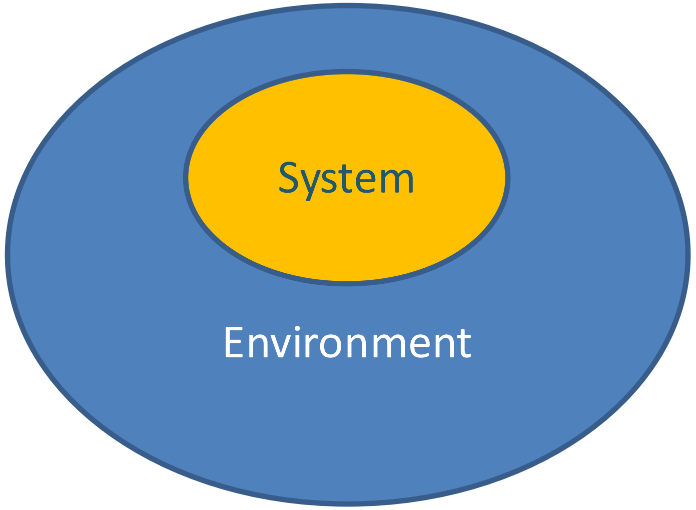

Master equation

$$\dot{\rho} = -\frac{i}{\hbar}[H, \rho] + \mathcal{L}(\rho) \qquad [H, \rho]=0$$

Only incoherent evolution

$$\dot{\rho} = \mathcal{L}(\rho) = \gamma(c\rho c^{\dagger} - \frac{1}{2}c^{\dagger}c\rho - \frac{1}{2}\rho c^{\dagger}c)$$

Example for an open quantum system: The spontaneous decay.

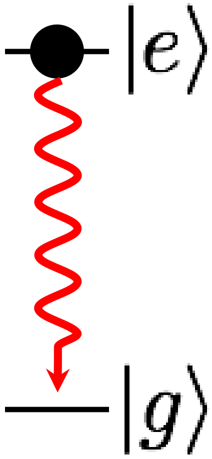

Master equation

$$\dot{\rho} = \mathcal{L}(\rho) = \gamma(c\rho c^\dagger - \frac{1}{2}c^\dagger c\rho - \frac{1}{2}\rho c^\dagger c)$$

Example: Spontaneous emission

Jump operator $c = |g\rangle\langle e|$

Action $c|g\rangle = 0$

$c|e\rangle = |g\rangle$

Dark state is $|g\rangle$.

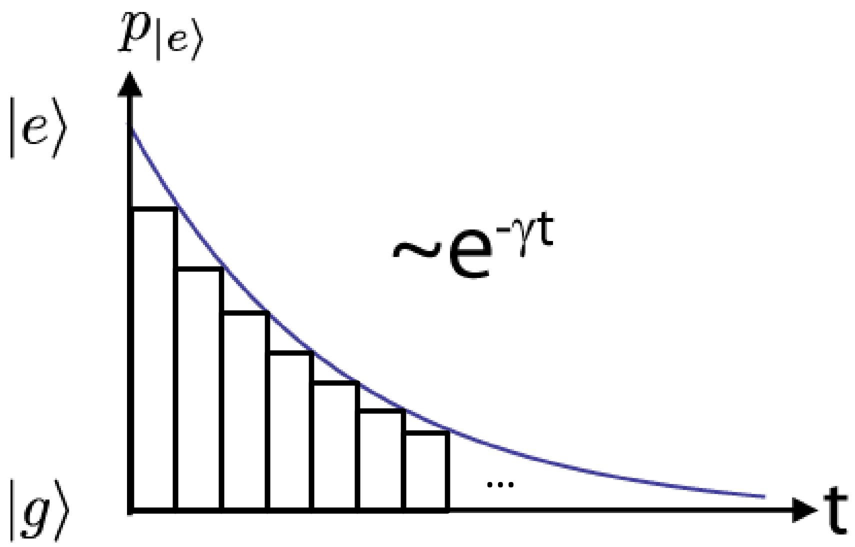

One can engineer a multi-qubit environment that maps two qubits into an entangled state.

Two-body jump operator

$$c = \frac{1}{2}\sigma_1^x(1 - \sigma_1^z\sigma_2^z)$$

Dark state is

$$c|\psi^-\rangle = 0$$

$$c|\phi^-\rangle = |\psi^-\rangle$$

Bell state pumping

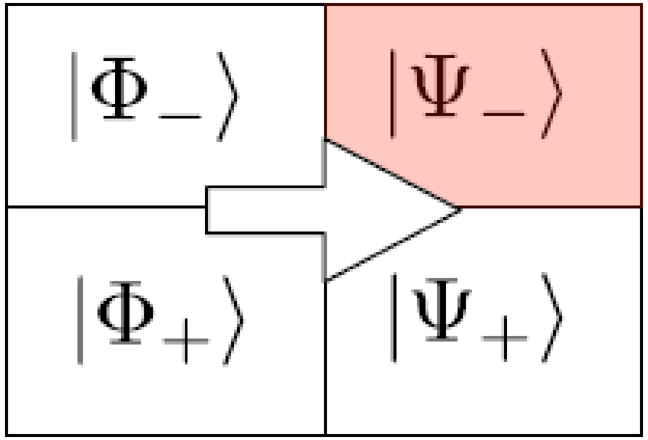

J.T. Barreiro, M. Müller, et al., *Nature* **470**, 486-491 (2011).

Engineering a multi-qubit environment

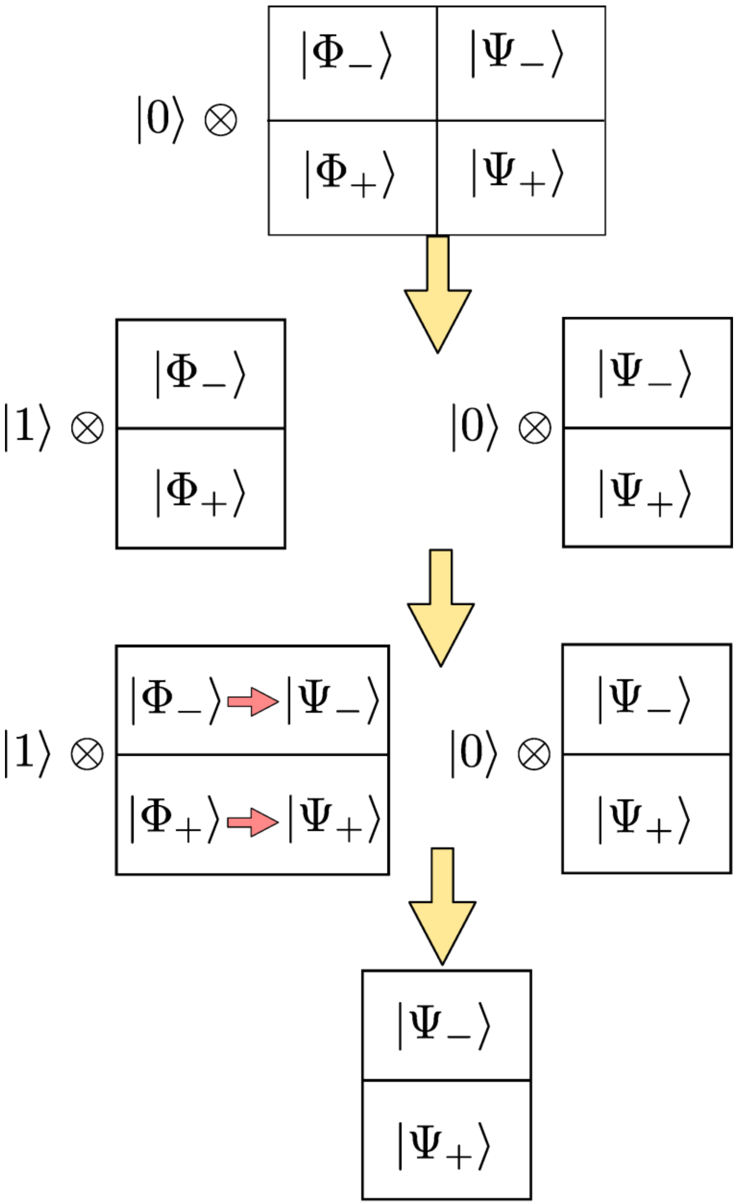

Use an ancilla to engineer the environment

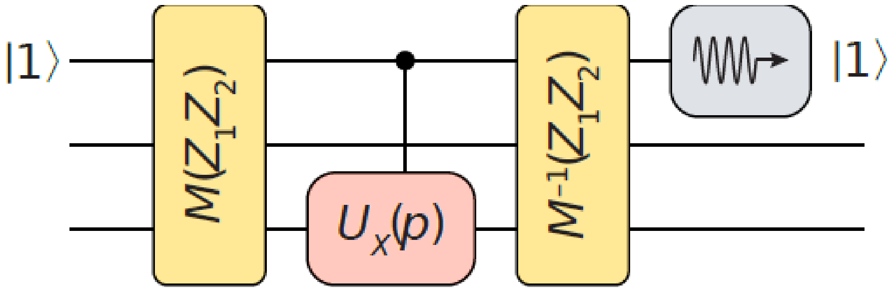

- Map information of |Ái /|Ãi onto the ancilla.
- Controlled rotation on the system qubits
- Undo the mapping
- Reset the ancilla

The engineered environment pumps two qubits from a mixed state to a entangled Bell state.

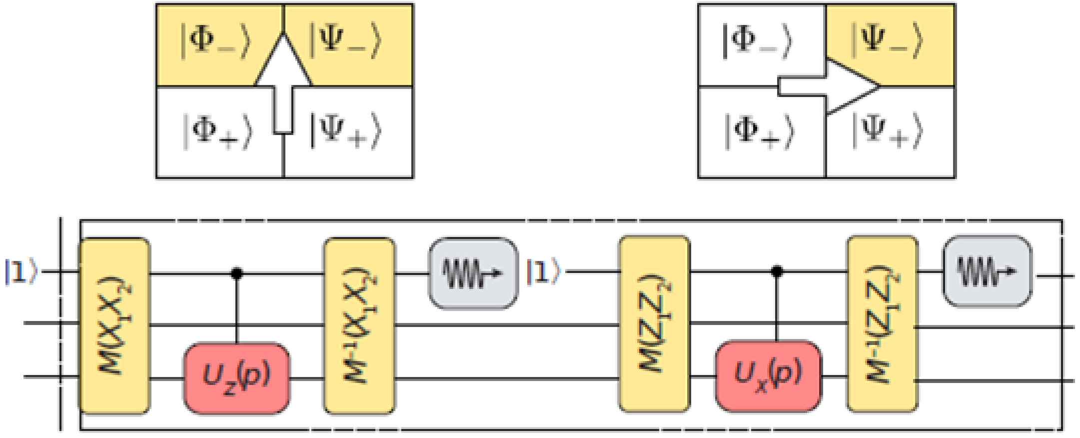

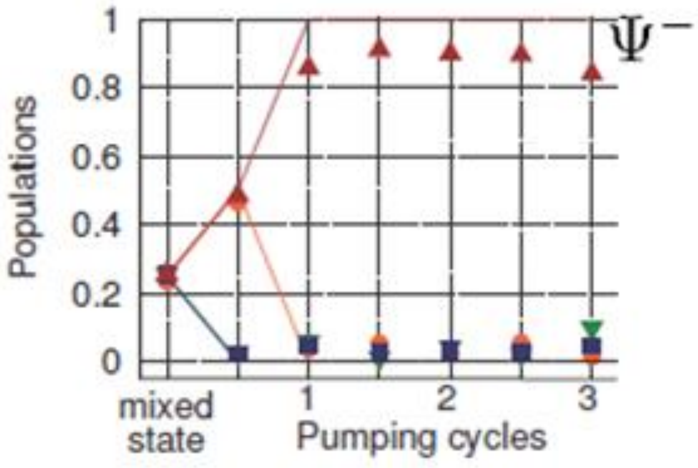

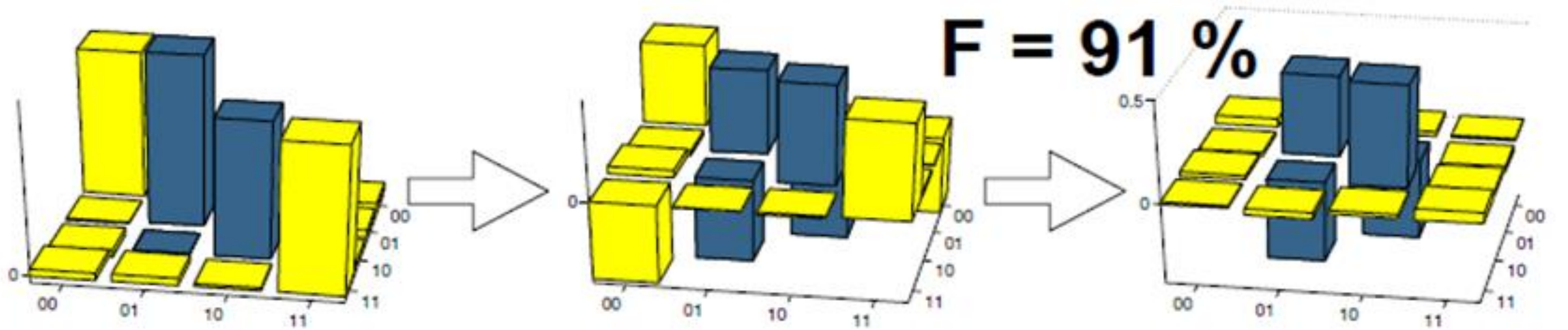

J.T. Barreiro et al., *Nature* **470**, 486-491 (2011).

Application: Factorization of the number 15 with 5 trapped ion qubits.

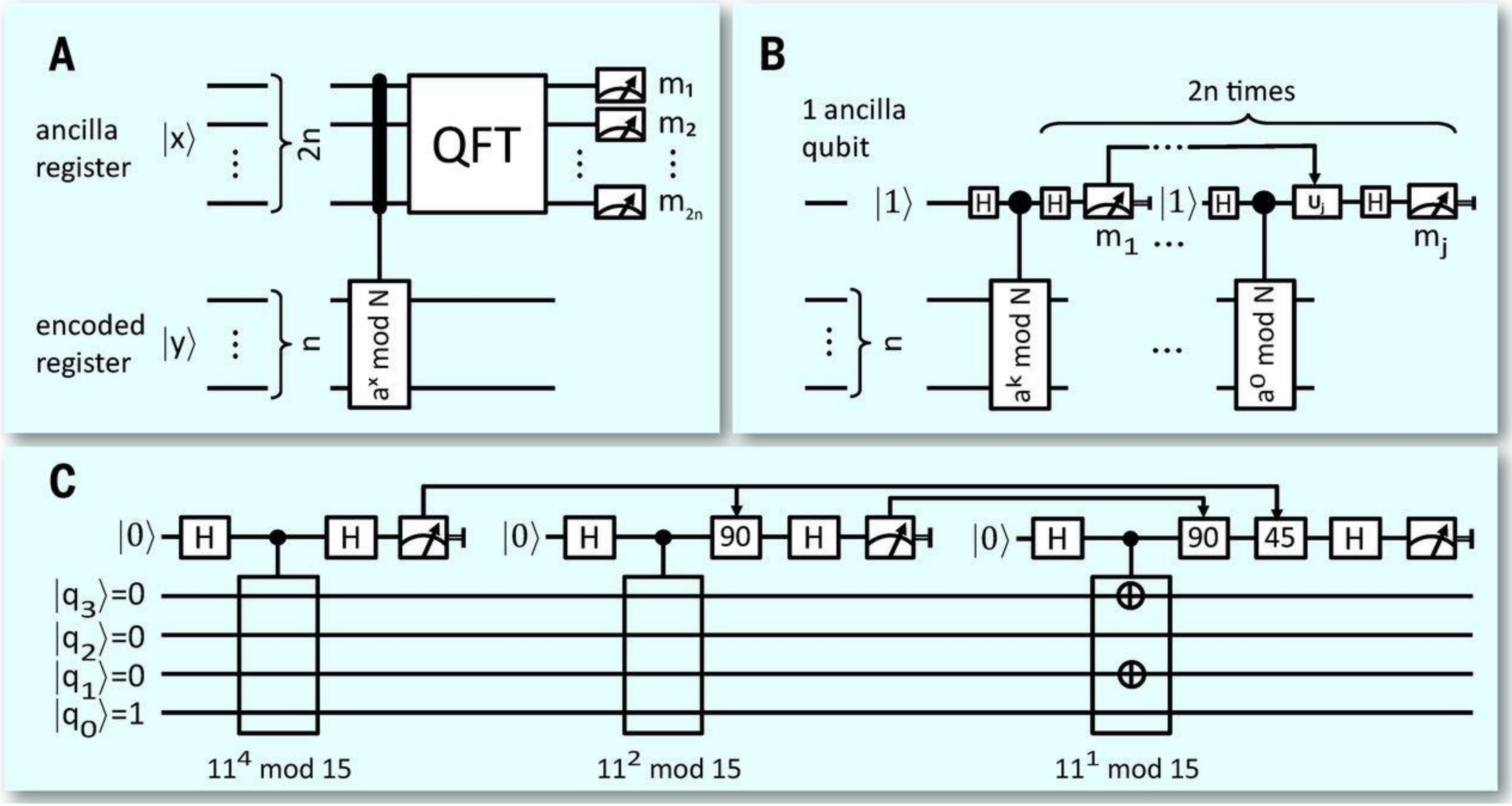

T. Monz et al., Science 351, 1068 (2016).

Application: Factorization of the number 15 with 5 trapped ion qubits.

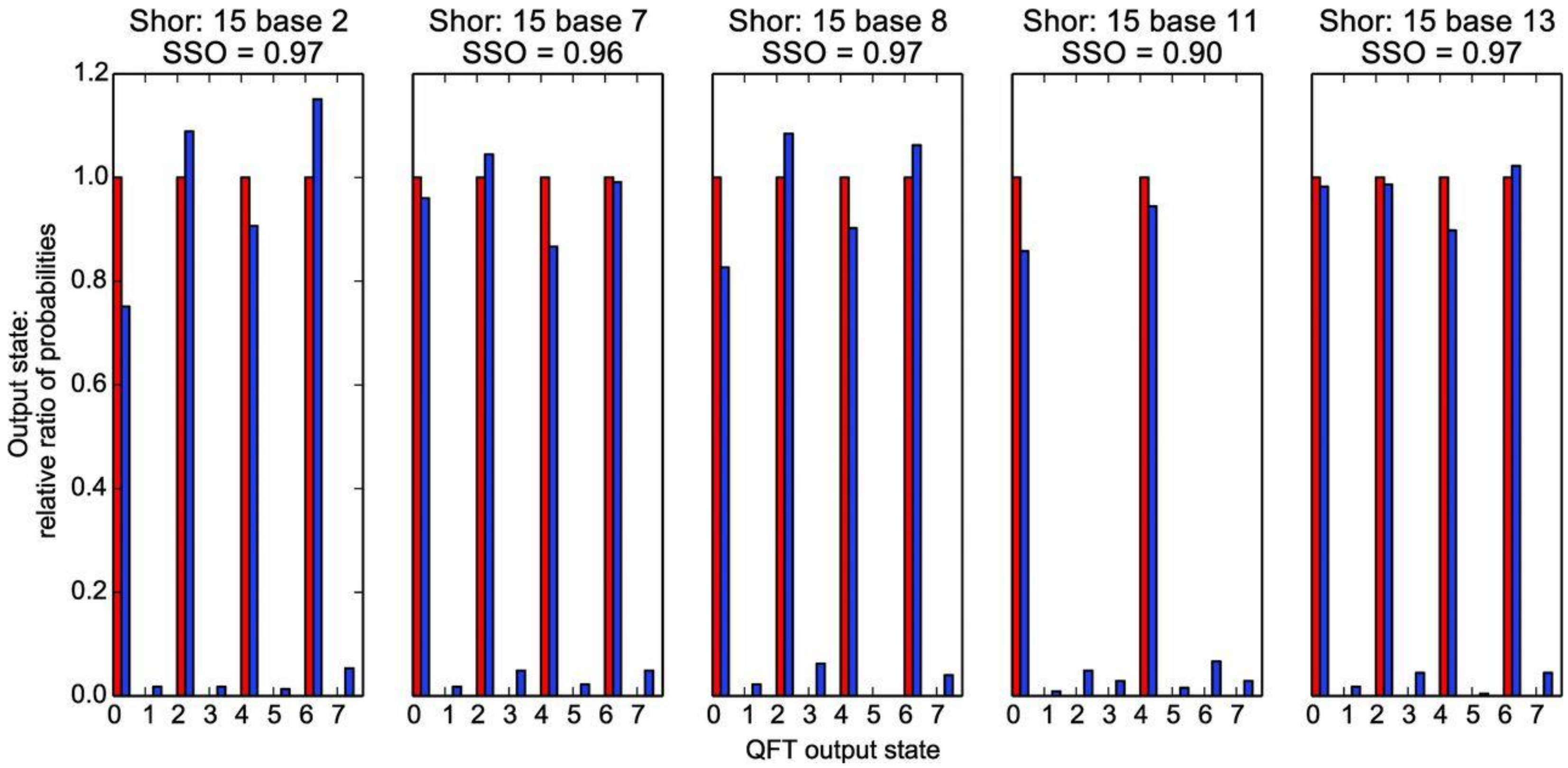

T. Monz et al., Science 351, 1068 (2016).

Ion trap quantum computing research groups and companies

Research groups:

- Innsbruck, Austria
- Stockholm, Sweden
- Oxford, UK
- Mainz, Germany
- ETH Zürich, Switzerland
- Sussex, UK
- Maryland, USA
- NIST, USA
- Berkeley, USA
- MIT LL, USA
- Tsinghua, China
- Duke Univ., USA
- Seoul, Korea
- Sydney, Australia
- UCLA, USA

Trapped ion QC companies:

AQT
infineon
IONQ
QUANTINUUM
QUDORA TECHNOLOGIES
Universal Quantum
eleQtron
OXFORD IONICS
NEQxT
Quantum Art

For a more complete list and map,
see https://qtech.fysik.su.se/links.html

From research lab to commercial product

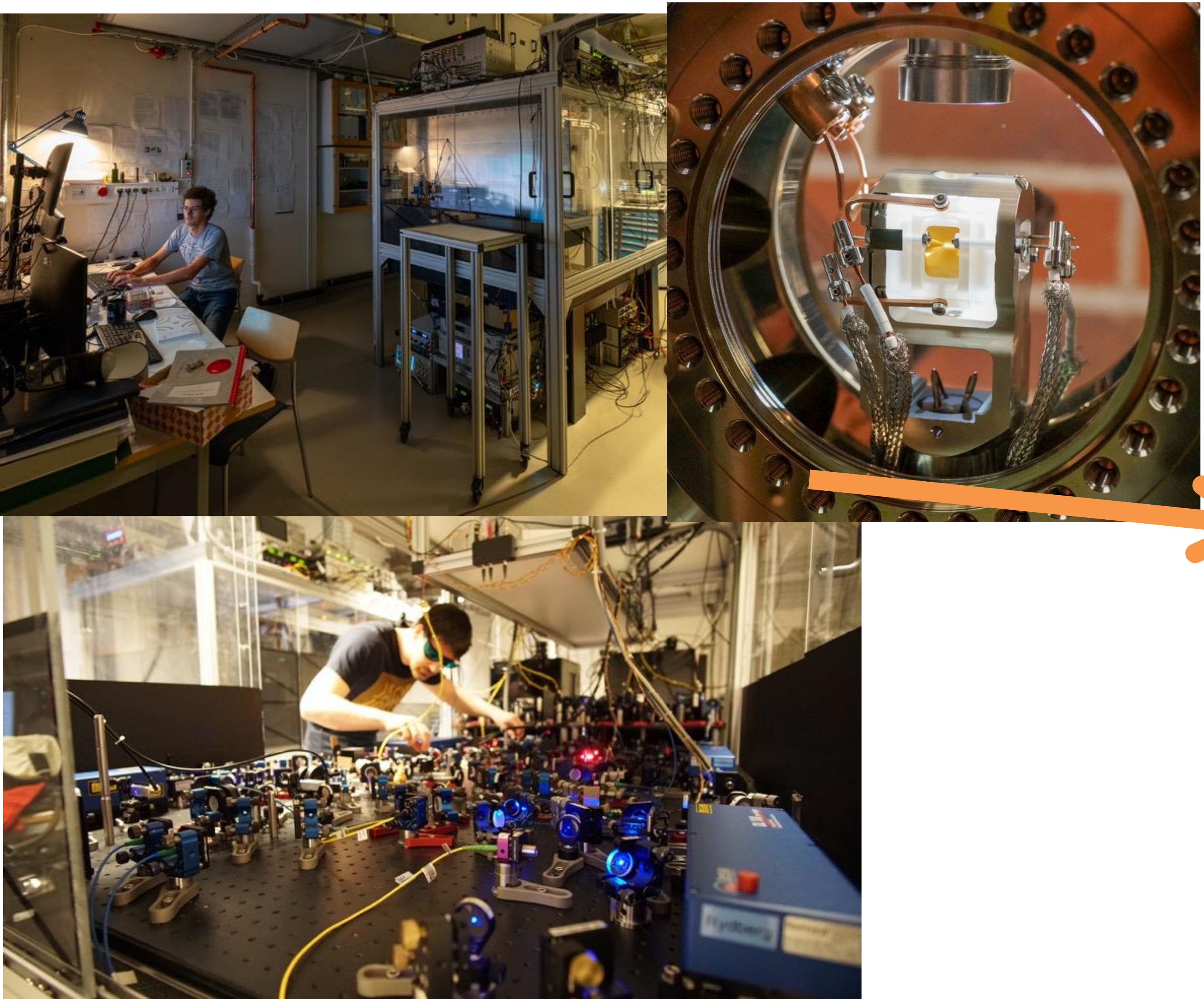

Trapped ions feature high gate fidelities, long coherence and trapping times.

State-of-the-art:

- Individual rotation of >70 ion qubits
- 24-ion entanglement
- Quantum simulations with >50 ions
- All gate errors $<10^{-3}$

- Standard entangling gates are rather slow (~50 µs/gate)

- Fast entangling gates?
- Larger ion crystals?
- Better scalability?

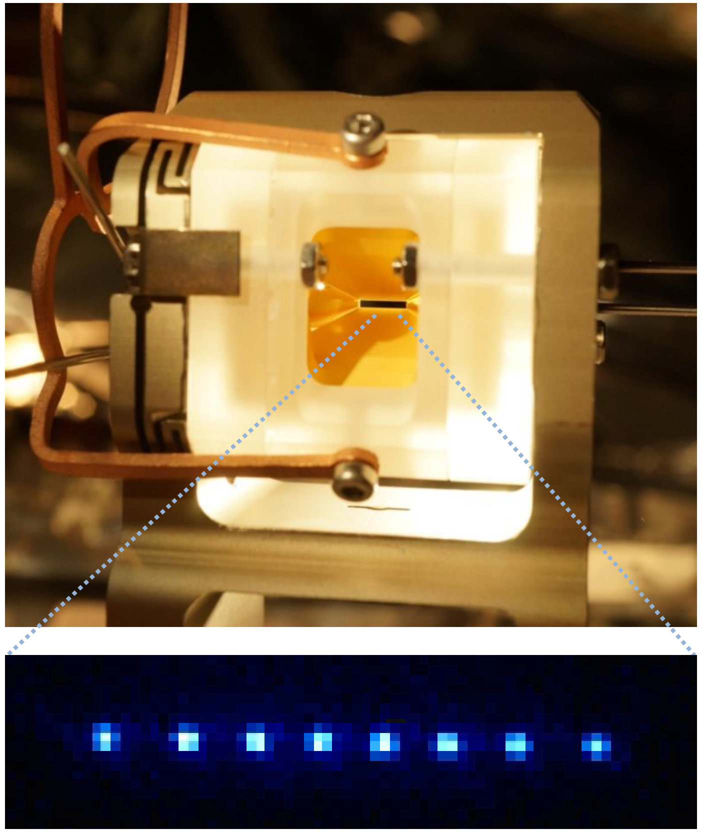

Scalability of trapped ion technology

Idea of a scalable ion trap architecture (CCD)

(ideas pioneered by D. Wineland, NIST)

Segmented trap electrode allow to transport ions and to split ion strings

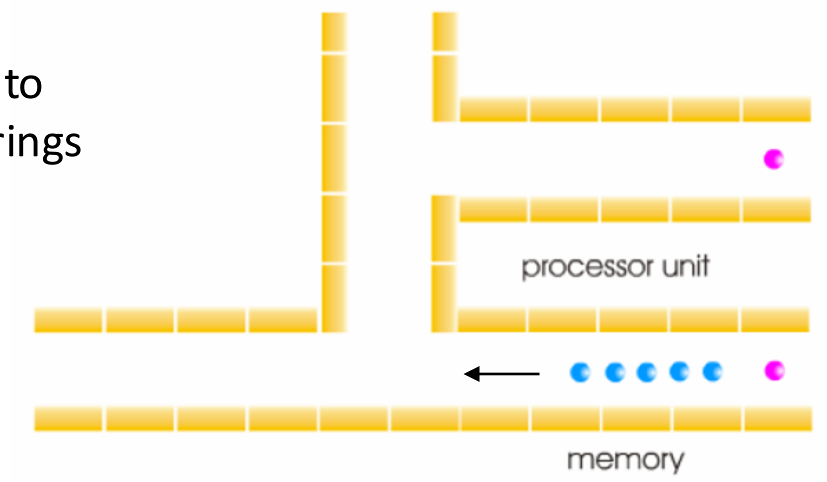

State of the art:

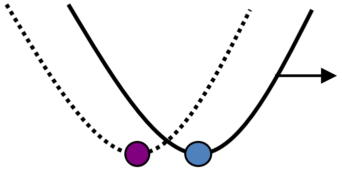

<u>Transport of ions</u>

1 mm within 50 µs

no motional heating

<u>Splitting of two-ion crystal</u>

$t_{separation} \approx 200\ \mu s$

small heating n ≈1

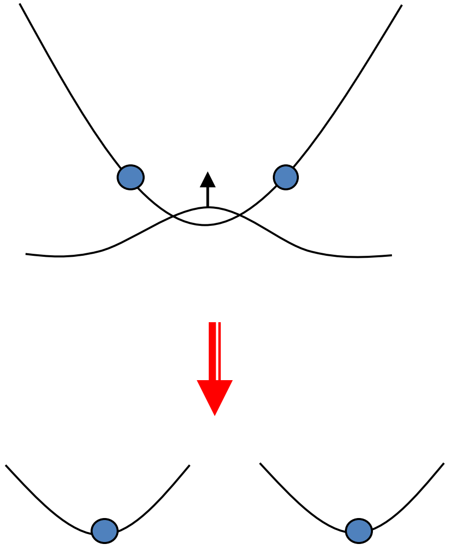

„Architecture for a large-scale ion-trap quantum computer“, D. Kielpinski et al, Nature 417, 709 (2002)

„Transport of quantum states“, M. Rowe et al, quant-ph/0205084

Scalability: Ion traps on chip

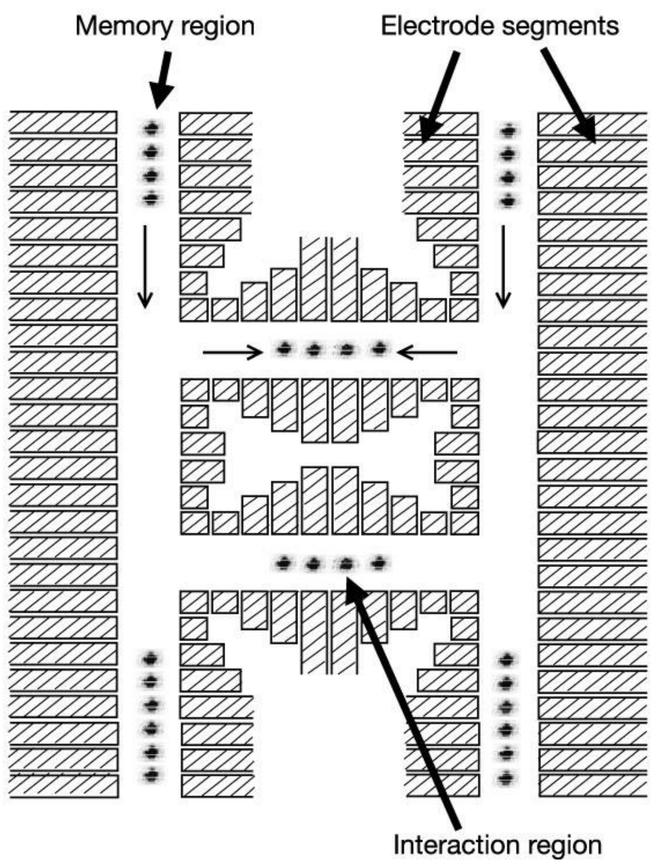

D. Kielpinski, et al., Nature 417, 709-711 (2002).

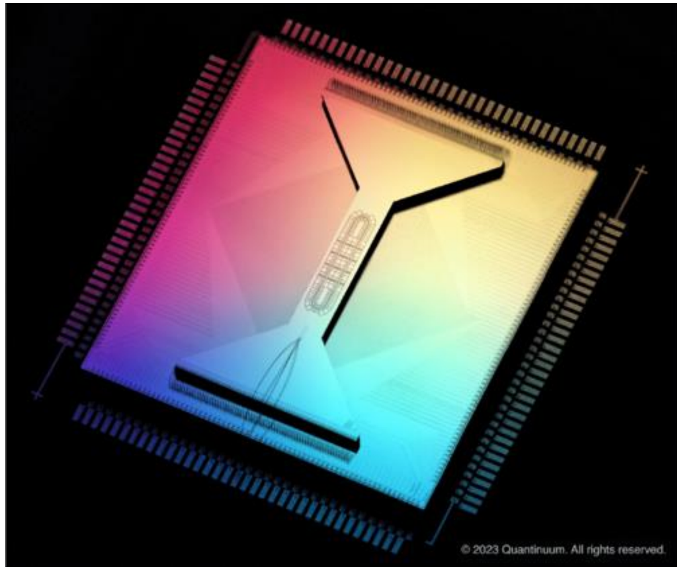

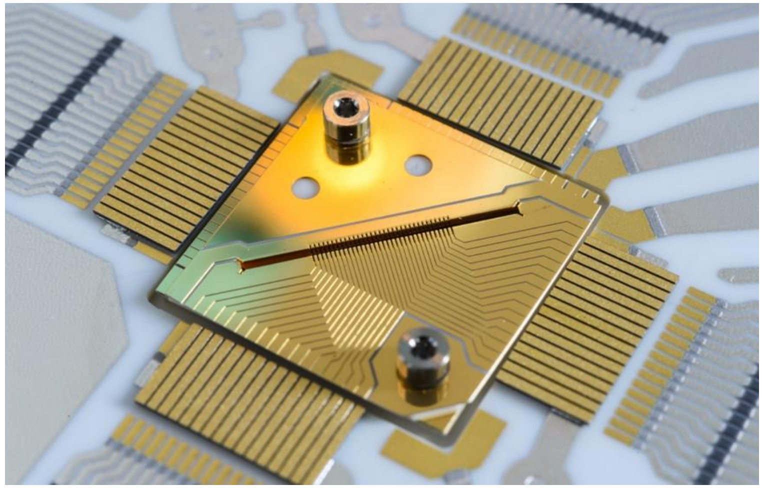

QUANTINUUM

S. A. Moses *et al.*, Phys. Rev. X 13, 041052 (2023)

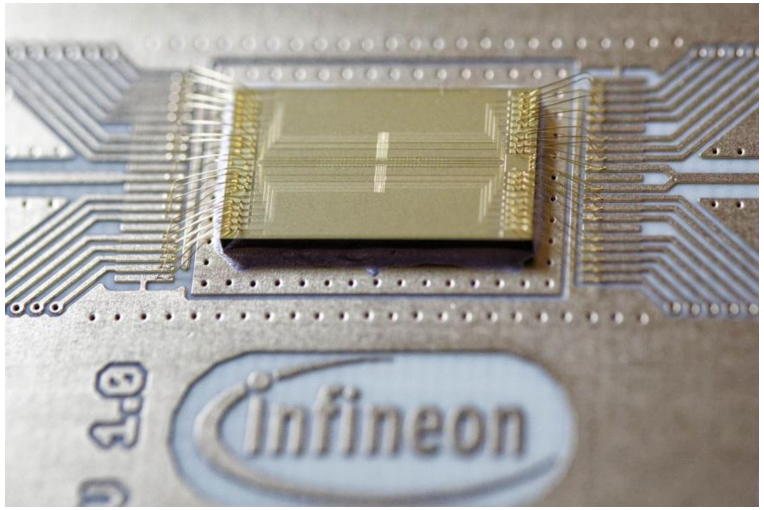

infineon

NEXT

Chip ion traps:

- Different regions which act as processing, memory, or readout unit
- Ions can be moved around on the chip between different functional units

Integrate trapped ion quantum memory with integrated optics & waveguide structures

- Combine advanced QC system of trapped ion with efficient photonic interface
- Integration of atomic/ionic quantum memories in chips

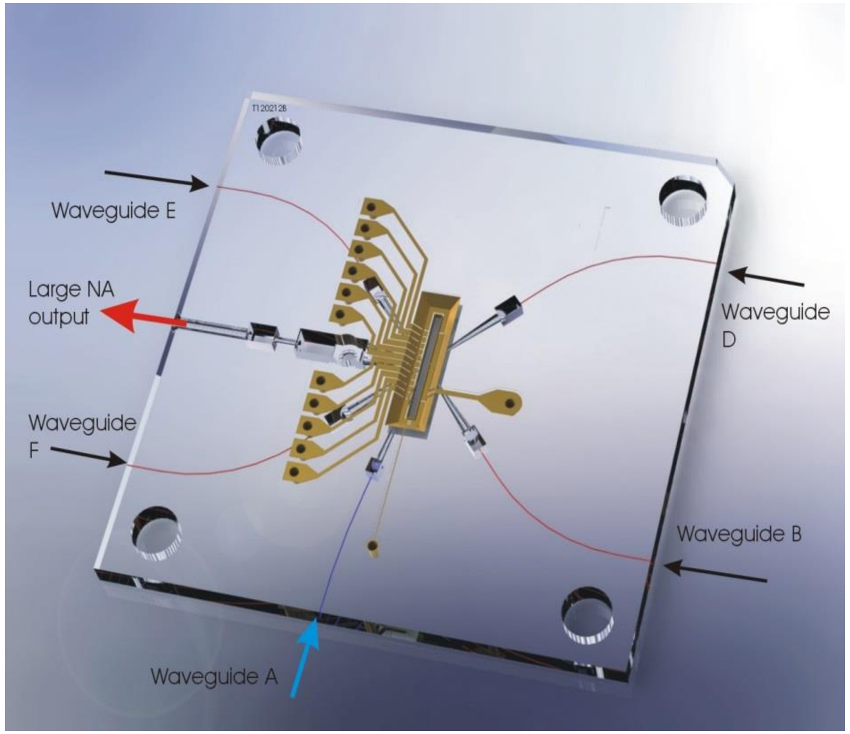

Chip-integrated optics

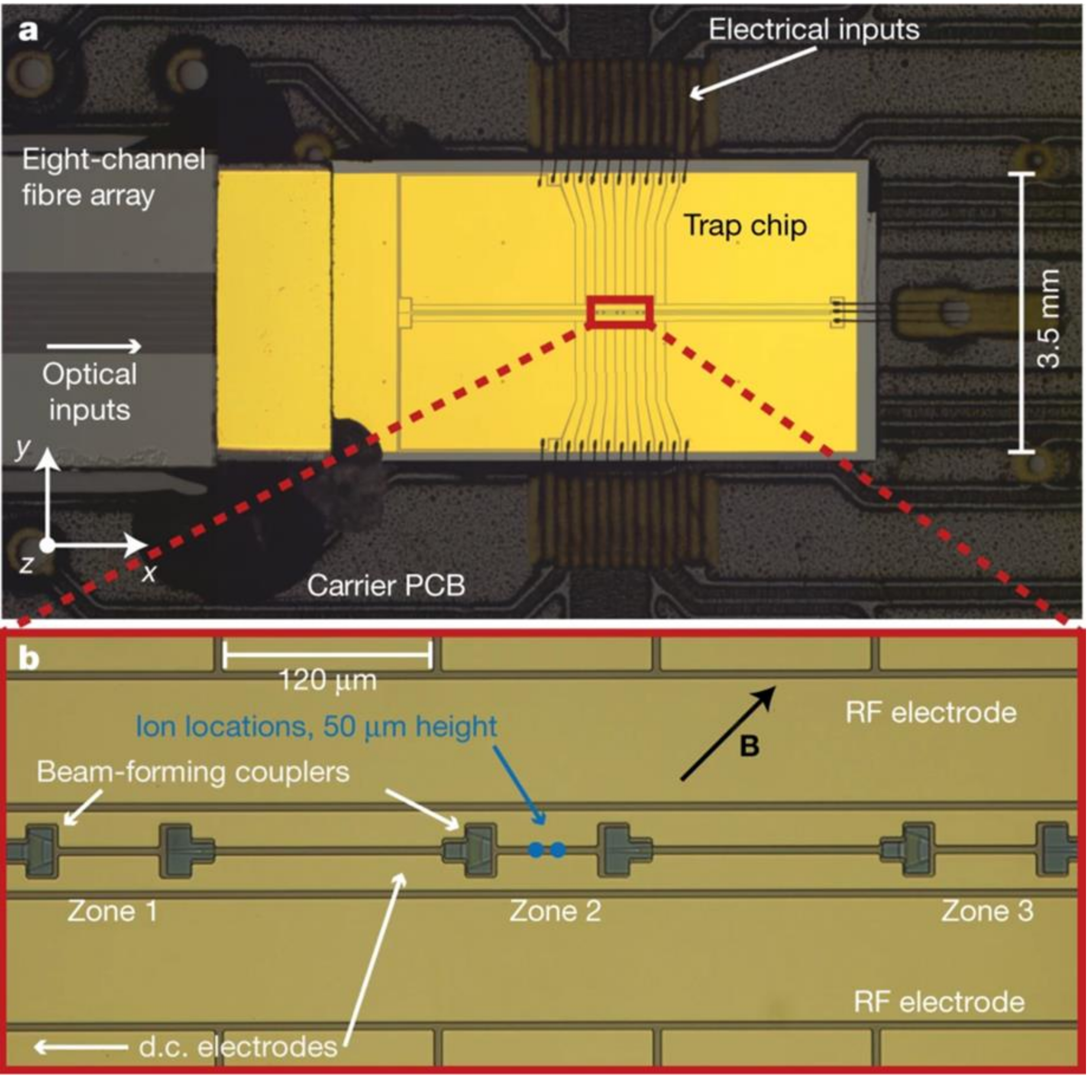

ETH Zurich,
K. K. Mehta, et al., Nature 586, 533-537 (2020)

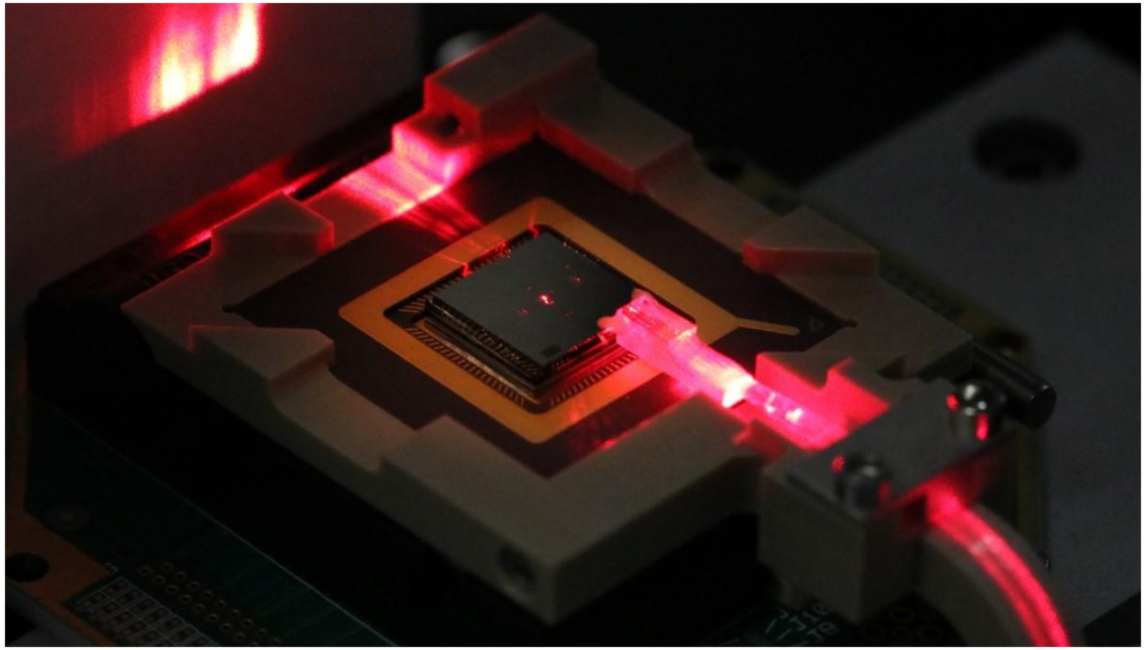

MIT Lincoln Laboratory
Niffenegger, et al., Nature 586, 538–542 (2020).

Coulomb-mediated coupling between ions in nearby trapping wells

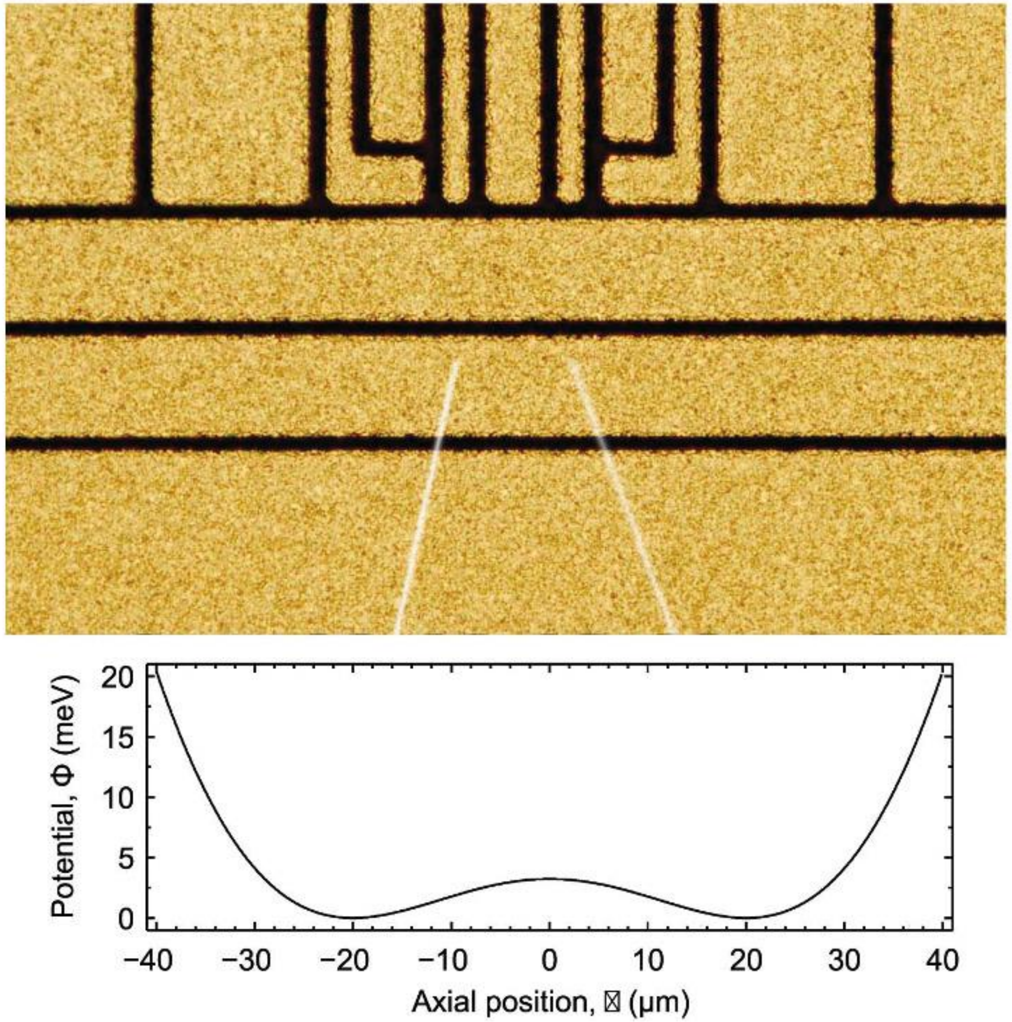

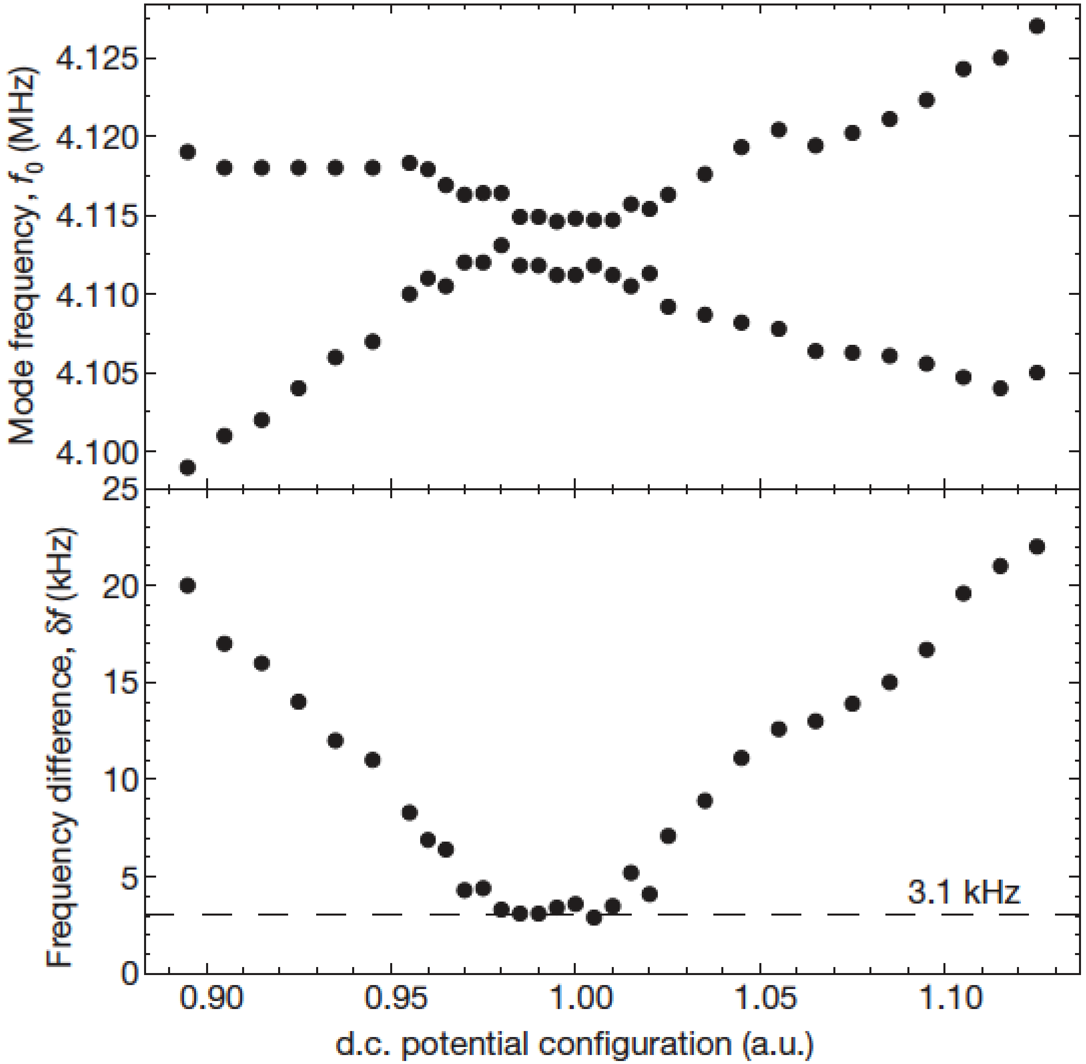

K. R. Brown, et al., *Nature* **471**, 196–199 (2011).
M. Harlander, et al., *Nature* **471**, 200–203 (2011).

2D array of coupled ions

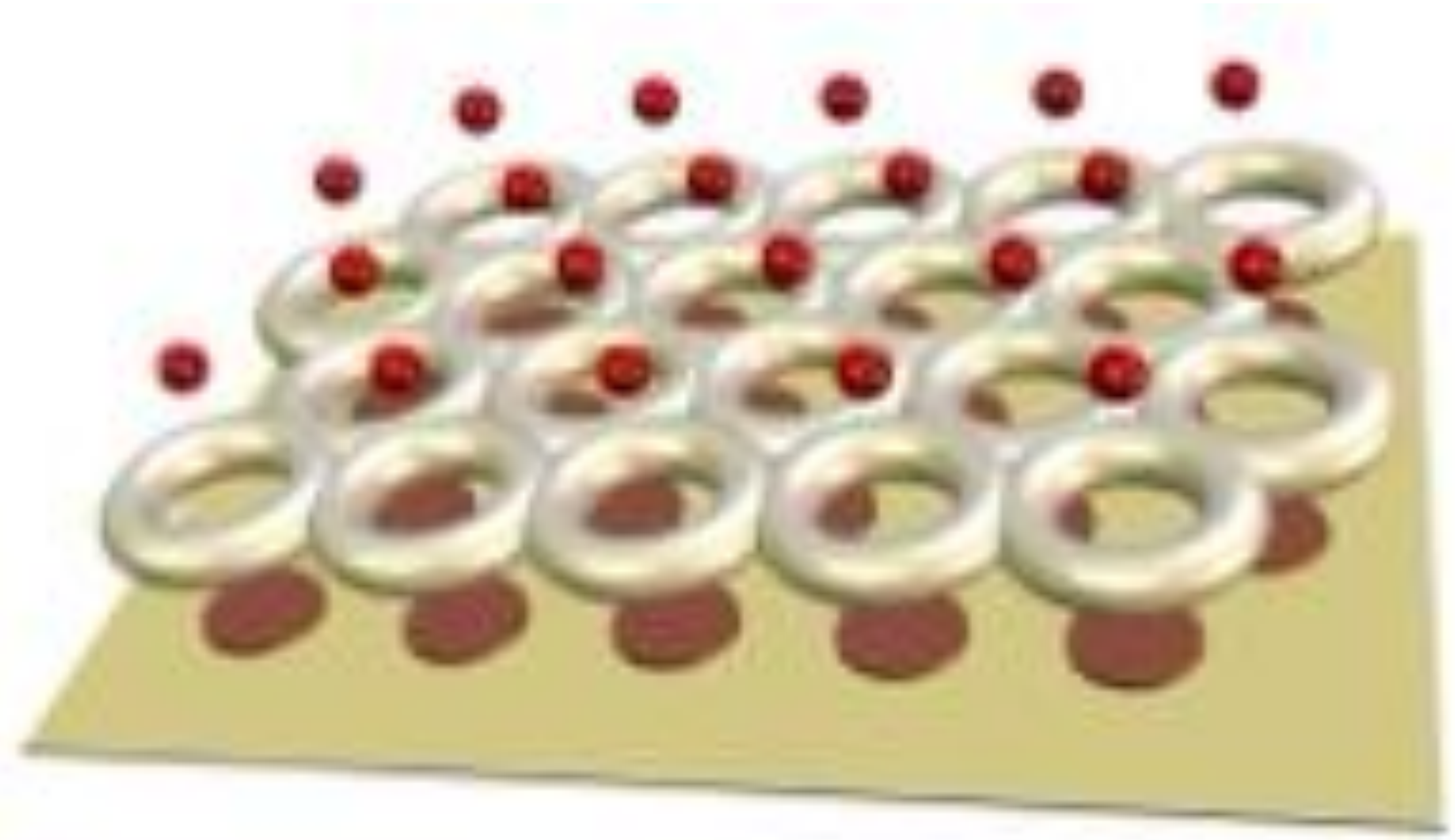

Quantum networks

Atom-photon interaction

…in free space

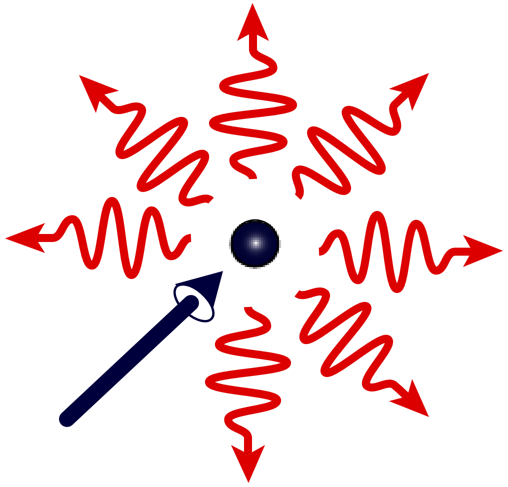

+ simple setup
- frequency?
- direction?

…via a cavity

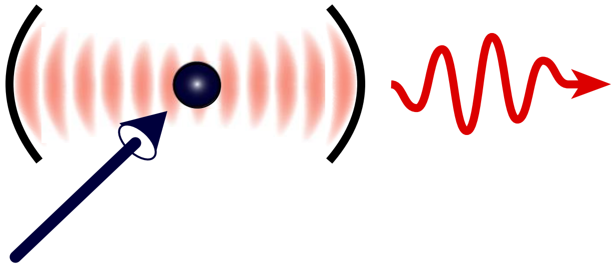

- complex setup
+ frequency!
+ direction!

Ion trap with high-numerical aperture objectives

High aperture lenses NA = 0.4

Paul trap Innsbruck design

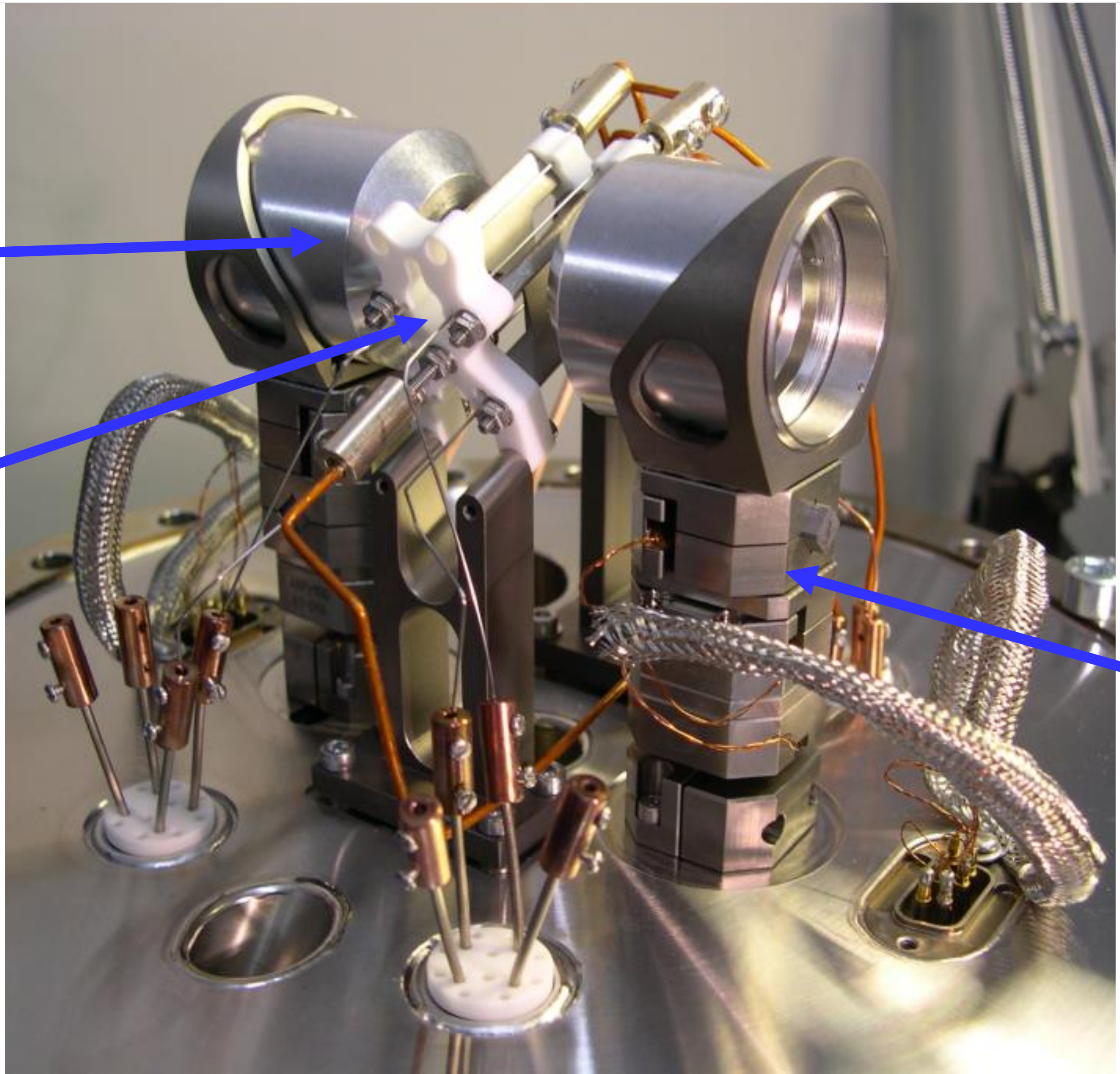

UHV translation stages resolution <1µm

Quantum networks: Ions in a cavity

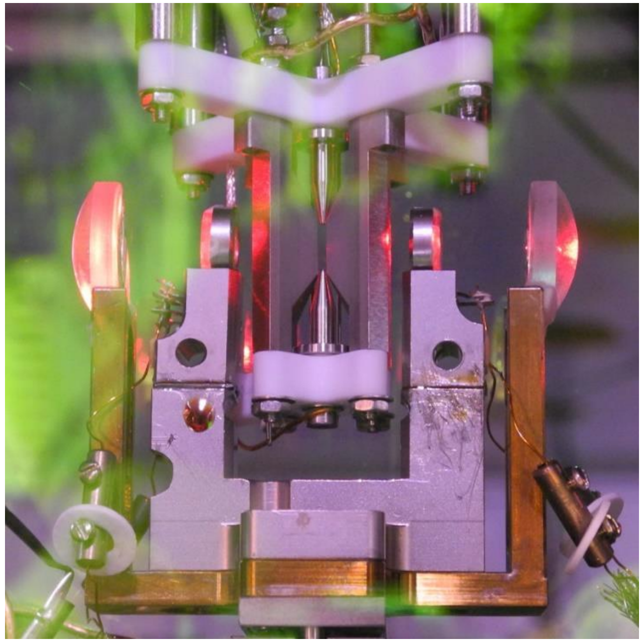

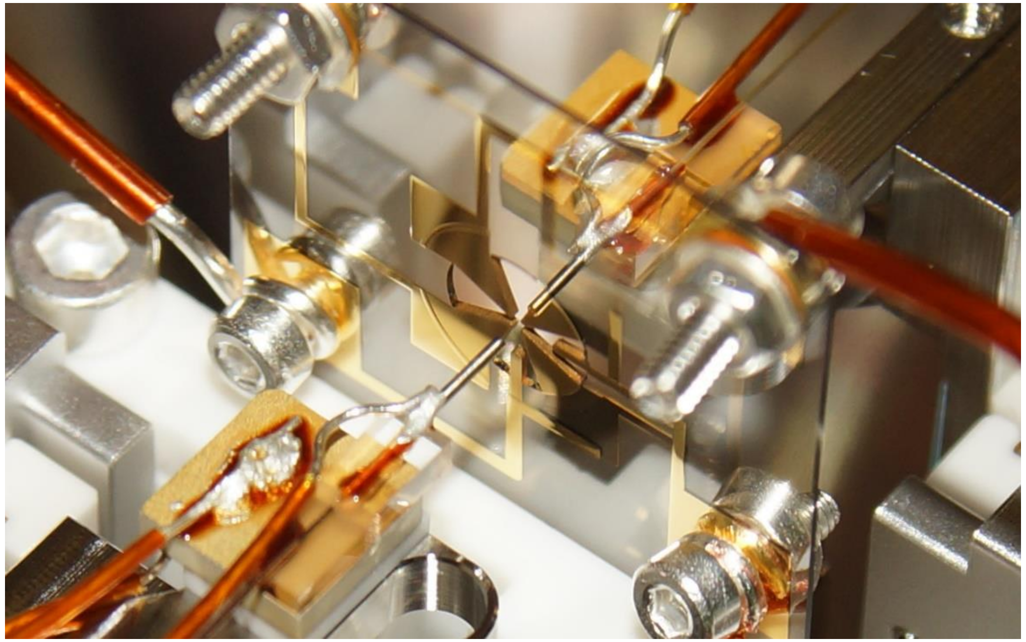

Optical resonators:

Efficient coupling to photons in single light mode

Atom-photon entanglement

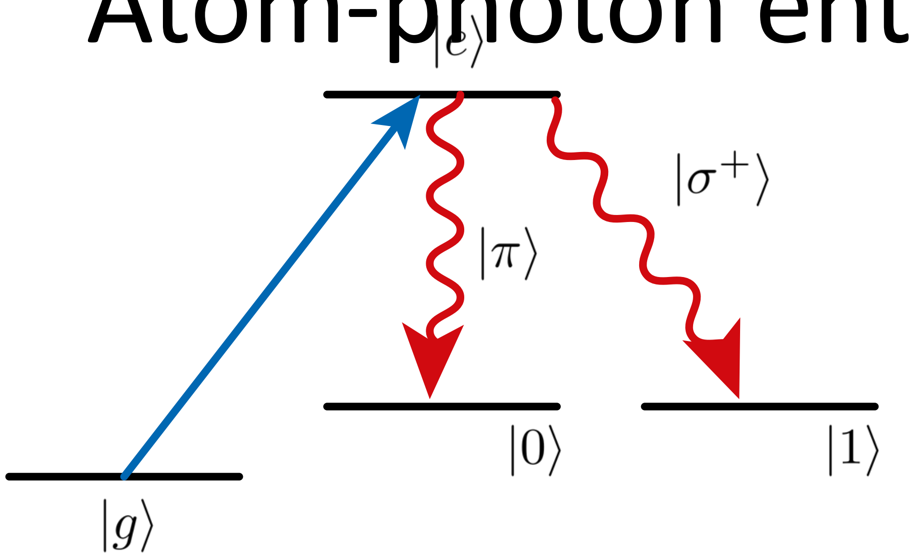

$$|\psi\rangle \propto |0,\pi\rangle + |1,\sigma^+\rangle$$

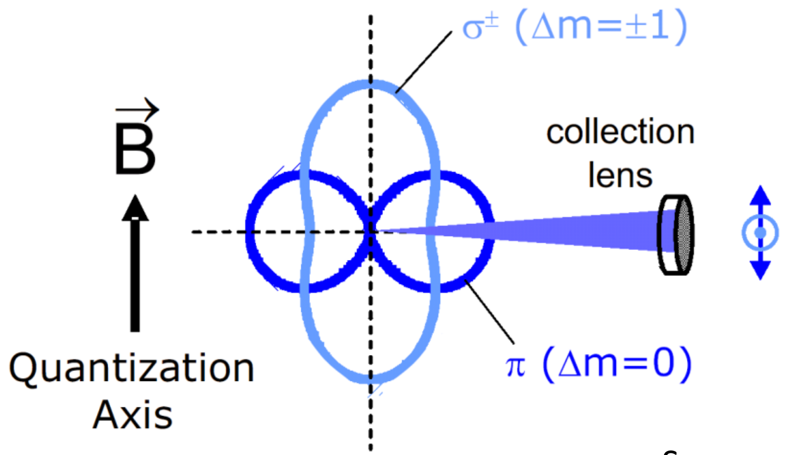

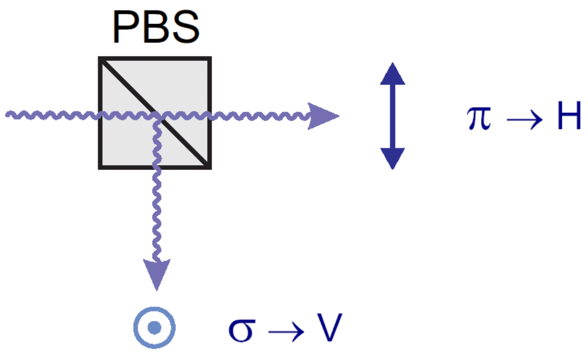

Some realisations:

B. B. Blinov, et al., Nature **428**, 153 (2004) (free-space)

A. Stute, et al., Nature **485**, 7399 (2012) (cavity)

P. Kobel, et al., Npj Quantum Information **7**, 1 (2021) (fiber cavity)

Entanglement swapping

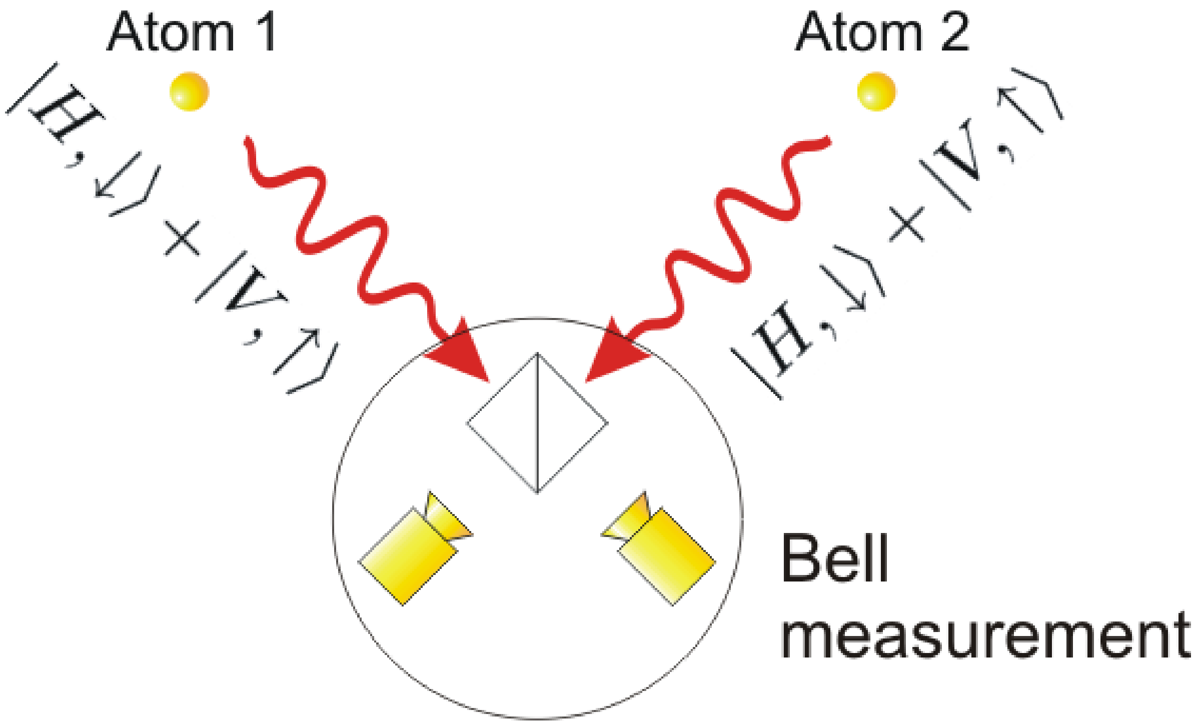

L.-M. Duan, M. D. Lukin, J. I. Cirac, and P. Zoller, Nature **414**, 413 (2001).
C. Simon and W. T. M. Irvine, Phys. Rev. Lett. **91**, 110405 (2003).
Exp.: D.L. Moehring, et al., Nature **449**, 68-71 (2007).

Single photon entanglement protocol (exp): L. Slodička, et al., PRL **110**, 083603 (2013)

Hong-Ou-Mandel interference (HOM)

two photons → four alternatives

$|1\rangle_1 |1\rangle_2$

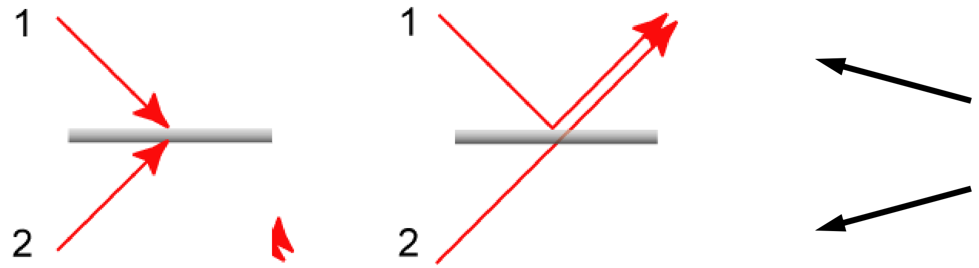

no coincidences !!!

$\frac{1}{\sqrt{2}} \, |2\rangle_1 |0\rangle_2$ $\quad$ $-\frac{1}{\sqrt{2}} \, |0\rangle_1 |2\rangle_2$

$$\longrightarrow \quad \text{final state} = \frac{1}{\sqrt{2}} \left(|2\rangle_1 |0\rangle_2 - |0\rangle_1 |2\rangle_2 \right)$$

Hong-Ou-Mandel interference (HOM)

two photons → four alternatives

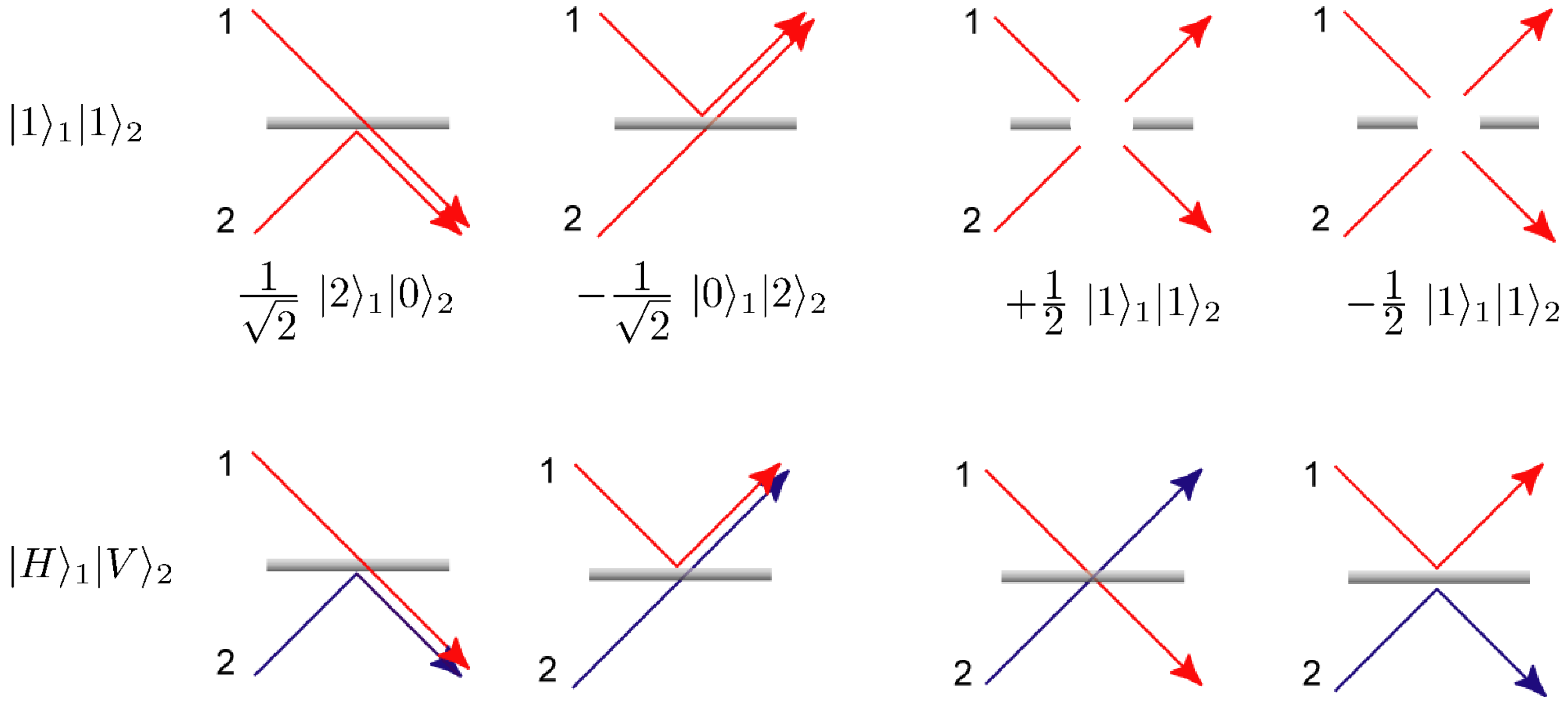

Coincidence probability

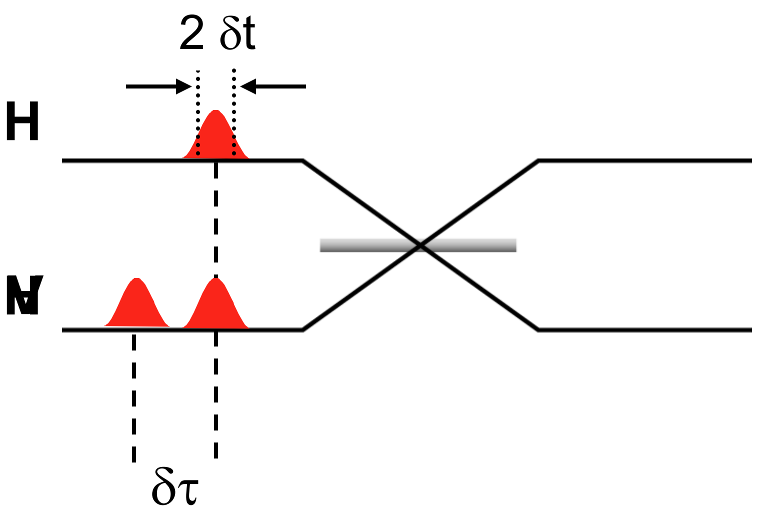

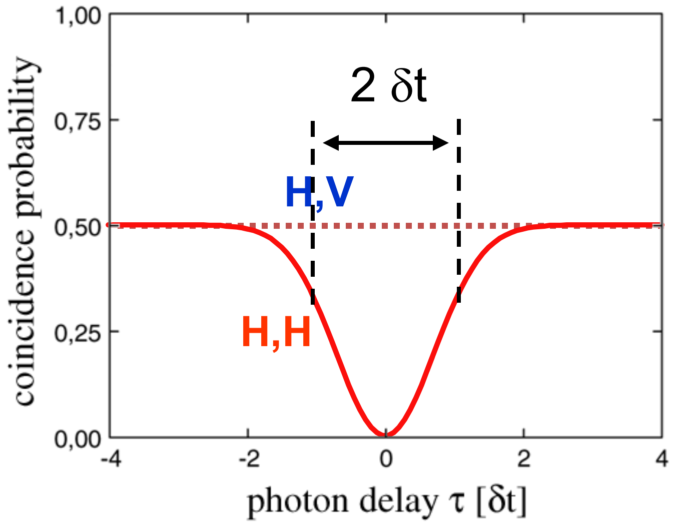

Coincidence detection = Bell state measurement

$$|\psi^+\rangle = \frac{1}{\sqrt{2}}(|H,V\rangle + |V,H\rangle)$$

no coincidence due to symmetry

$$|\psi^-\rangle = \frac{1}{\sqrt{2}}(|H,V\rangle - |V,H\rangle)$$

1 out of 4 Bell states detected by coincidence

$$|\phi^-\rangle = \frac{1}{\sqrt{2}}(|H,H\rangle - |V,V\rangle)$$

Identical photons → no coincidence

$$|\phi^+\rangle = \frac{1}{\sqrt{2}}(|H,H\rangle + |V,V\rangle)$$

Entanglement swapping

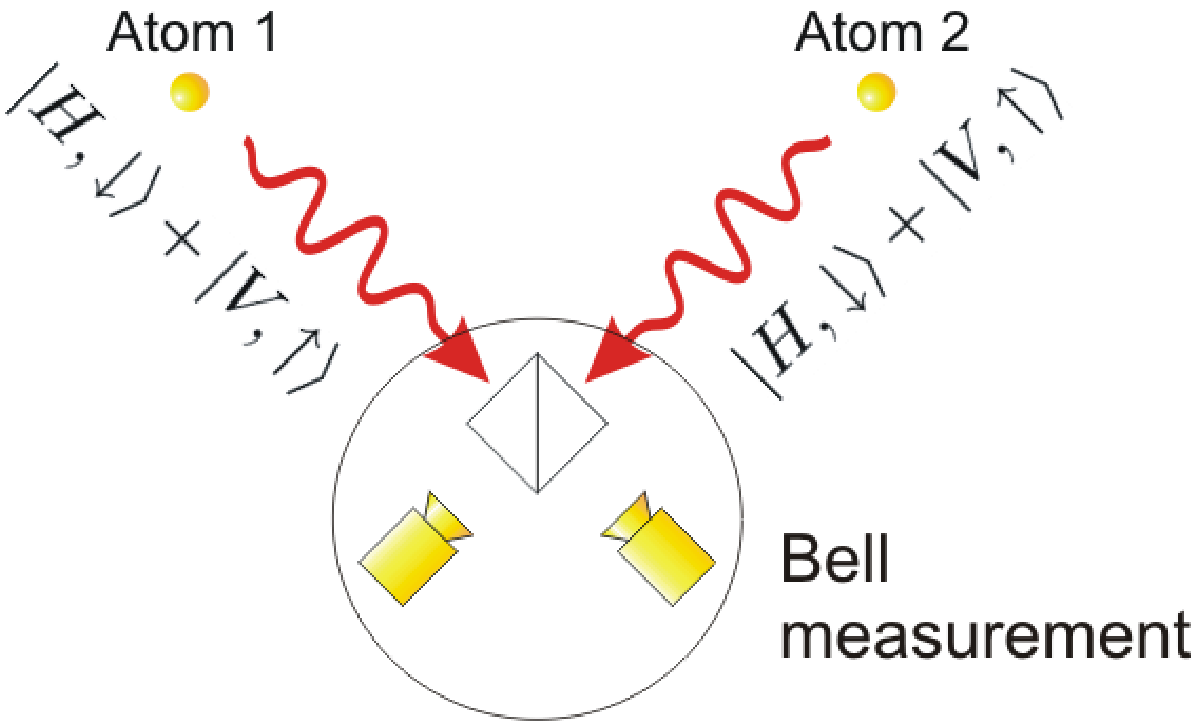

Theory: L.-M. Duan, M. D. Lukin, J. I. Cirac, and P. Zoller, Nature **414**, 413 (2001).
C. Simon and W. T. M. Irvine, Phys. Rev. Lett. **91**, 110405 (2003).

Exp.: D.L. Moehring, et al., Nature **449**, 68-71 (2007).

Single photon entanglement protocol (exp): L. Slodička, et al., PRL **110**, 083603 (2013)

Example application: Network of optical clocks

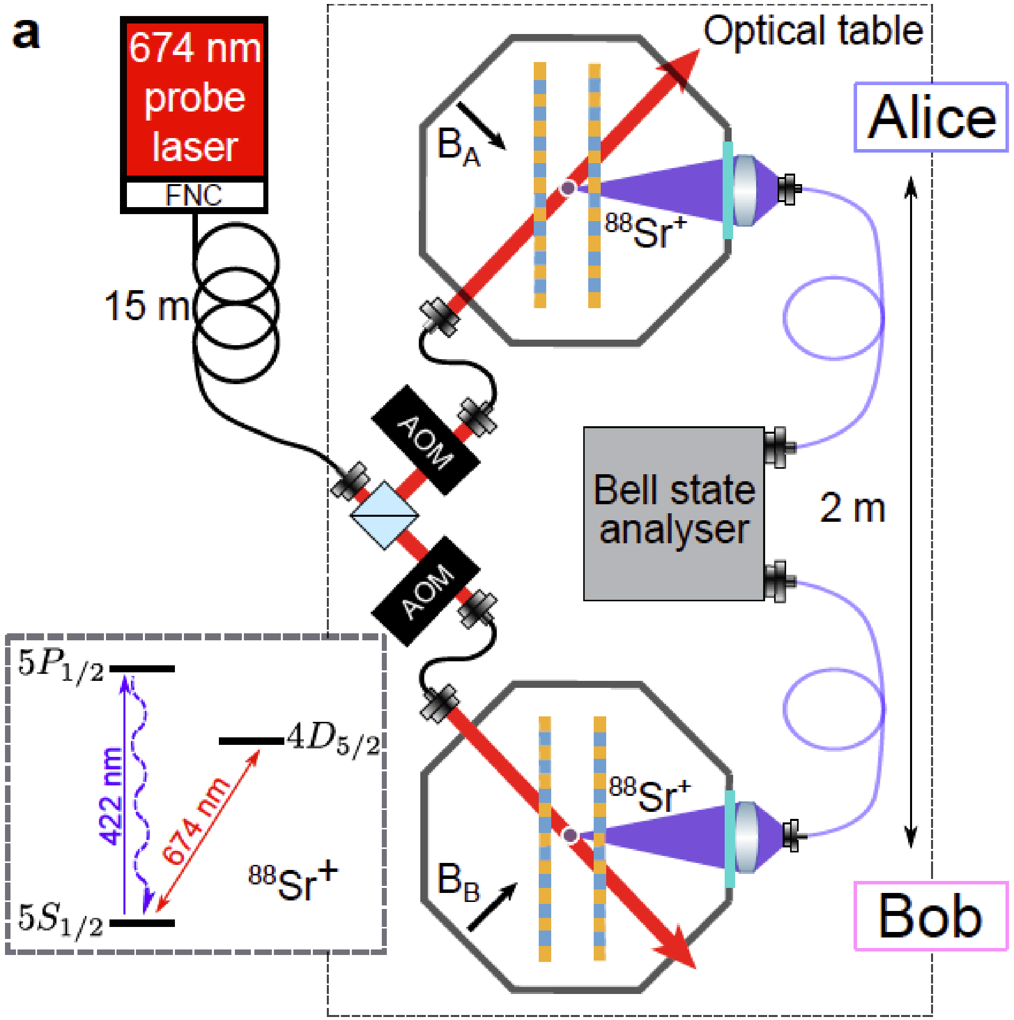

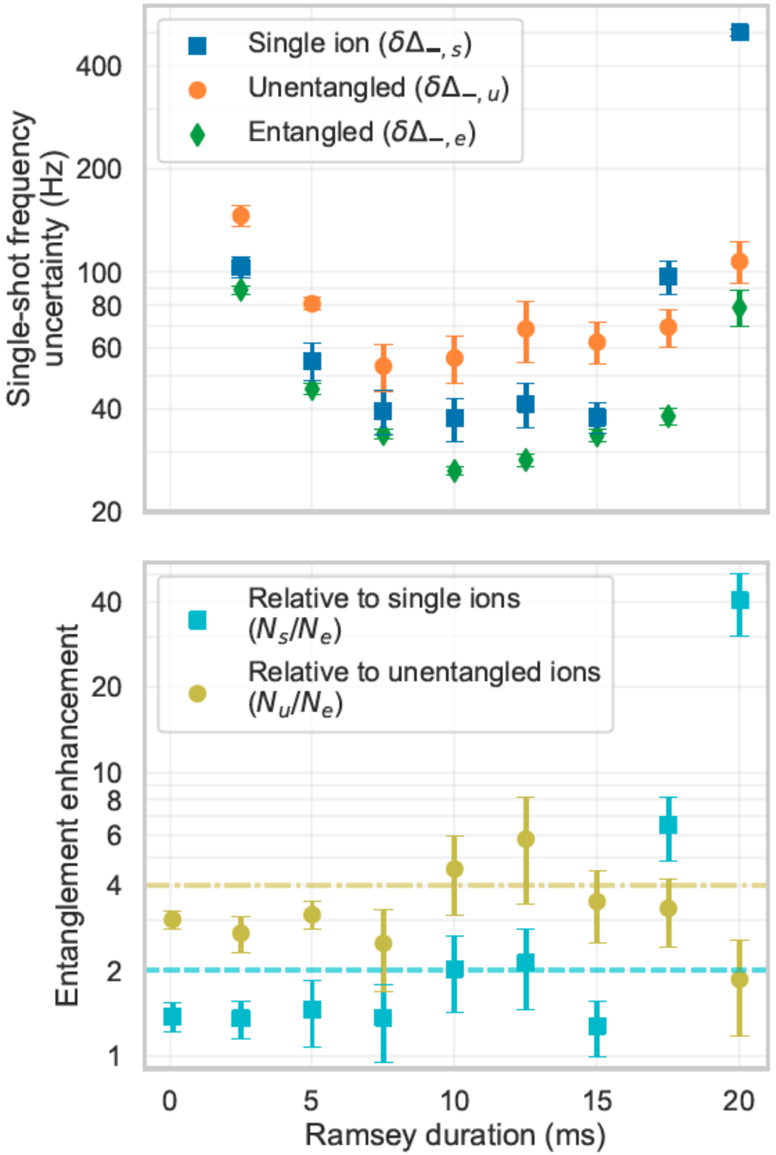

B. C. Nichol, et al. *Nature* **609**, 689–694 (2022).

Motivation: Quantum network

- Atom – photon interface:
  transmission of quantum information between two systems
  J.I. Cirac et al., Phys. Rev. Lett. 78, 3221 (1997).

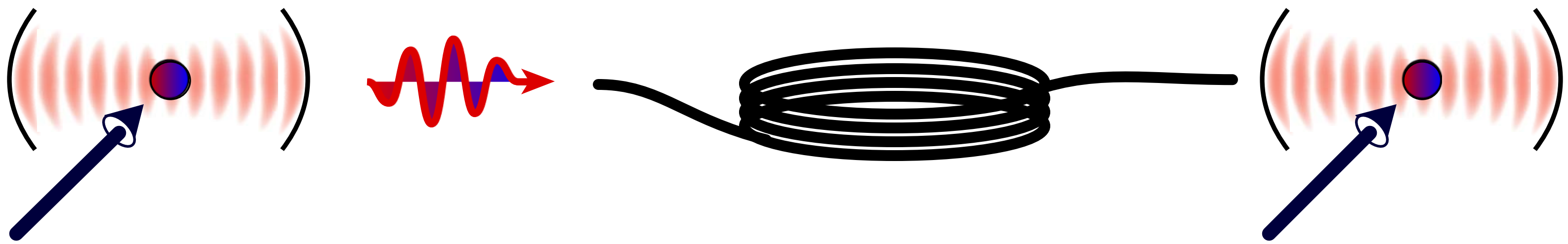

Why telecom?

transmission after 50km optical fibre

Losses @800nm:	2dB/km	→	10^{-10}
Losses @1550nm:	0.2dB/km	→	10%

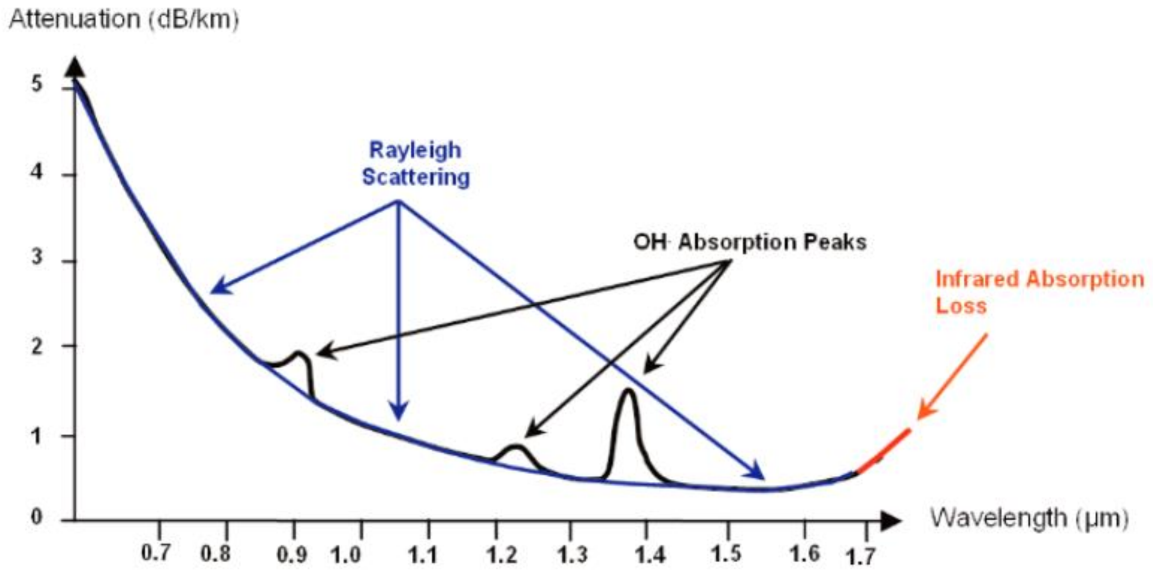

Frequency conversion to telecom wavelength

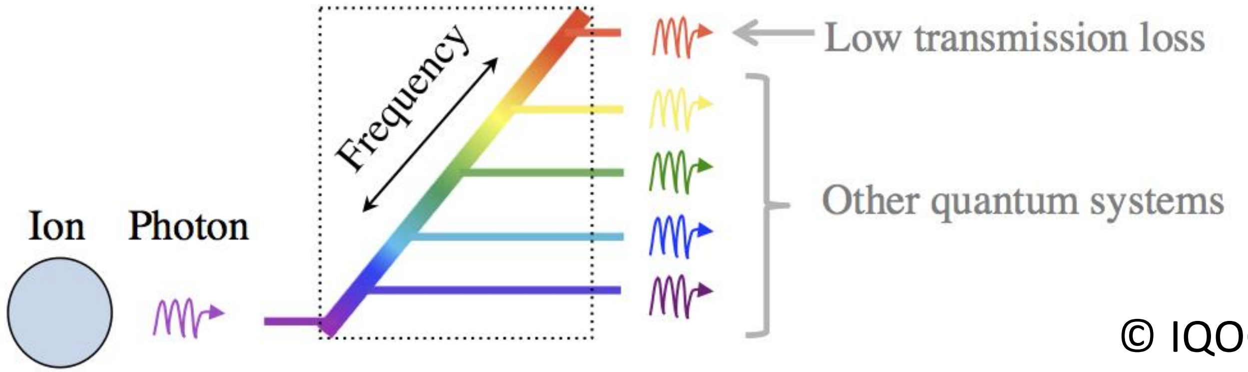

© IQOQI Innsbruck

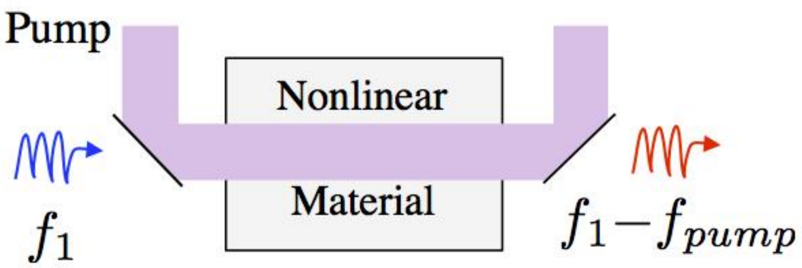

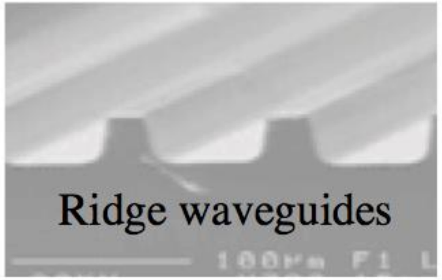

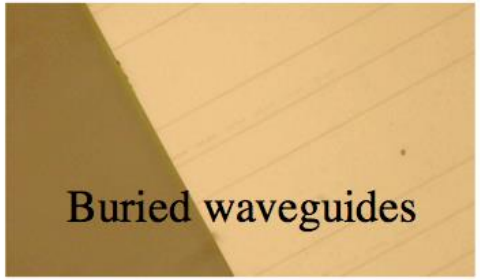

M. Bock, et al., Nature Communications **9**, 1 (2017).
T. Walker, et al., Physical Review Letters **120**, 203601 (2018).
V. Krutyanskiy, et al., Npj Quantum Information **5**, 1 (2019).

Application: Ion-Photon Entanglement over 101 Kilometers

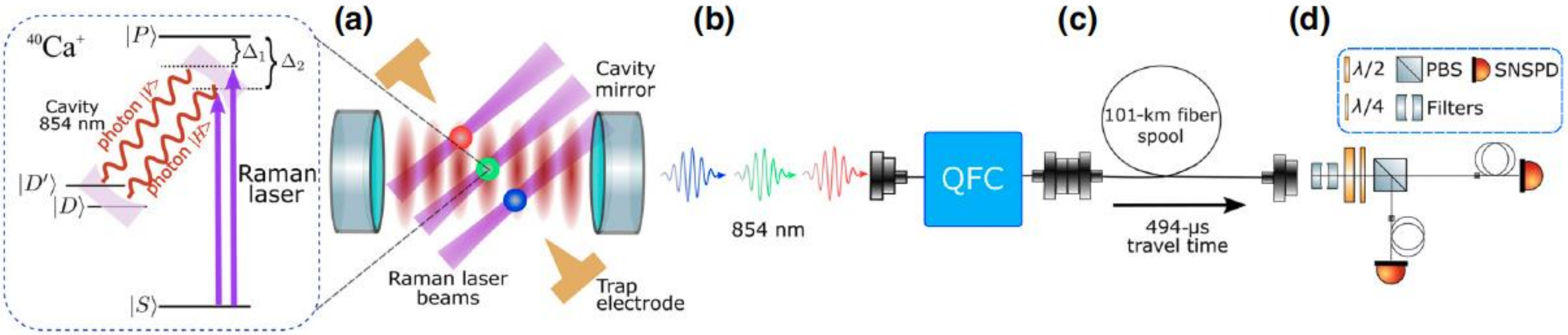

V. Krutyanskiy, et al., *PRX Quantum* **5**, 020308 (2024).

Trapped Rydberg ions

Trapped Rydberg ions

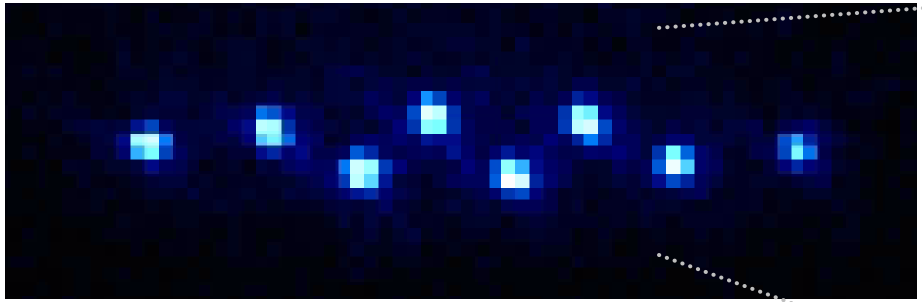

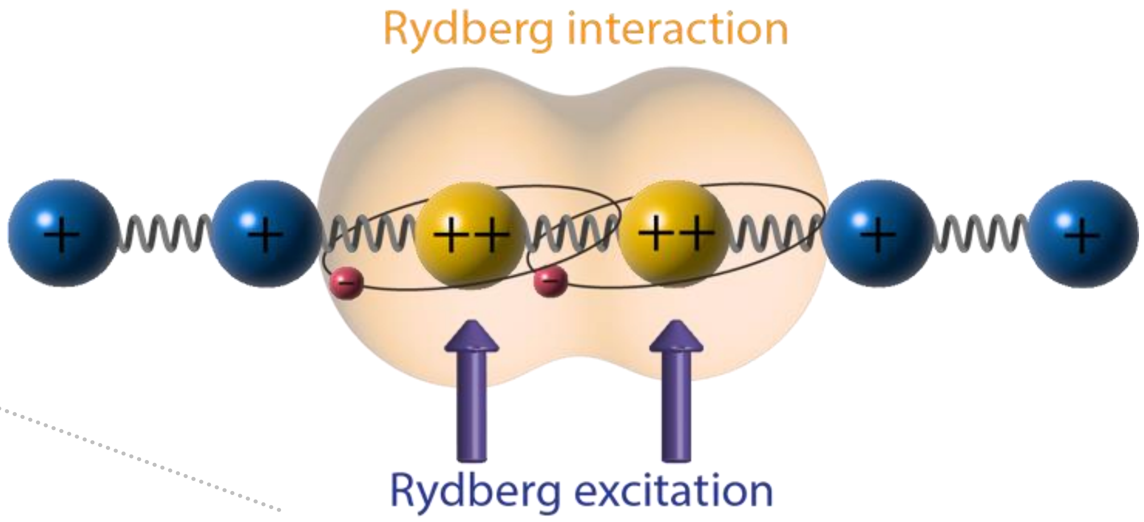

The idea: Combine **trapped ions** and **fast Rydberg interaction**.

M. Müller, L.-M. Liang, and I. Lesanovsky, P. Zoller, New J. Phys. 10, 093009 (2008).

What is a Rydberg atom/ion?

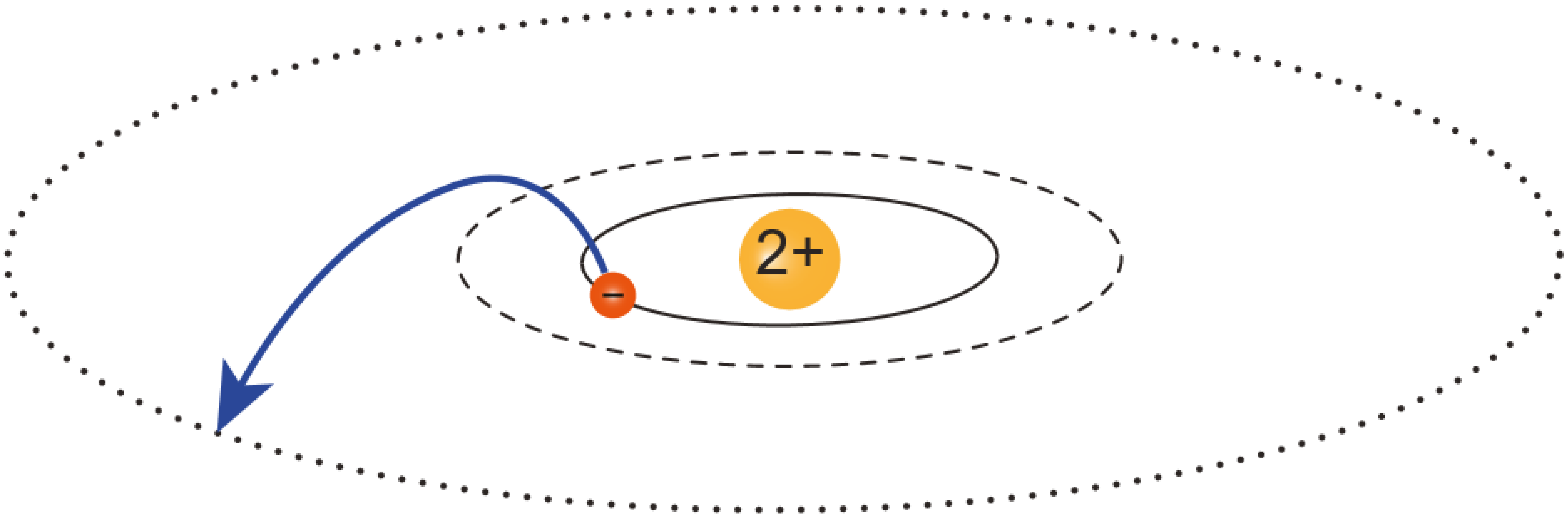

In a Rydberg atom / ion one electron is lifted into orbitals far away from the atomic core.

Johannes Robert Rydberg
(1854 –1919)
Swedish physicist

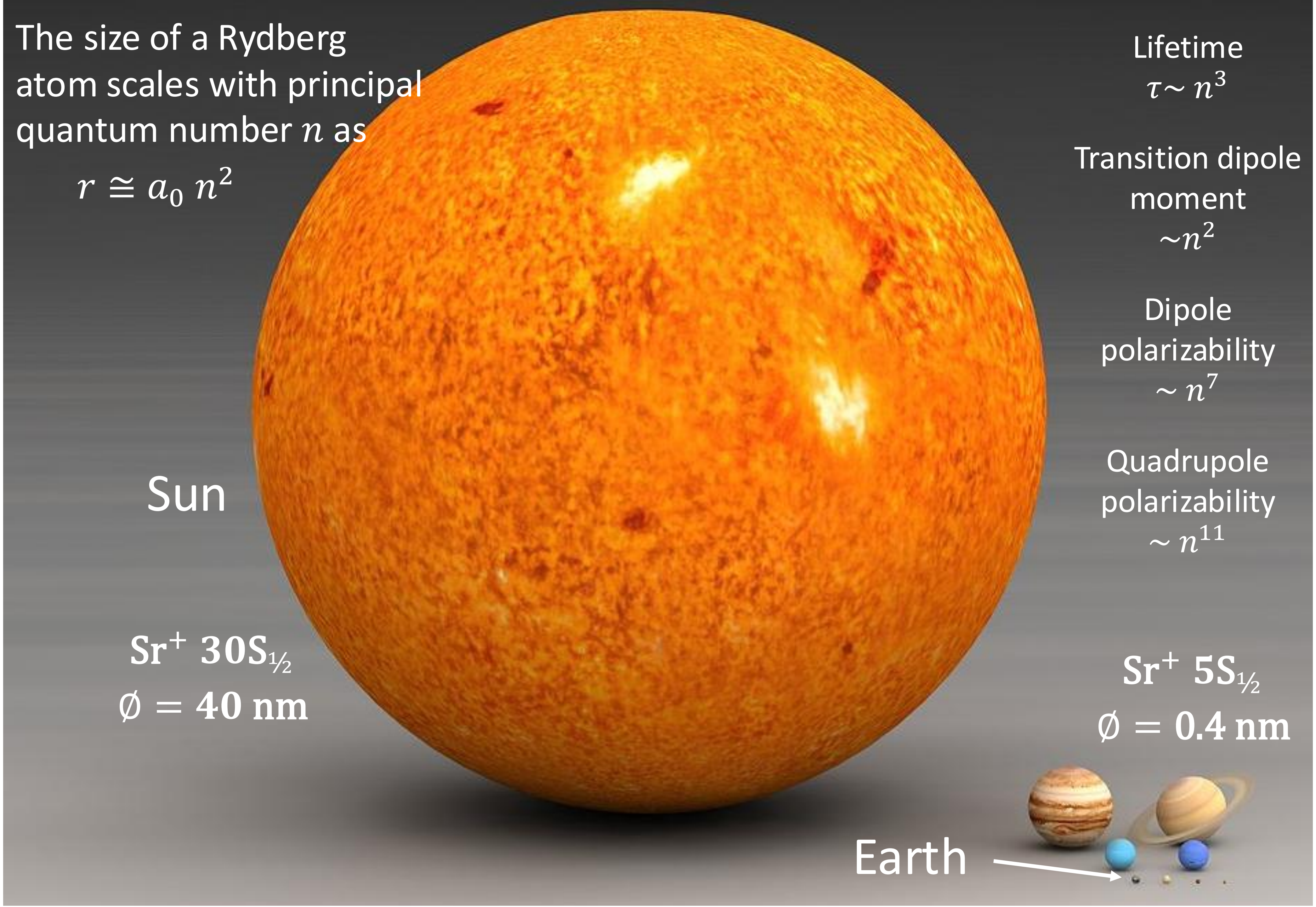
The size of a Rydberg atom scales with principal quantum number n as
$r \cong a_0 n^2$
Sun
$\mathbf{Sr^+ \ 30S_{1/2}}$
$\boldsymbol{\emptyset = 40 \ \mathrm{nm}}$
Lifetime
$\tau \sim n^3$
Transition dipole moment
$\sim n^2$
Dipole polarizability
$\sim n^7$
Quadrupole polarizability
$\sim n^{11}$
$\mathbf{Sr^+ \ 5S_{1/2}}$
$\boldsymbol{\emptyset = 0.4 \ \mathrm{nm}}$
Earth

Rydberg blockade

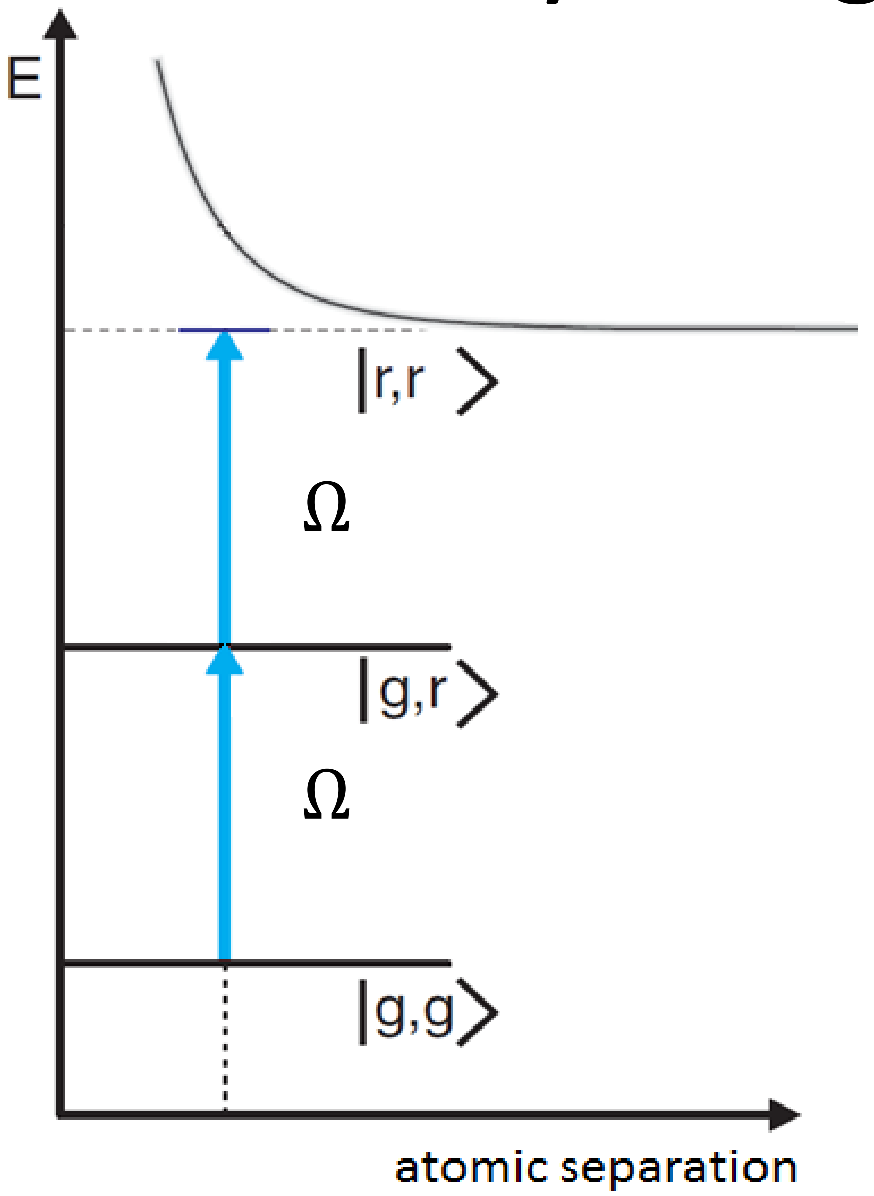

Two interacting
Rydberg atoms / ions

↓

Doubly excited Rydberg state
is shifted in energy

↓

Laser is shifted out of resonance
and double excitation is blocked

Rydberg ions are big, well localized, and can be individually manipulated by a laser.

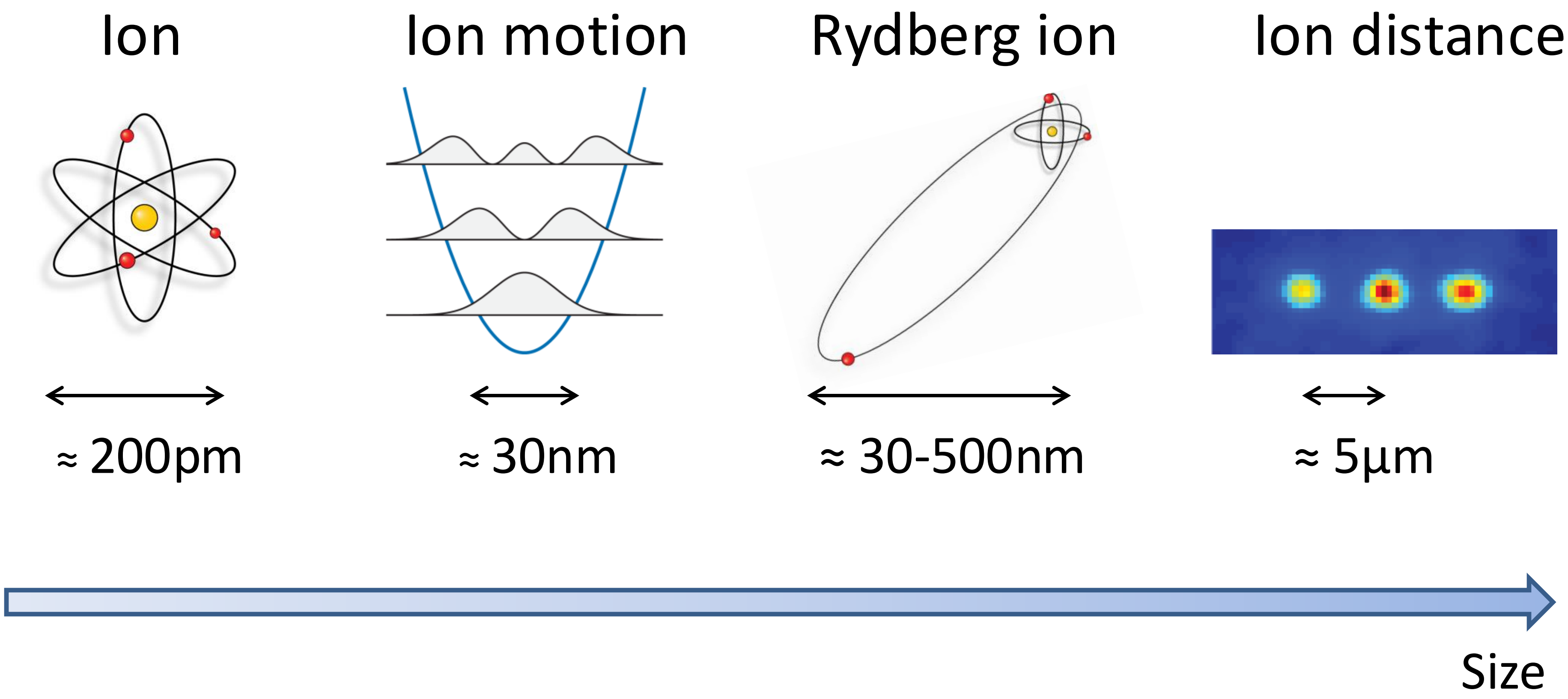

Ionization energies of typical ion species

Ion species	GS ionization limit in wavenumbers	one photon photoionization wavelength	D-state ionization limit in wavenumbers	D-state one photon photoionization wavelength
Ba^+	80686 cm^{-1}	123.9 nm	75012 cm^{-1}	133.3 nm
Sr^+	88964 cm^{-1}	112.4 nm	74128 cm^{-1}	134.9 nm
Ca^+	95752 cm^{-1}	104.4 nm	82042 cm^{-1}	121.9 nm (Lyman α =121.6nm)
Mg^+	121267 cm^{-1}	82.5nm		
Be^+	146882 cm^{-1}	68.1 nm		
Yb^+	98207 cm^{-1}	101.8 nm	75246 cm^{-1}	132.9 nm
Cd^+	136374 cm^{-1}	73.3 nm		
Hg^+	151284 cm^{-1}	66.1 nm		
Al^+	151862 cm^{-1}	65.8 nm		

Rydberg excitation @ Mainz [1]

Wavelength < 200nm is absorbed by air. Light source needs to be in vacuum.

[1] T. Feldker, et al., Rydberg excitation of a single trapped ion, *PRL* **115**, 173001 (2015).

Room-temperature ion trap experiment

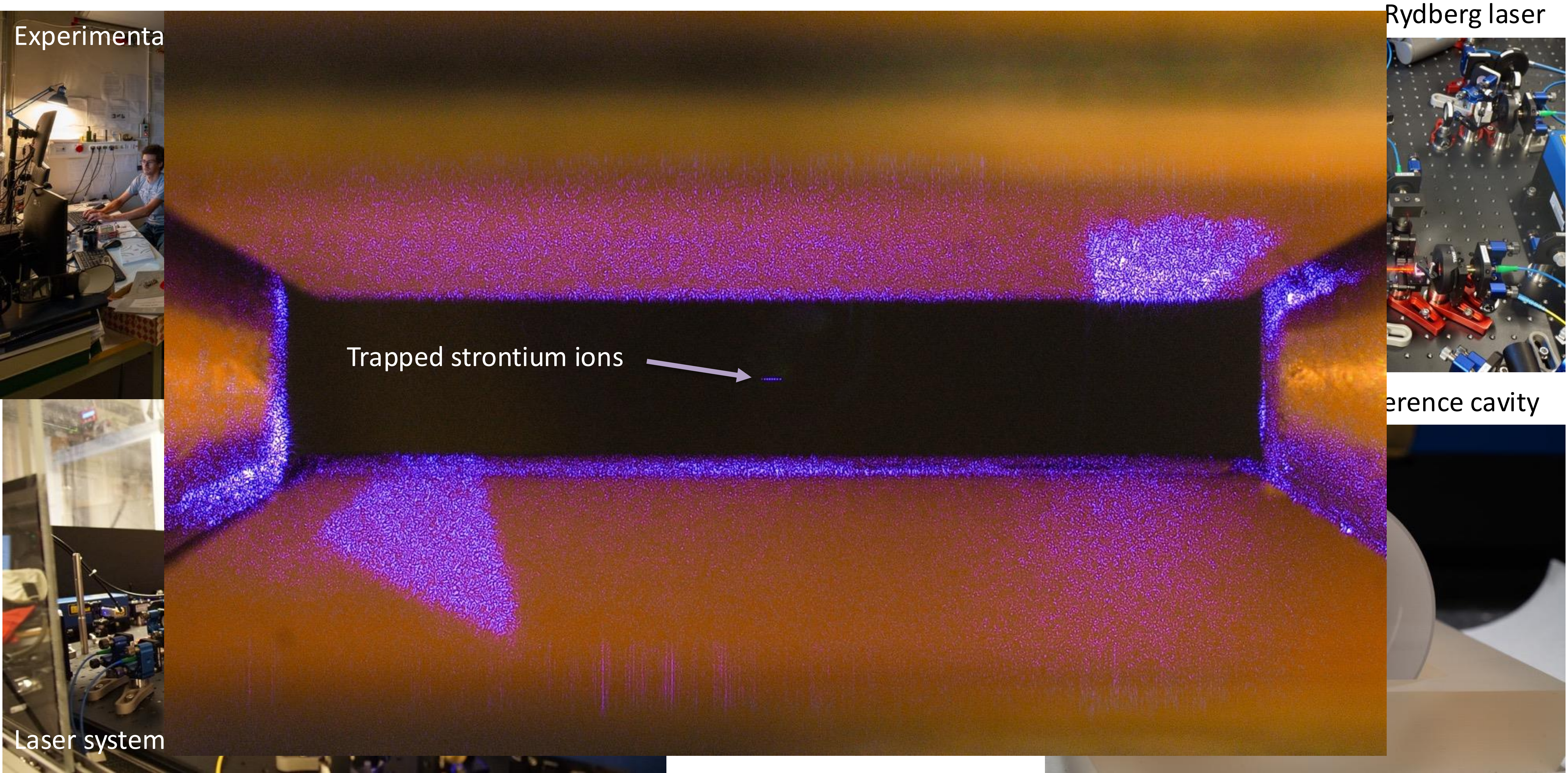

Two-photon Rydberg excitation of $^{88}Sr^+$

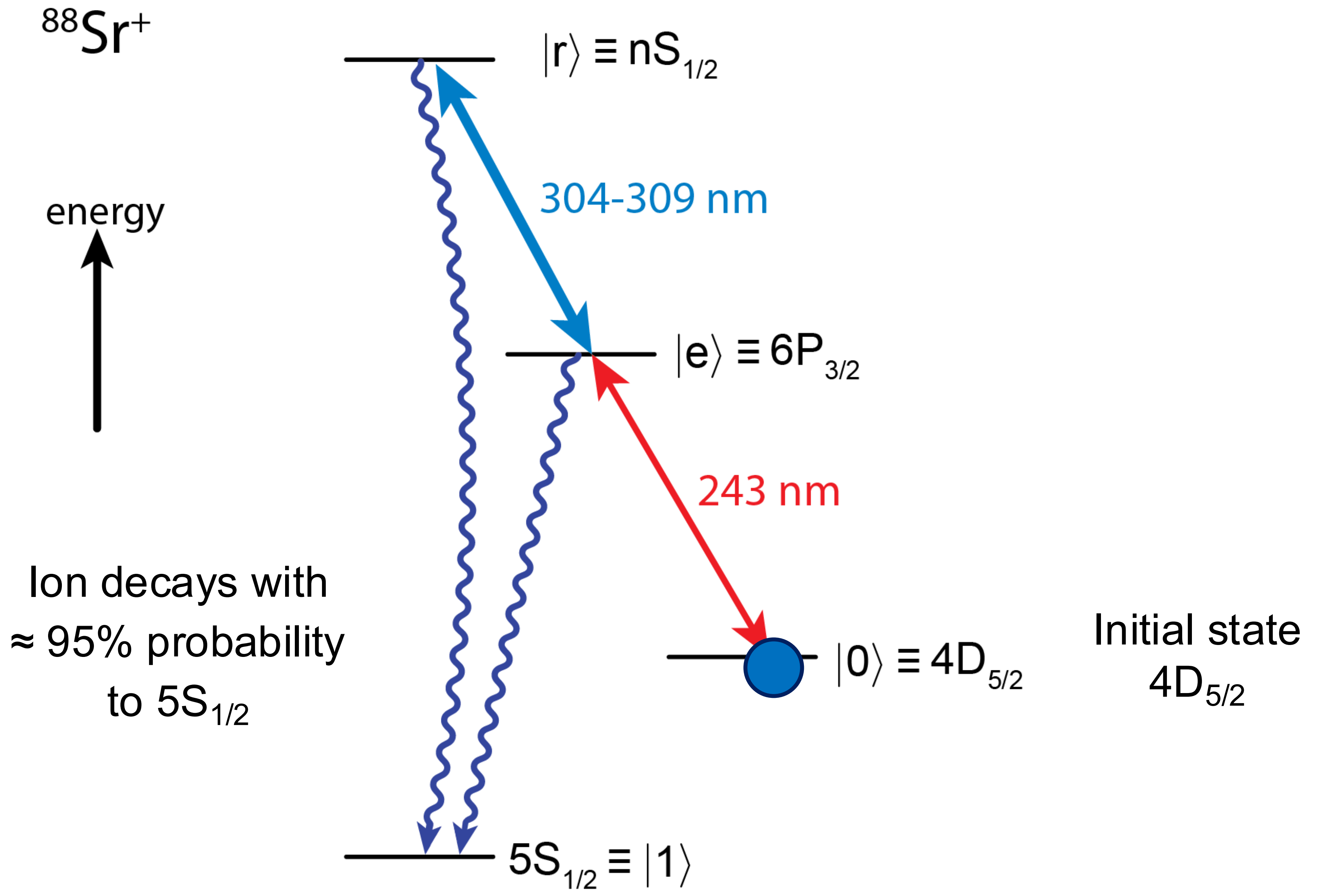

Stimulated two-photon adiabatic passage (STIRAP) for coherent Rydberg excitation.

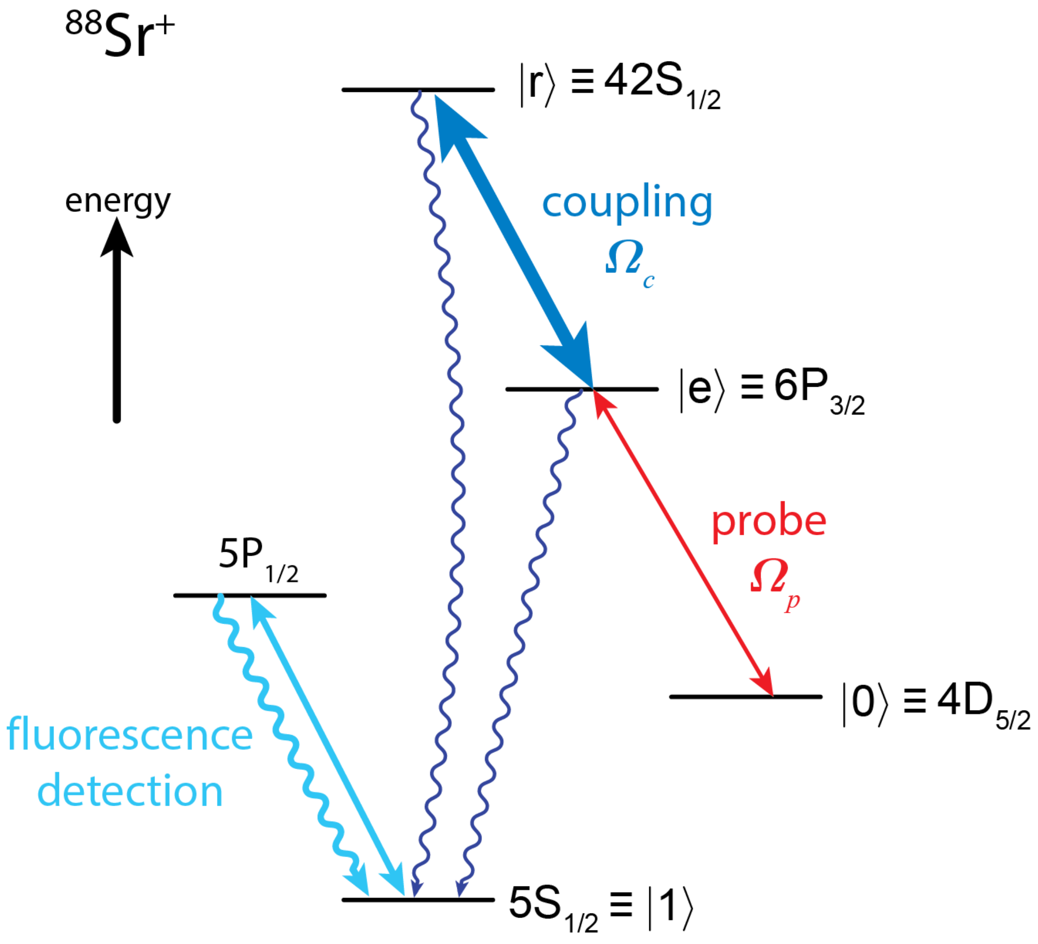

3-level Hamiltonian

$$\begin{pmatrix} 0 & \Omega_P & 0 \\ \Omega_P & 0 & \Omega_C \\ 0 & \Omega_C & 0 \end{pmatrix} \begin{pmatrix} |0\rangle \\ |\mathrm{e}\rangle \\ |\mathrm{r}\rangle \end{pmatrix}$$

Dark eigenstate

$$|\phi_{dark}\rangle \propto \Omega_C |0\rangle - \Omega_P |\mathrm{r}\rangle$$

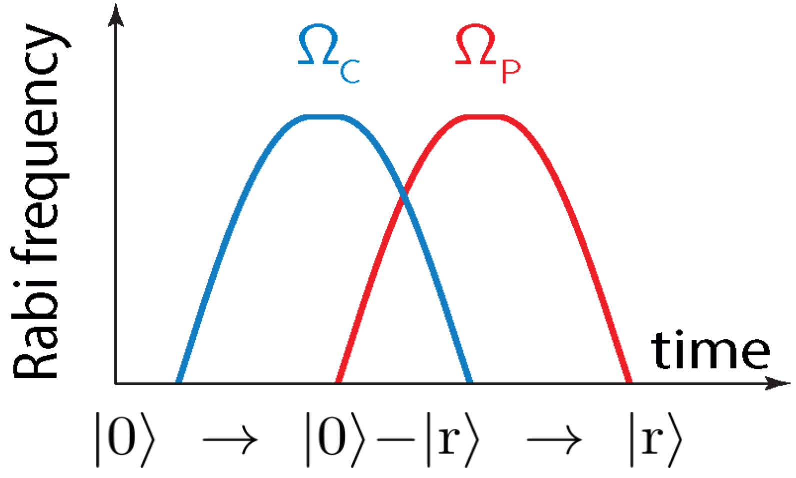

G. Higgins, et al., PRL 119, 220501 (2017).

Mapping the population to the Rydberg state and back.

Short double-STIRAP
$(83^{+5}_{-6})\%$ returned to $|0\rangle$

STIRAP efficiency =
$\sqrt{(83^{+5}_{-6})\%} = (91\pm3)\%$

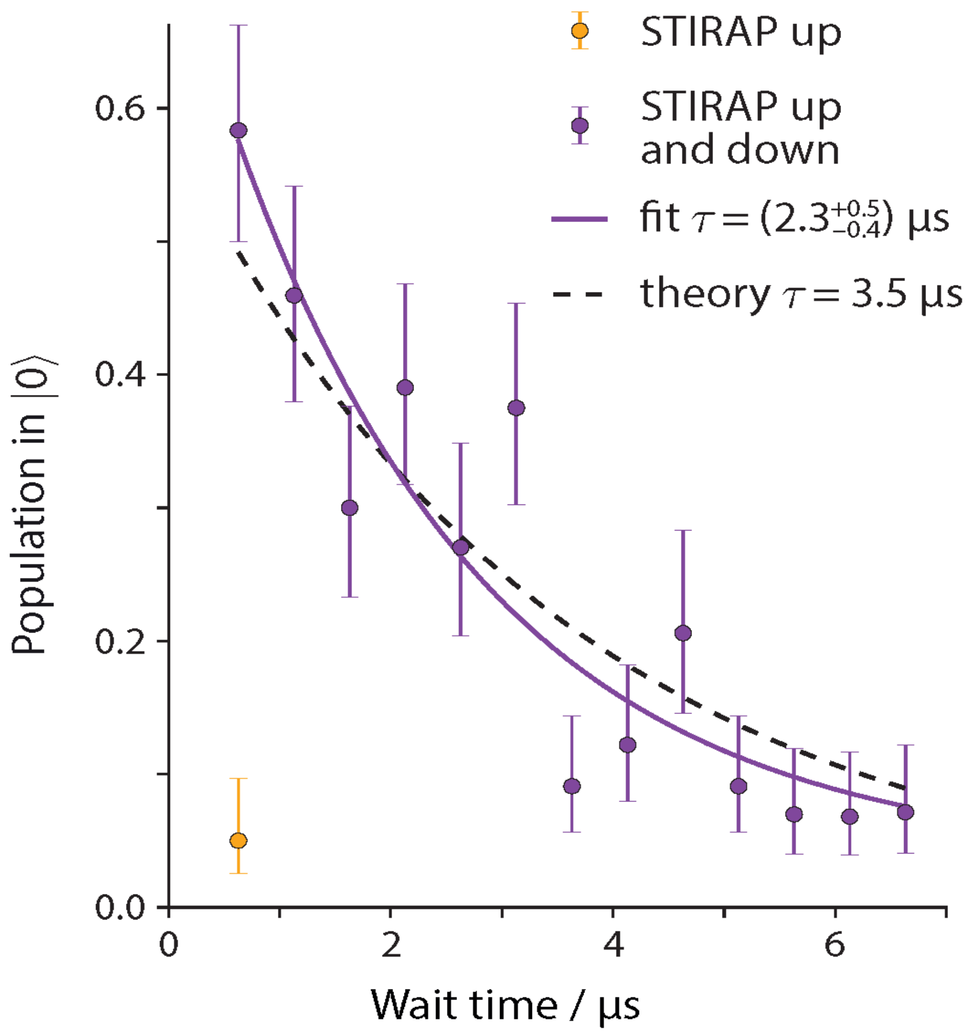

G. Higgins, et al., PRL 119, 220501 (2017).

The strong interaction between Rydberg ions blocks the excitation of a neighboring ion.

Rydberg blockade

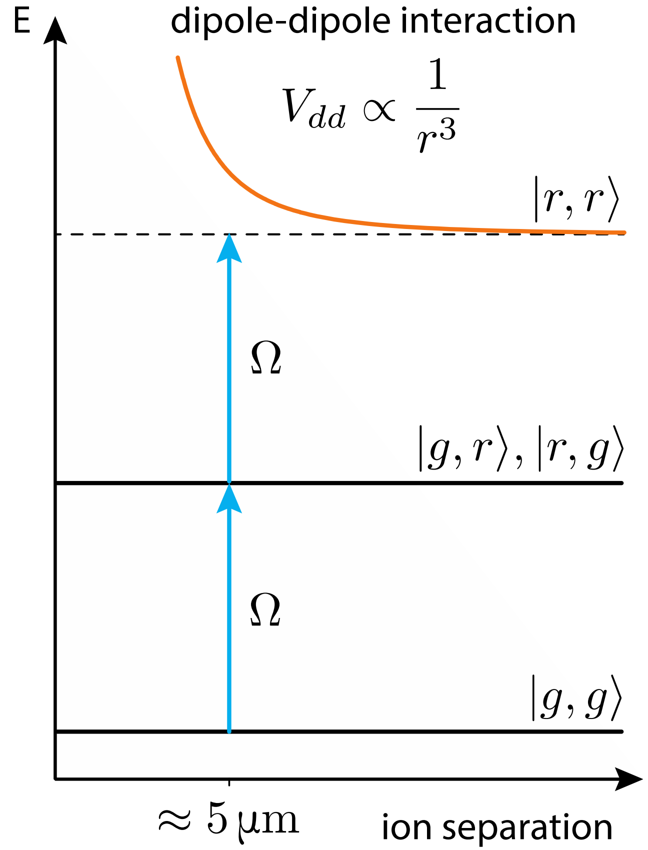

Coherent Rydberg excitation of 1 vs 2 ions

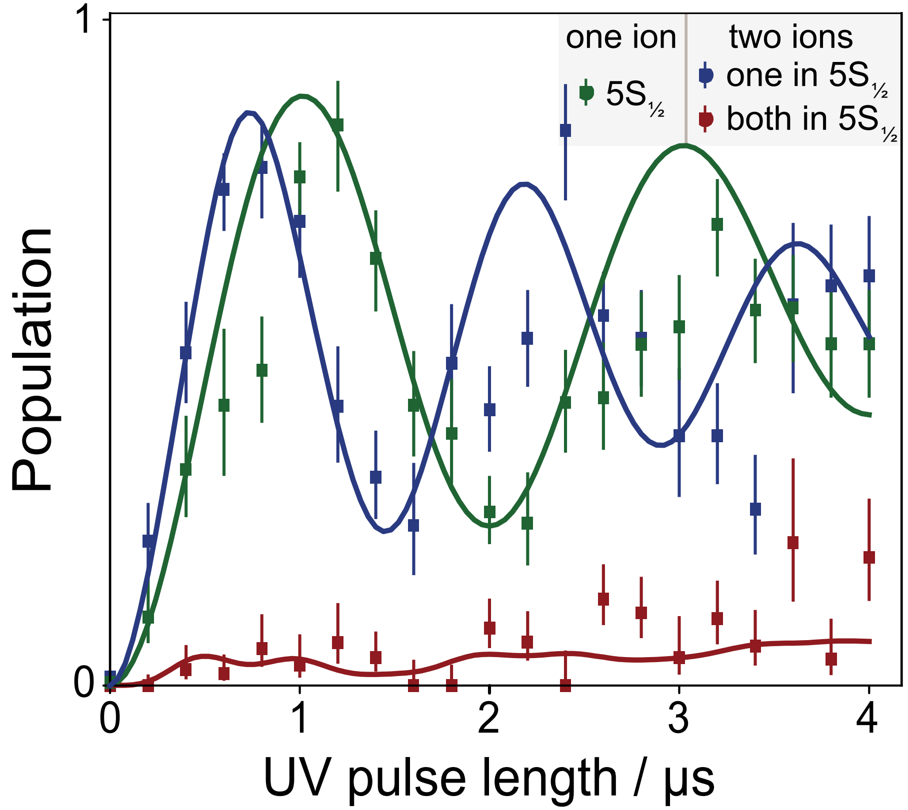

Double-excitation is suppressed due to Rydberg interaction

Ion distance 2-5μm
Interaction strength 1-20MHz

Chi Zhang, et al., Nature **580**, 345 (2020).

We perform a two-qubit controlled phase gate in <1μs.

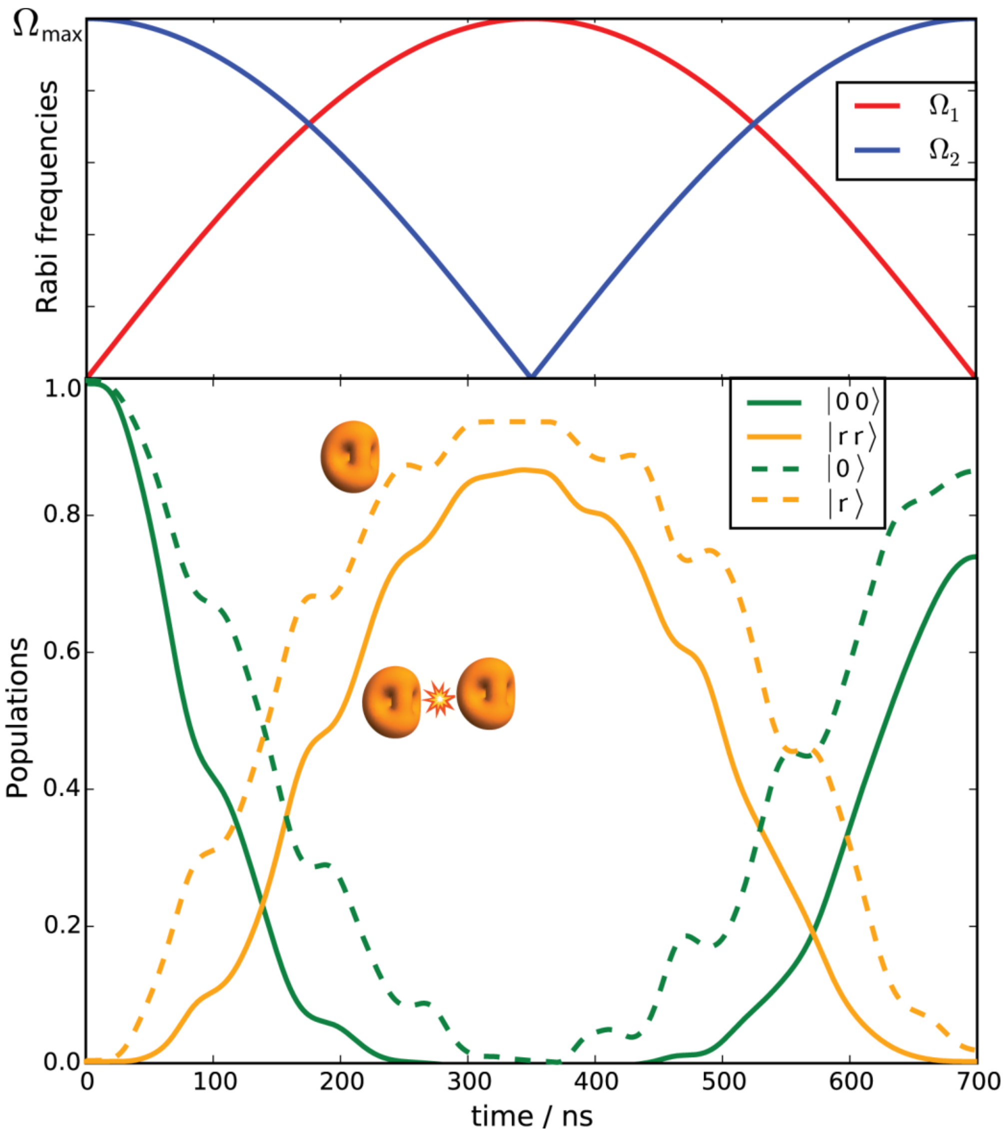

Apply STIRAP of 2 ions to MW-dressed interacting states

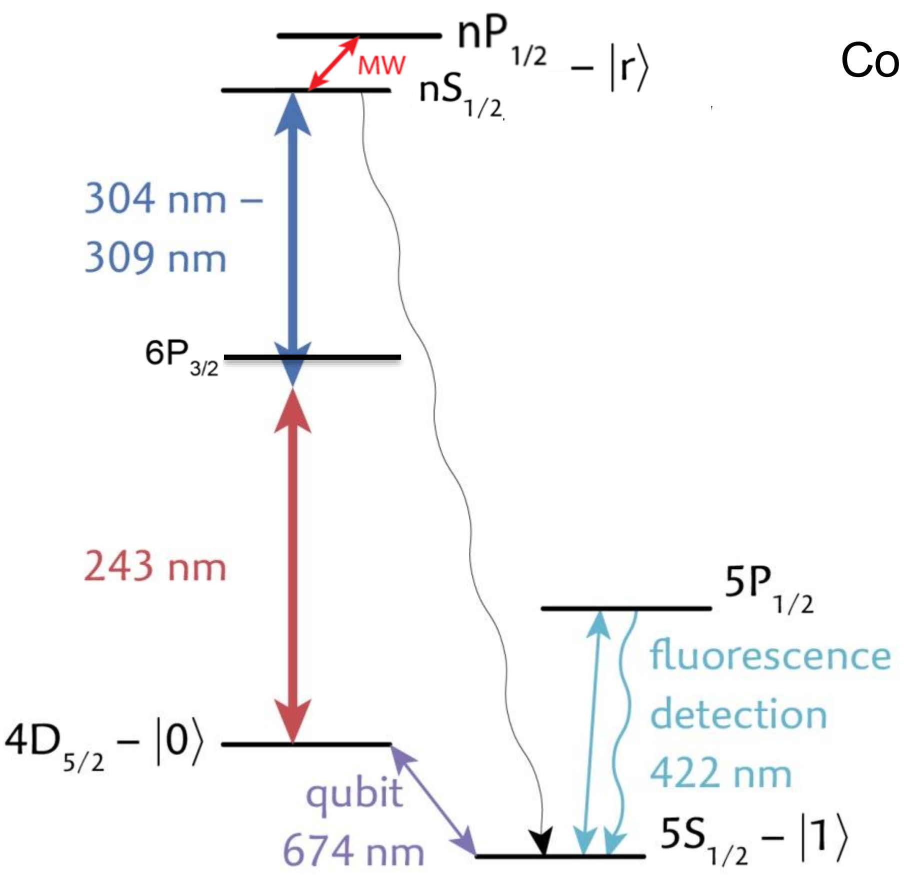

Controlled phase gate

$$
\begin{aligned}
|00\rangle &\rightarrow -|00\rangle \\
|01\rangle &\rightarrow |01\rangle \\
|10\rangle &\rightarrow |10\rangle \\
|11\rangle &\rightarrow |11\rangle
\end{aligned}
$$

Theory: D. Rao Dasari, K. Mølmer, PRA 89, 030301 (2014).
W. Li, I. Lesanovsky, Appl. Phys. B 114, 37 (2014).

Exp.: Chi Zhang, et al., Nature 580, 345 (2020).

Interaction entanglement gate (=controlled-phase gate)

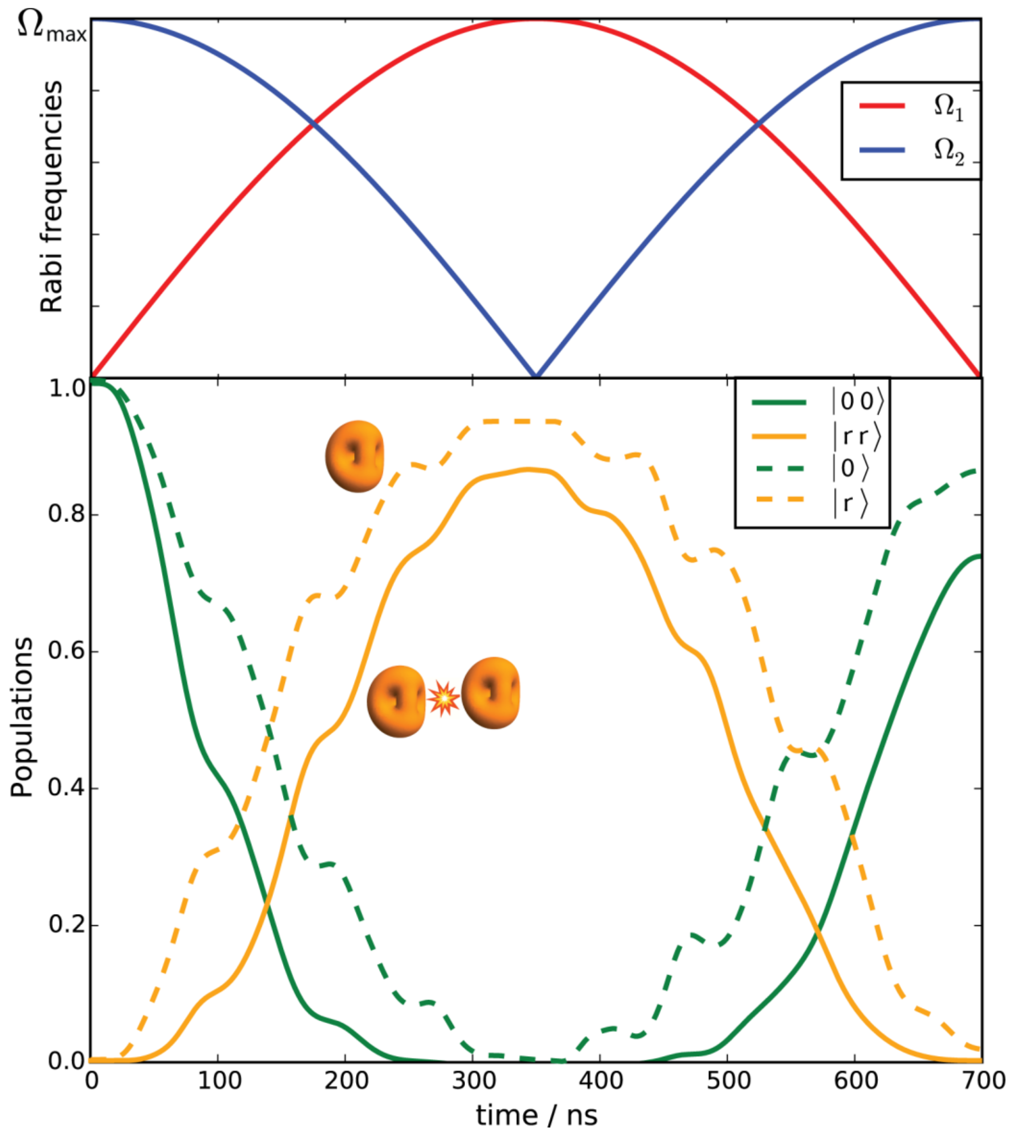

Apply STIRAP on 2 ions to MW-dressed interacting states

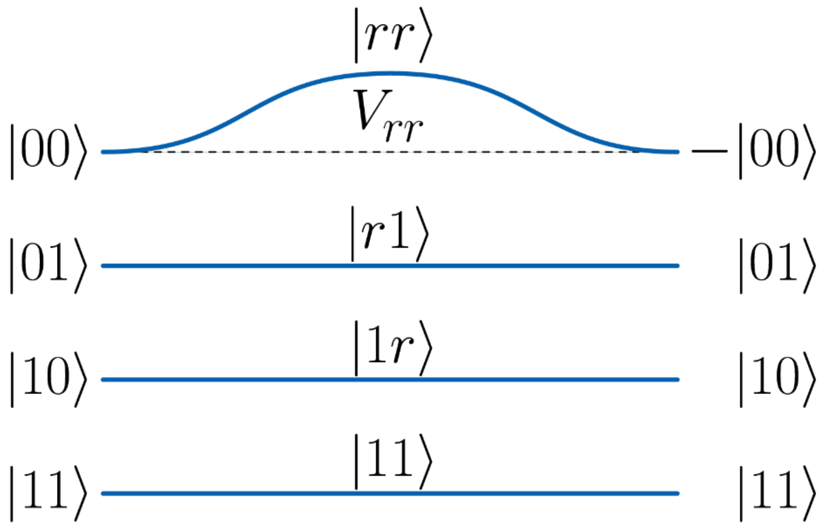

Rydberg interaction induces phase

$$\phi(t) = \frac{V_{rr}}{\hbar} \int_0^T \rho_{rr}(t)\, dt$$

→ Controlled-phase gate (CPhase)

We perform a two-qubit CPhase entangling gate in <1µs.

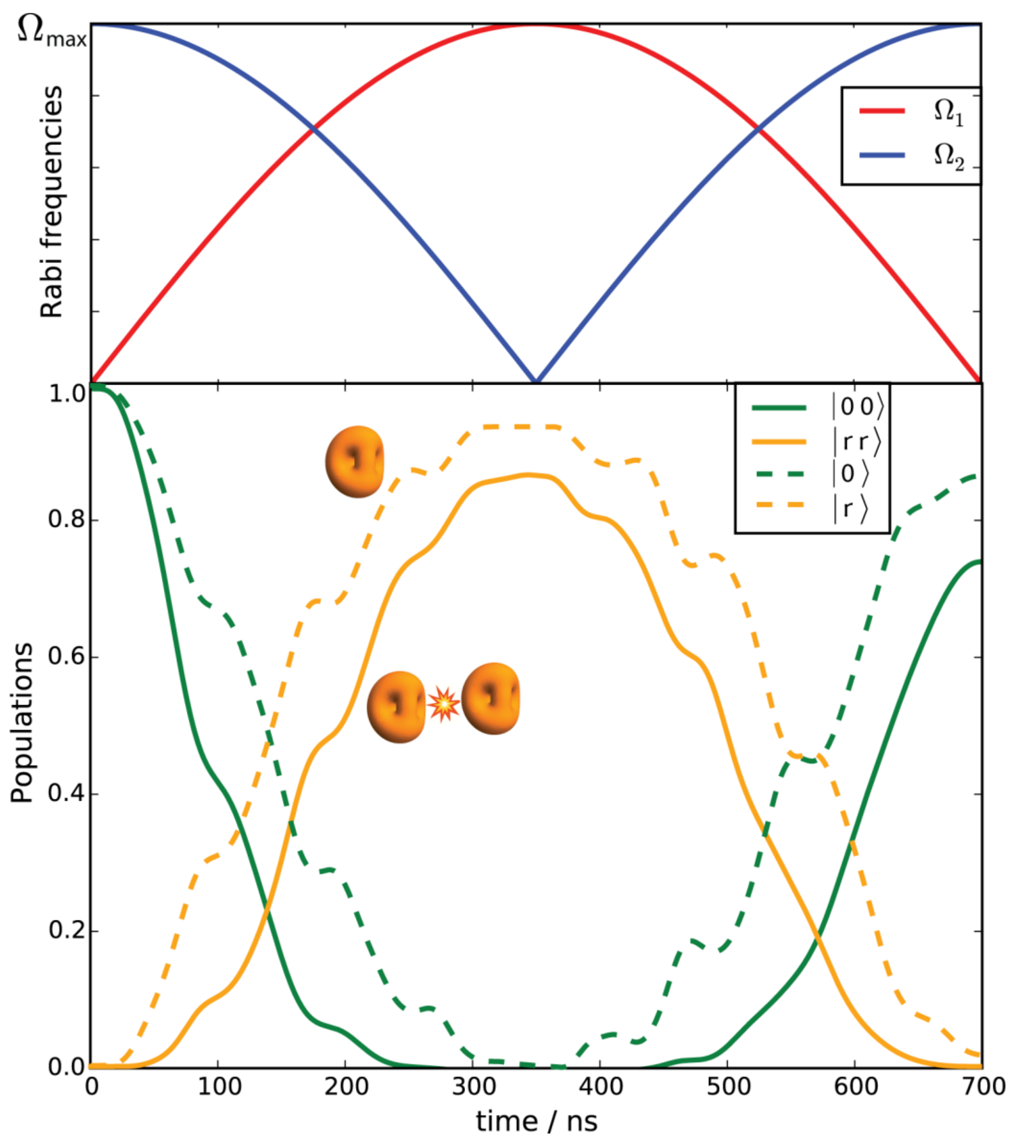

Maximally entangled state: $-|00\rangle + |01\rangle + |10\rangle + |11\rangle$

→ Measure fidelity by parity oscillations:

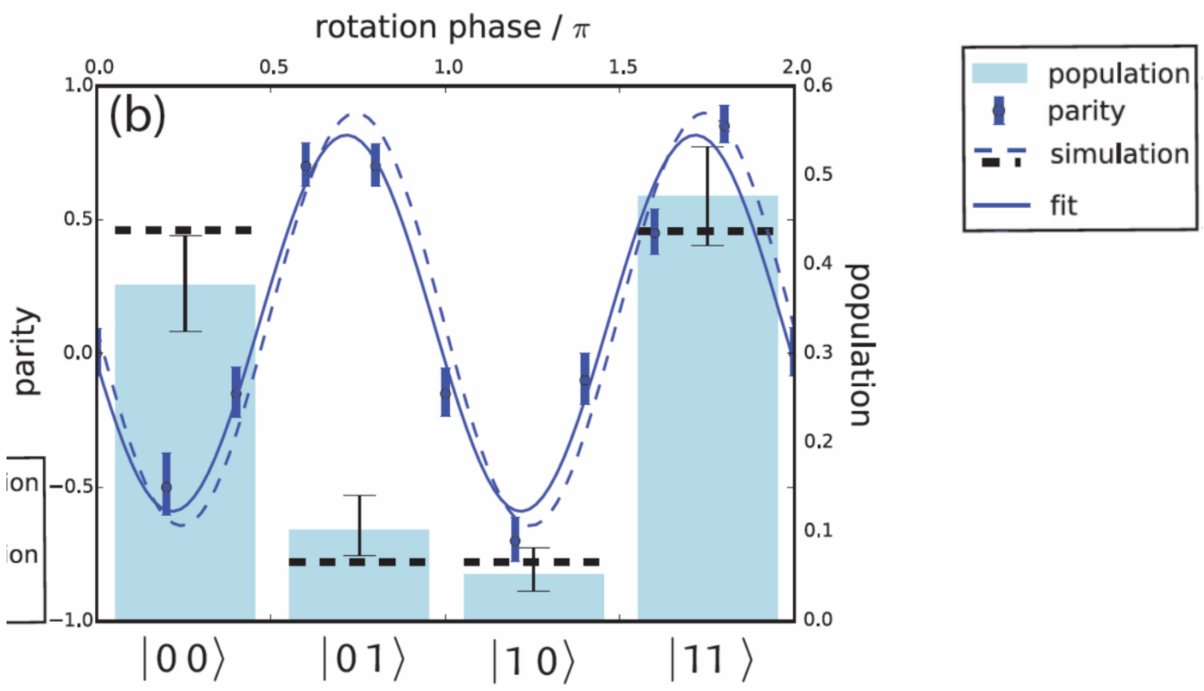

→ Bell state fidelity: 78% (technical limitations)

Chi Zhang, et al., Nature **580**, 345 (2020).

Interaction gate – error estimation and scaling

Error sources	Experiment (estimation)	Scaling
Rydberg state lifetime	3.5%	$n^{-7}\, r^3$
Laser linewidth	3%	$\Gamma_l\, n^{-4}\, r^3$
Decay of intermediate state	0.8%	$\Delta^{-2}\, n^4\, r^{-3}$
Non-adiabaticity of STIRAP	5.5%	$(\Omega_{max} - \Delta/2)^{-2}\, n^4\, r^{-3}$
Microwave power fluctuations	10%	$\delta\Omega_{MW}\, n^{-4}\, r^3$
Coupling to motion (due to interaction)	10^{-4}	$N^{1/12}$

→ Errors can be suppressed by technical improvements:

- Stability of microwave and lasers
- Higher laser power
- Smaller ion distance
- Higher principal quantum number

C. Zhang, et al., Nature **580**, 345 (2020).

We can speed up trapped ion quantum computers via Rydberg entangling gates.

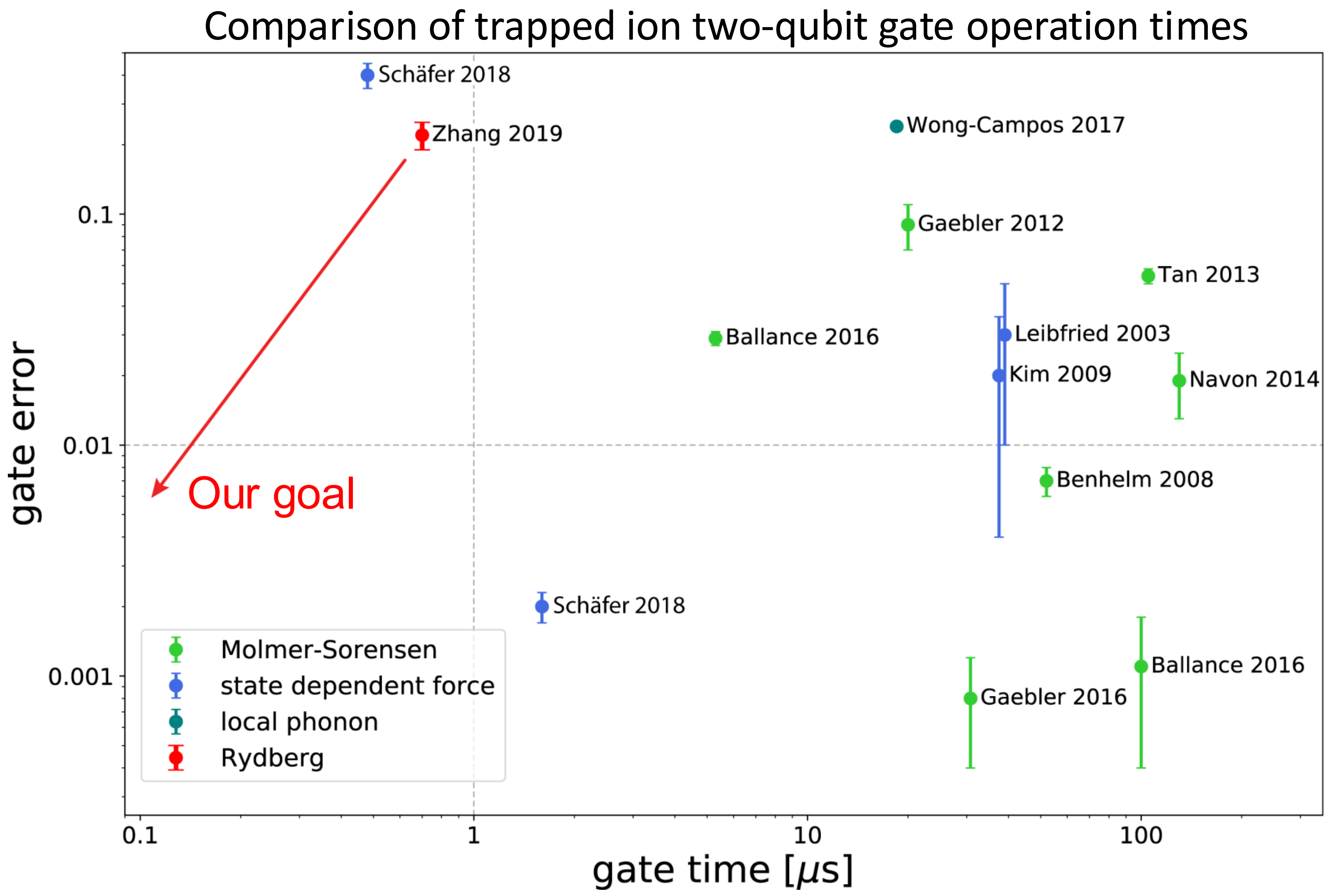

⇒ Our Rydberg two-qubit gates are 10-100 times faster than standard trapped ion gates via motion.

C. Zhang, et al., Nature **580**, 345 (2020)

V. M. Schäfer, et al., Nature 555, 75 (2018)

C. D. Bruzewicz, et al., Appl. Phys. Rev. 6, (2019)

Motional quantum gates slow down with the number of ions.

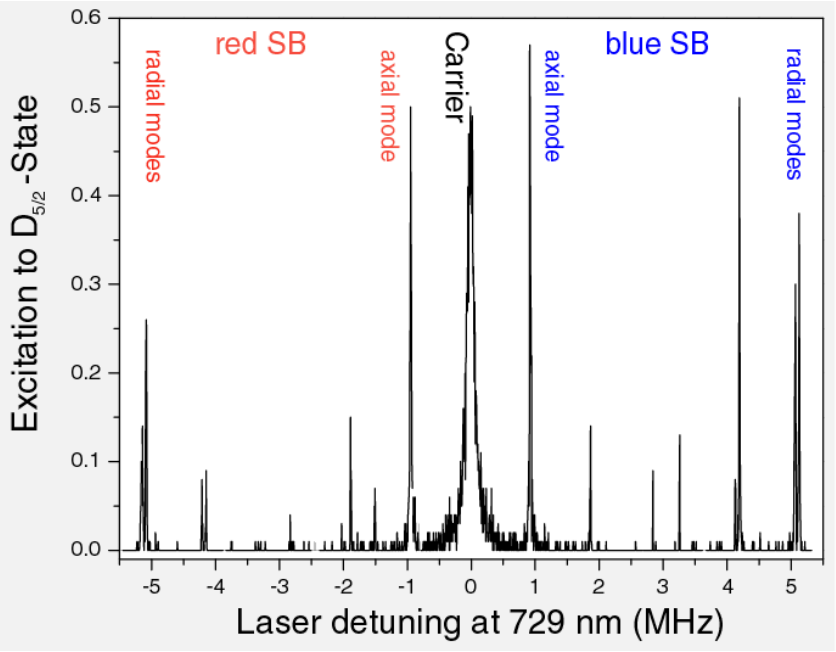

Excitation spectrum of single ion

ω_{ax} = 1.0 MHz

ω_{rad} = 5.0 MHz

For N-ion string there are 3N motional modes which are packed in a narrow spectral region.

Single motional mode needs to be addressed by a narrow (=long) laser pulse.

As a result, the gate time increases with $T_{gate} \sim N$.

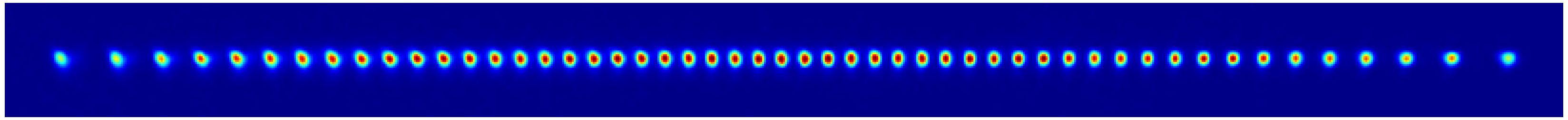

Rydberg gates speed up with the number of ions.

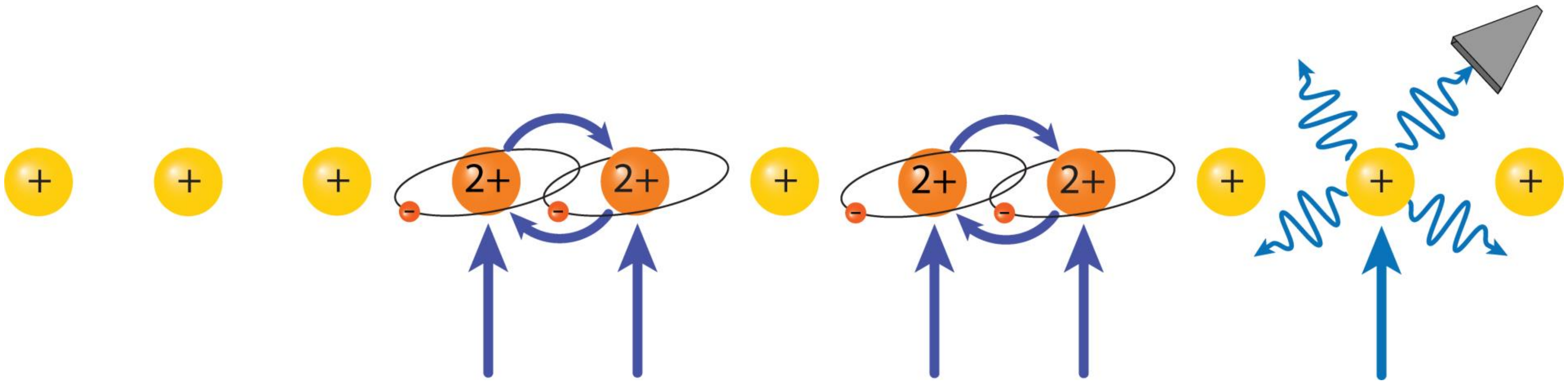

Minimum ion distance in a linear N-ion string scales as

$$r_{min} \propto N^{-0.596}$$

Thus, the maximum Rydberg interaction strength grows as

$$V_{max} \propto N^{1.788}$$

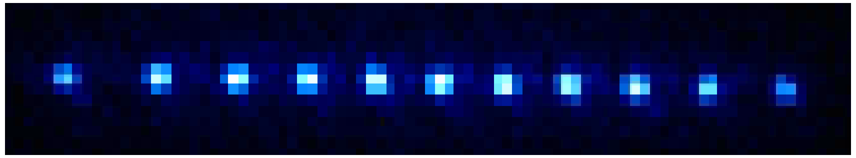

We have applied the two-ion gate in a 12-ion string.

Gate operation on 2 central ions in string cooled by polarization gradient cooling

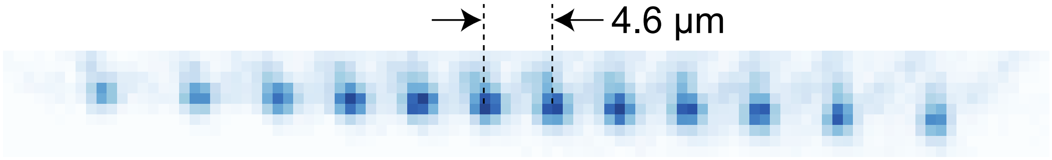

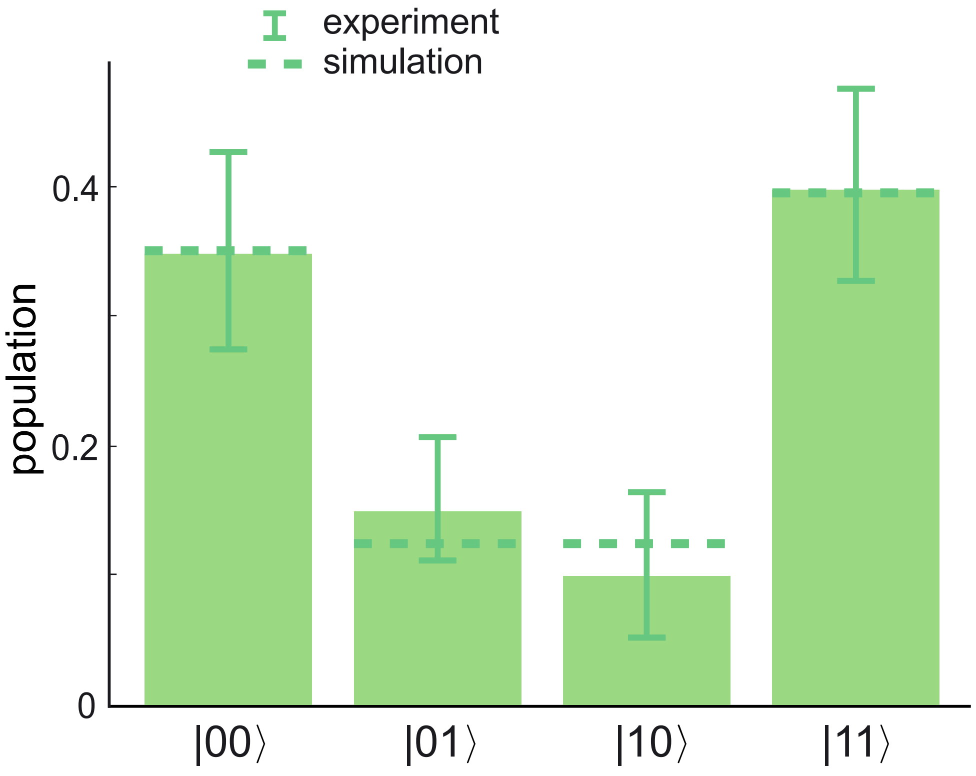

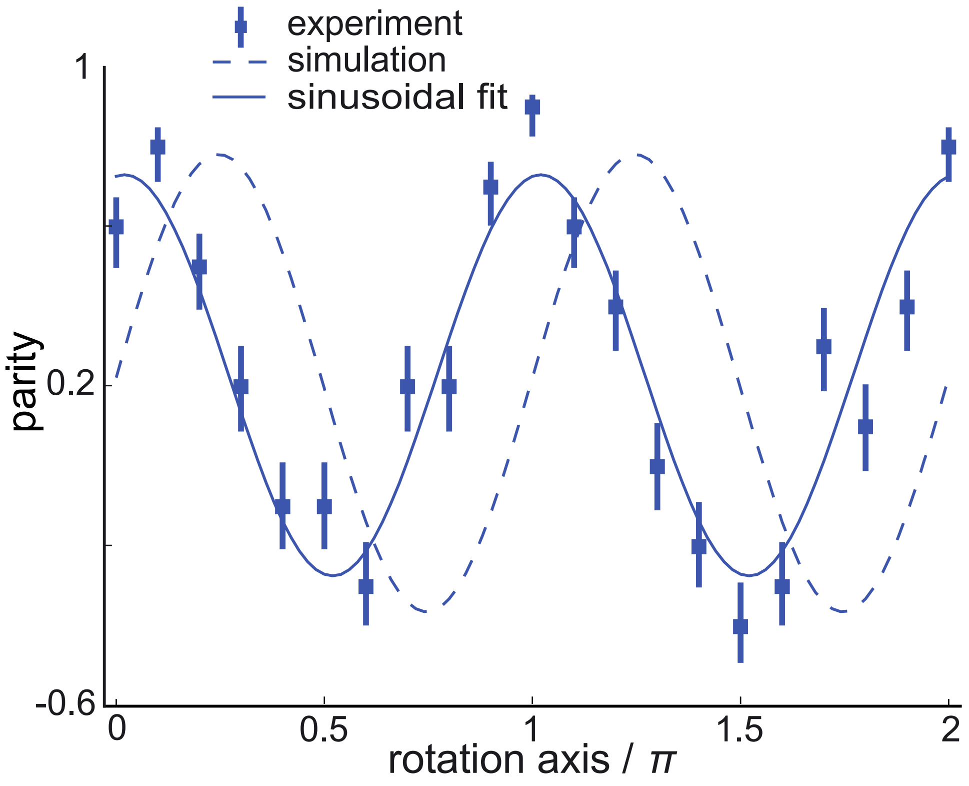

Gate time 700ns

→ Bell state fidelity: 63%

Rydberg states are highly polarizable $\rho \sim n^7$.

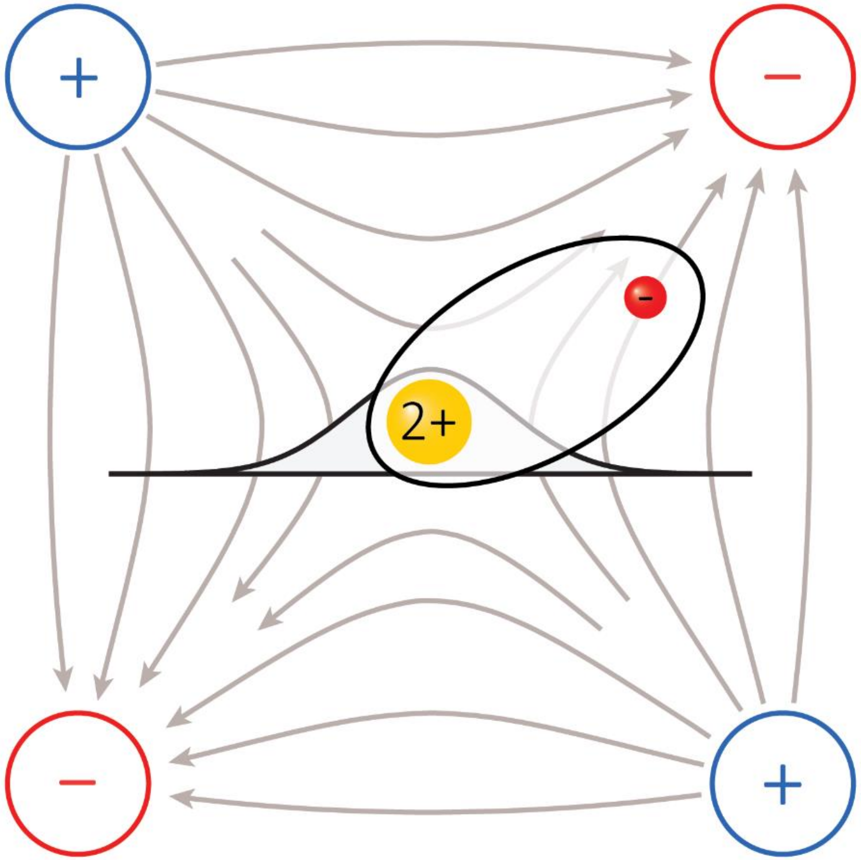

- Trapped ion has a non-zero spatial extent
- Ion experiences oscillating electric trapping field
- Additional harmonic potential from second order Stark effect

$$U_{add} = -\frac{1}{2}\rho\,\overline{E^2} \sim \rho\, r^2$$

Trapping potential
Rydberg state vs. low-lying state

- The transition energy depends on the motional state
- Phonon number conserving transitions are shifted by

$$\Delta E(n) = n \cdot \hbar\Delta\omega$$

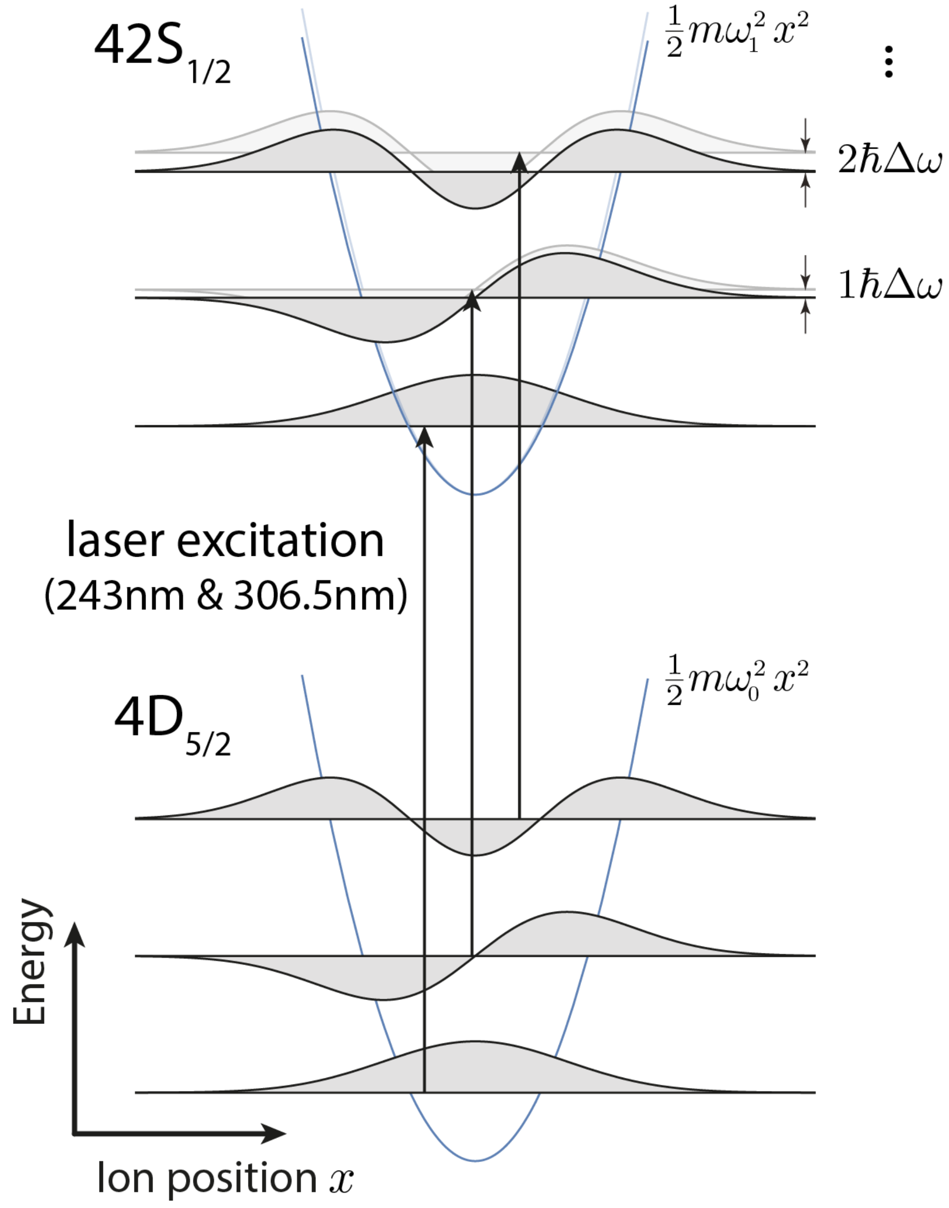

G. Higgins, W. Li, et al., PRX 7, 021038 (2017).
G. Higgins, et al., Phys. Rev. Lett. 123, 153602 (2019).

For $42S_{1/2}$ the measured frequency shift is consistent with theory.

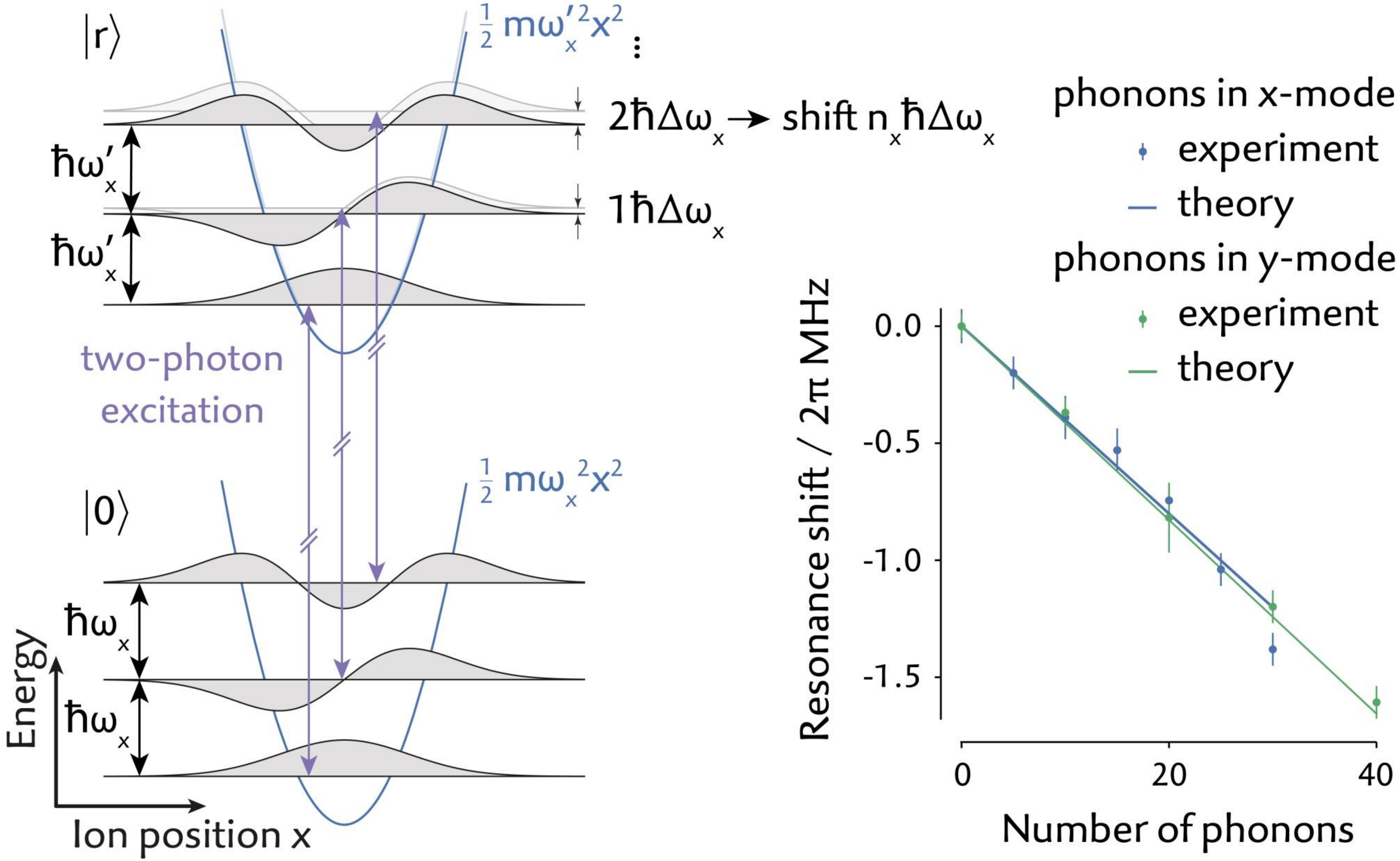

G. Higgins, et al., Phys. Rev. Lett. 123, 153602 (2019).

Microwave dressed Rydberg ions

- Microwave transition between Rydberg states $46S_{1/2} \leftrightarrow 46P_{1/2}$ (MW frequency @120GHz)

- $nS_{1/2}$ and $nP_{1/2}$ Rydberg states have opposite sign dc polarizability.

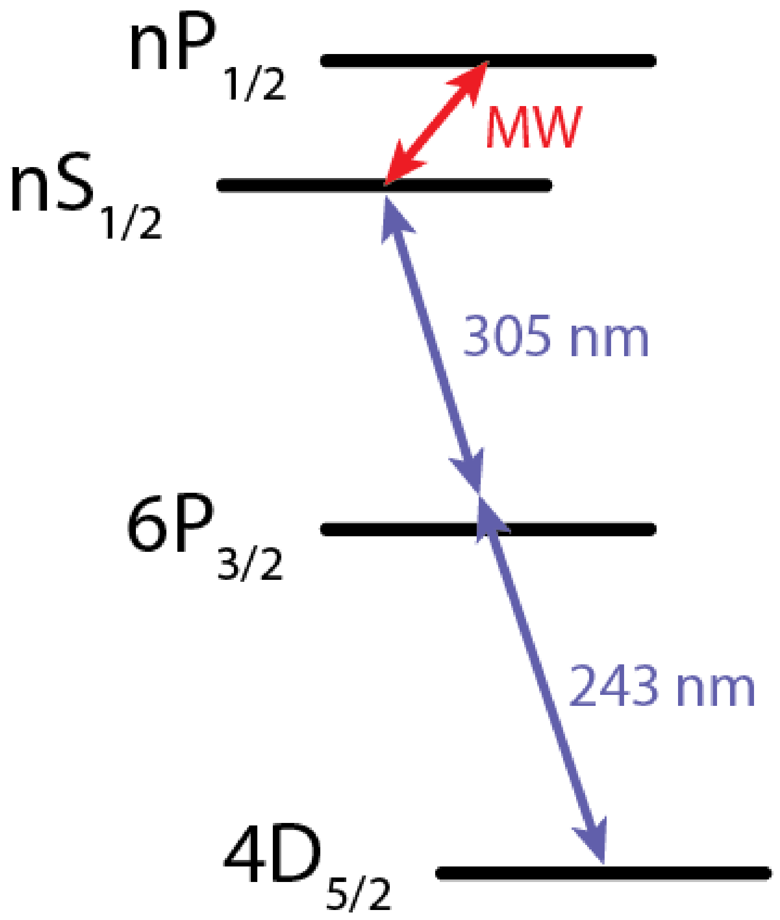

The polarisability can be tuned in microwave-dressed Rydberg states.

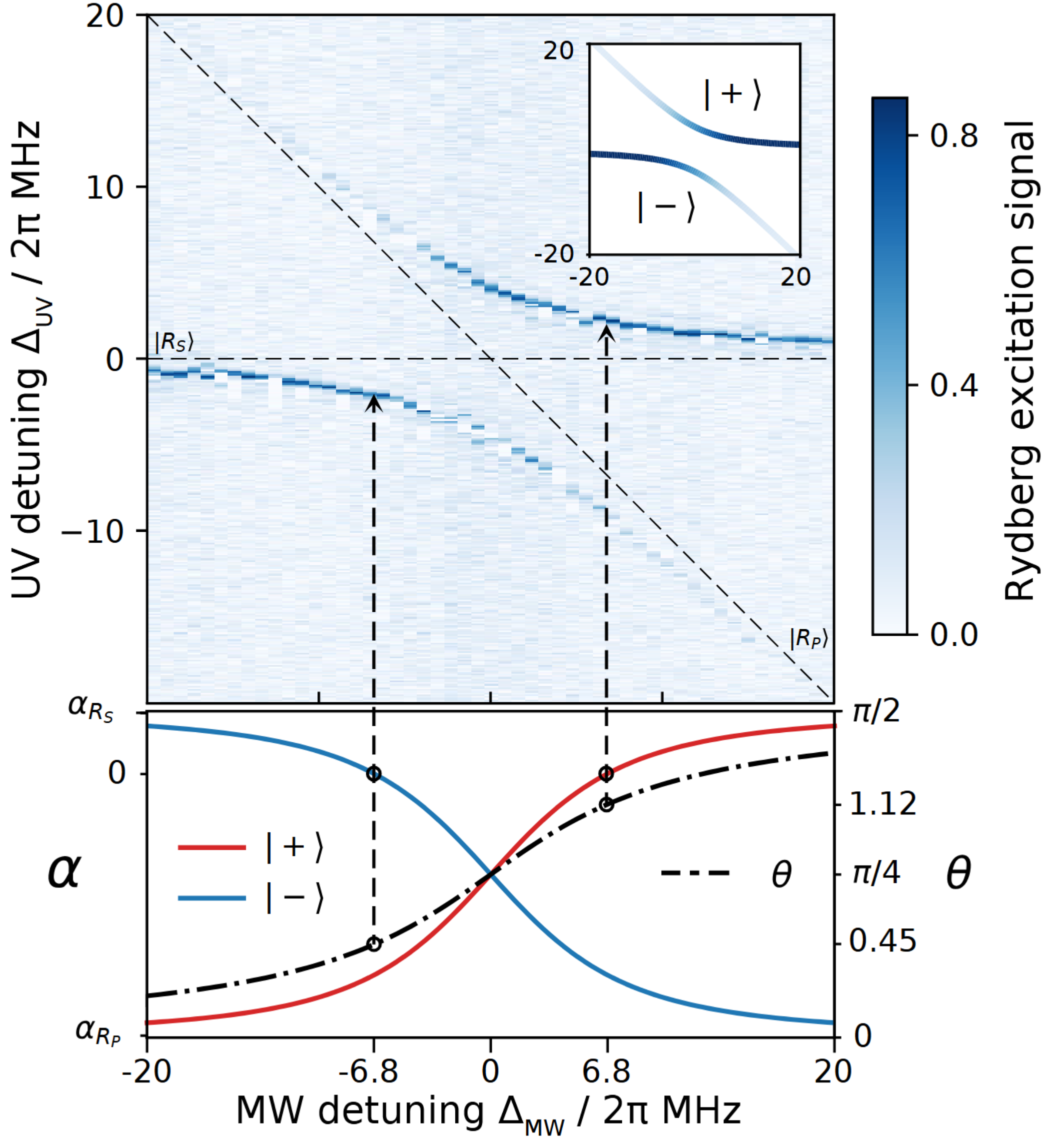

Dressed Rydberg states

$$|+\rangle = \sin\theta|nS\rangle + \cos\theta|nP\rangle$$

$$|-\rangle = \cos\theta|nS\rangle - \sin\theta|nP\rangle$$

$$\tan\theta = \frac{\Omega_{MW}}{\Delta_{MW}}$$

Polarisability of dressed state

$$\rho_- = \rho_{R_S}\cos^2\theta + \rho_{R_P}\sin^2\theta$$

The polarizability of mw-dressed Rydberg states can be tuned to zero.

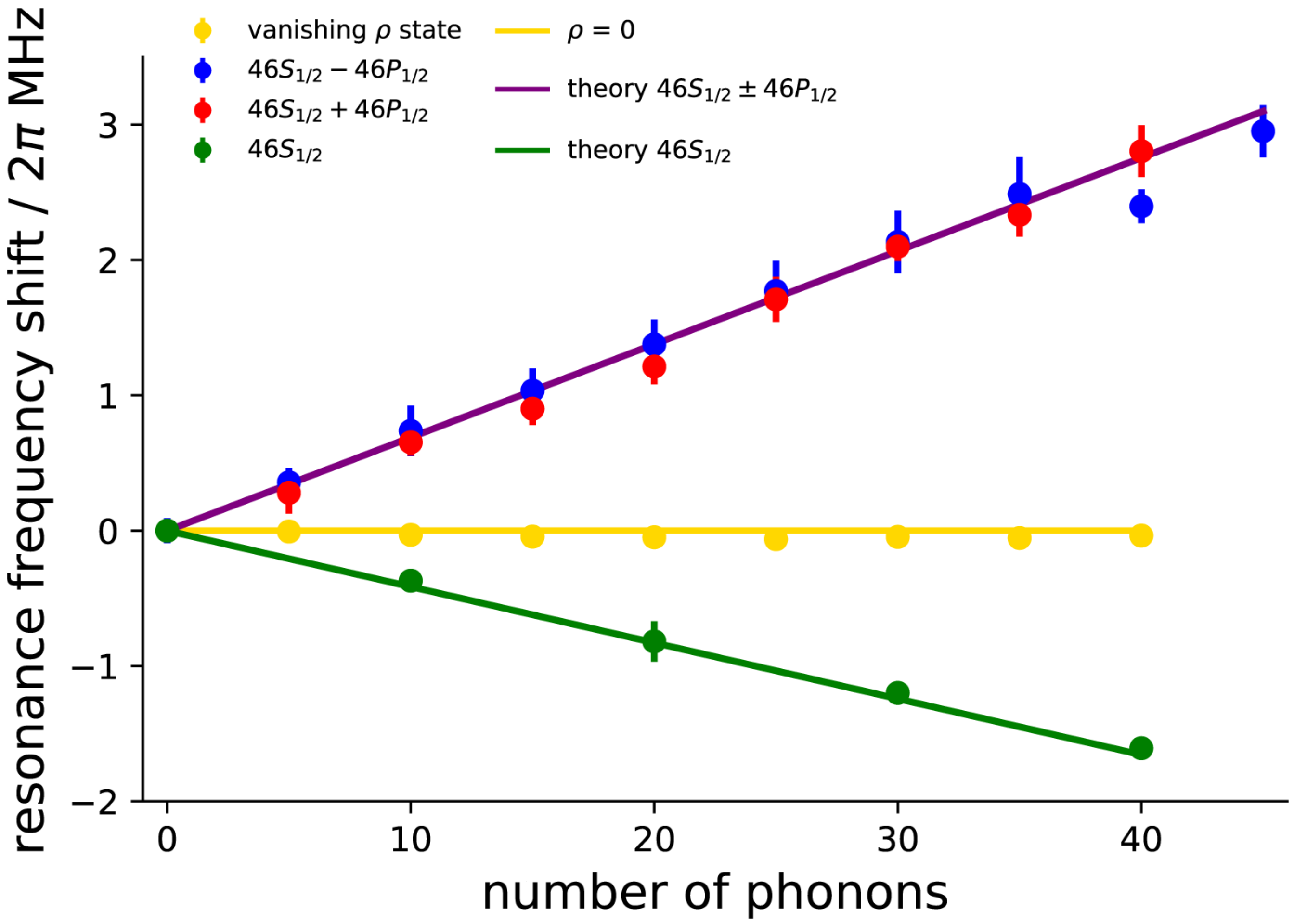

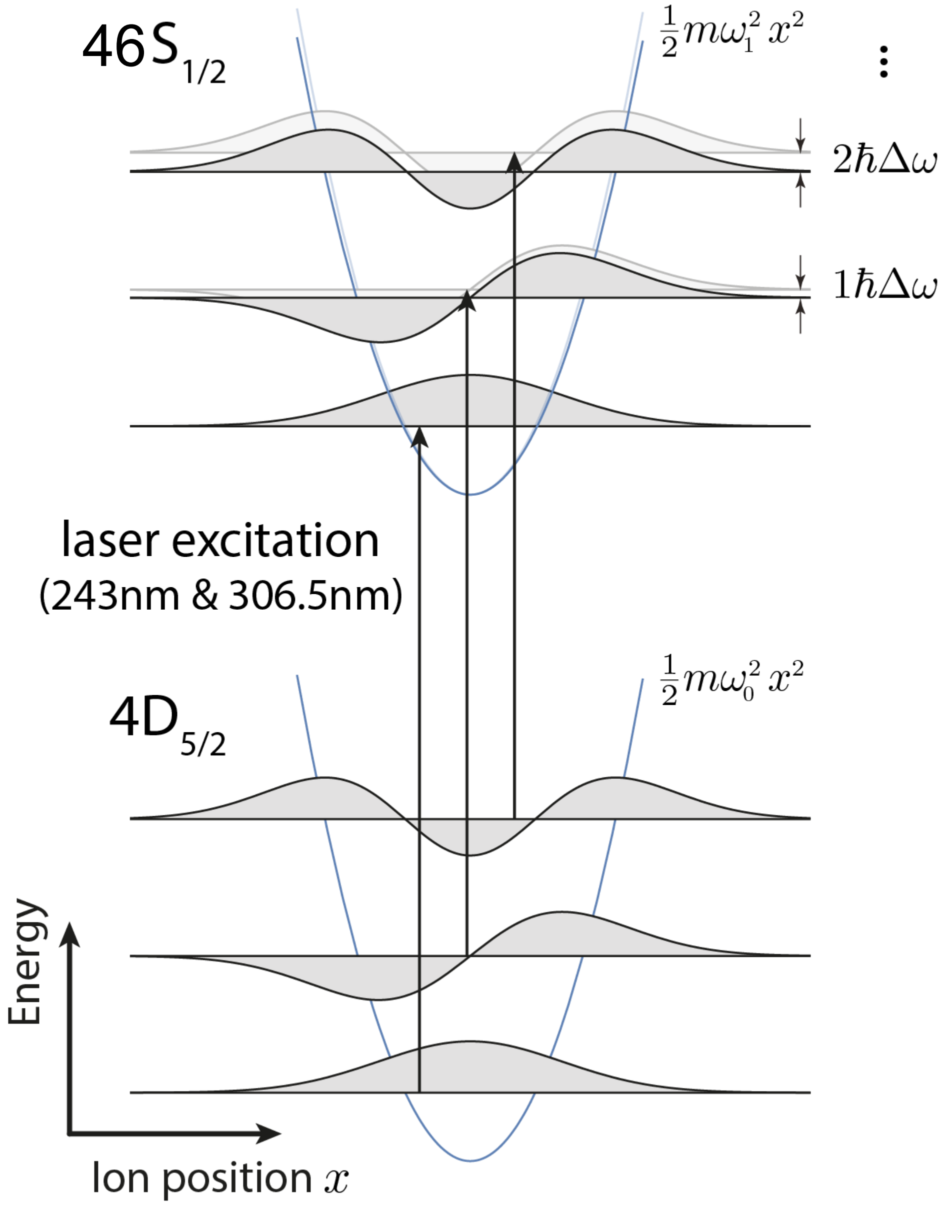

Theory: W. Li and I. Lesanovsky, Appl. Phys. B 114, 37 (2014).
Exp: F. Pokorny, et al., arXiv:2005.12422 (2020).

Transition from linear to zigzag ion configuration depending on the ratio of trapping frequencies.

$$\mathcal{A}_{\mathcal{C}} = \left(\frac{\omega_z}{\omega_x}\right)^2 \approx 2.53N^{-1.73}$$

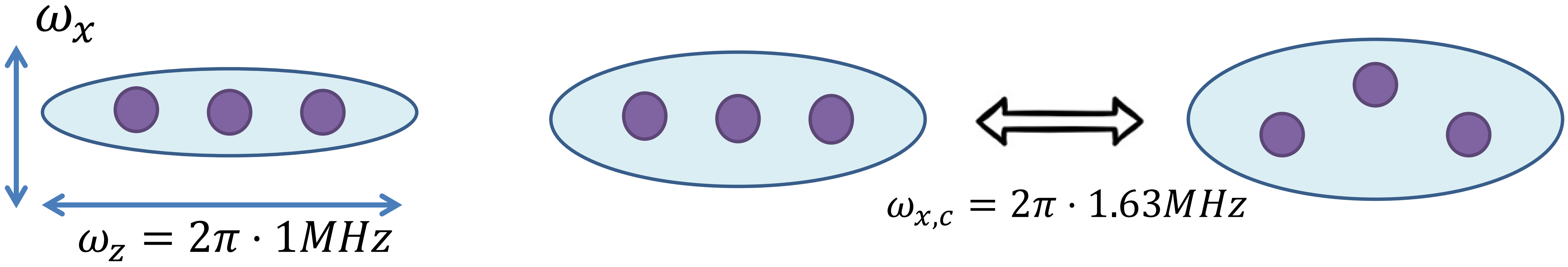

Linear to zigzag phase transition induced by Rydberg excitation

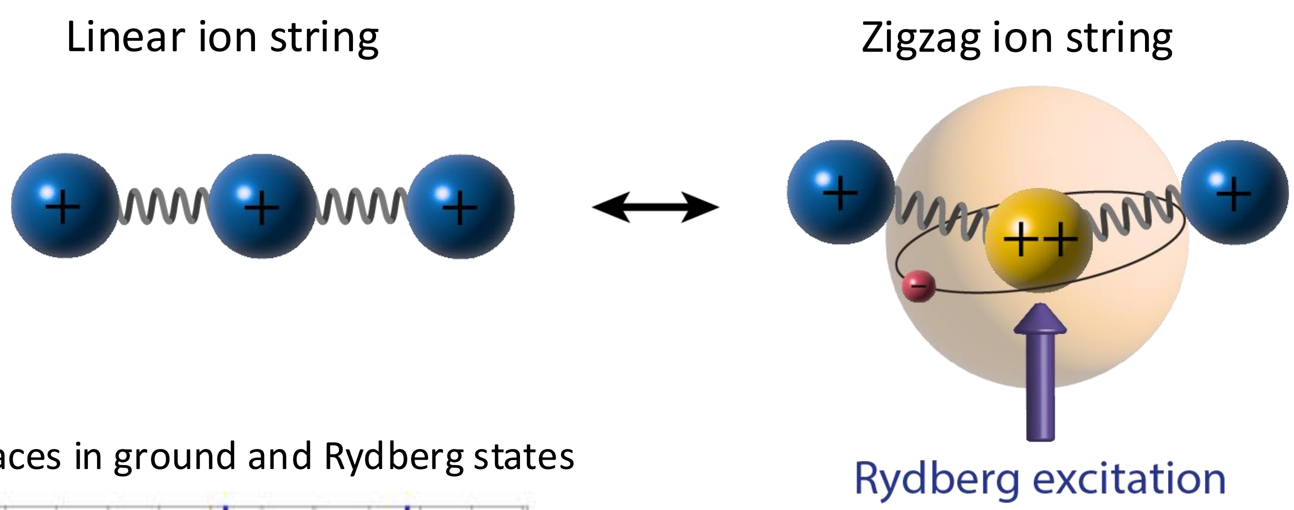

Radial potential surfaces in ground and Rydberg states

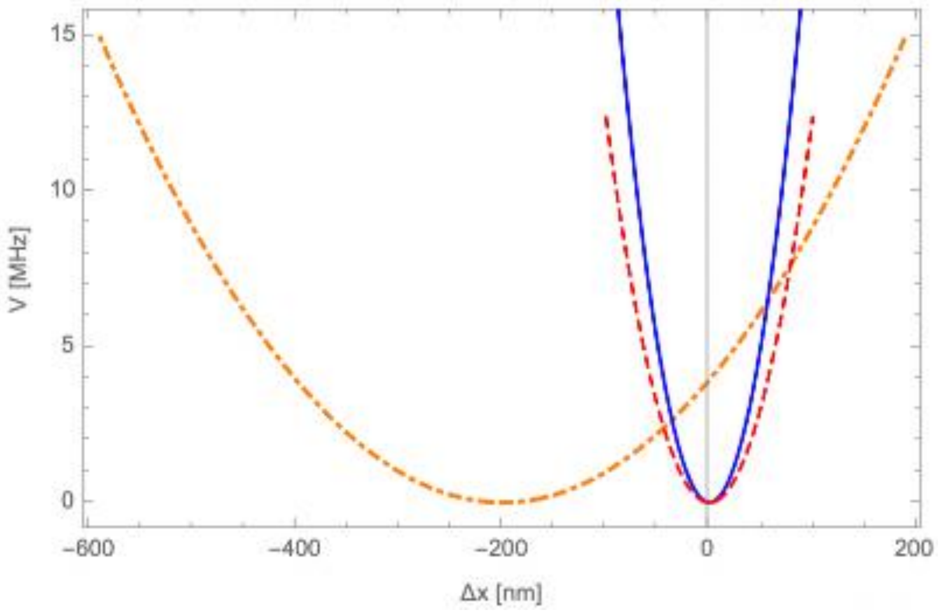

Marion Mallweger

The Rydberg ion system provides a platform to simulate the physics of molecular dynamics.

M. Mallweger et al, arXiv:2507.23631

Theory proposal:
W. Li, I. Lesanovsky, PRL **108**, 023003 (2012).

The amplitude of the resonance decreases approaching the linear-to-zigzag transition.

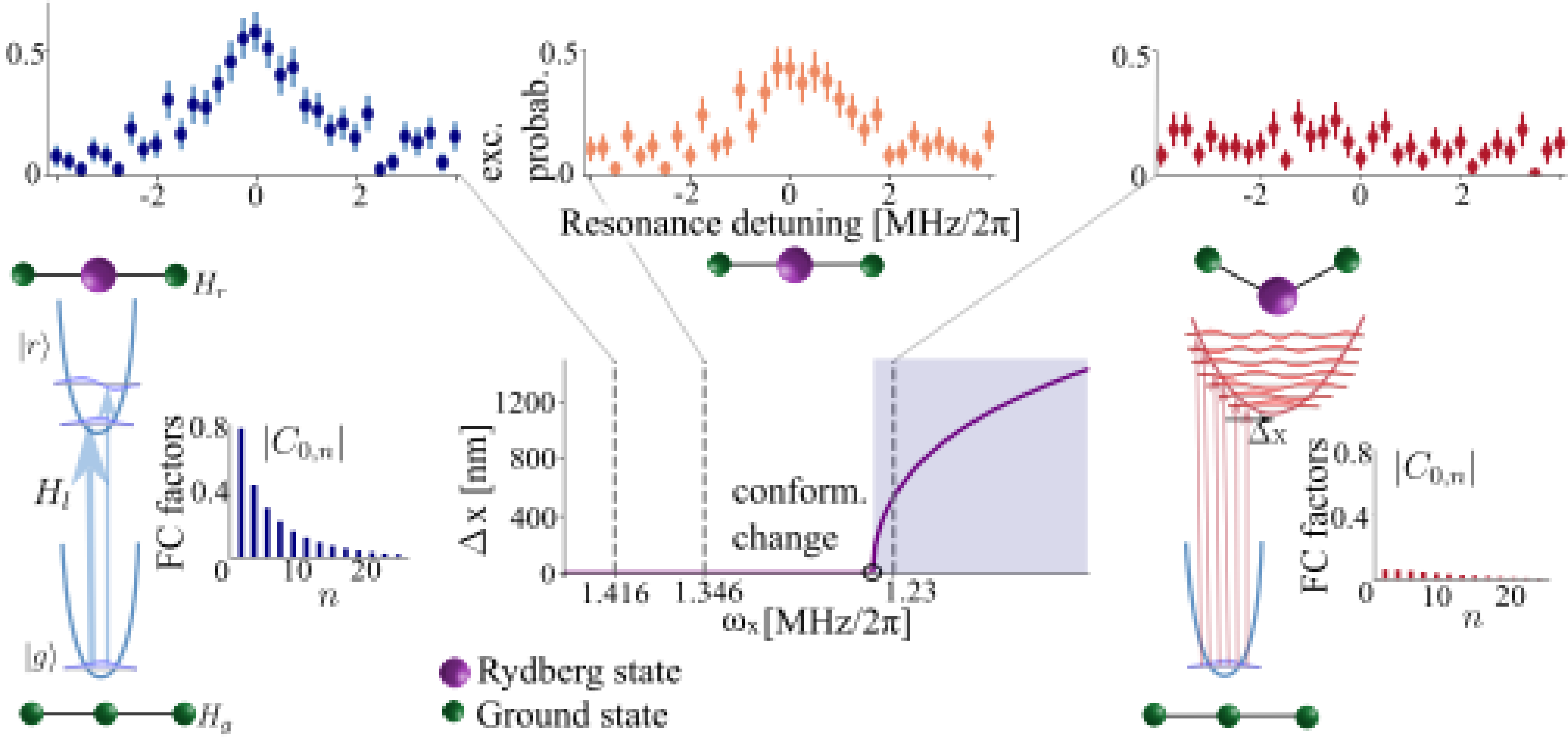

M. Mallweger et al, arXiv:2507.23631

Investigation of the structural phase transition for different trap settings.

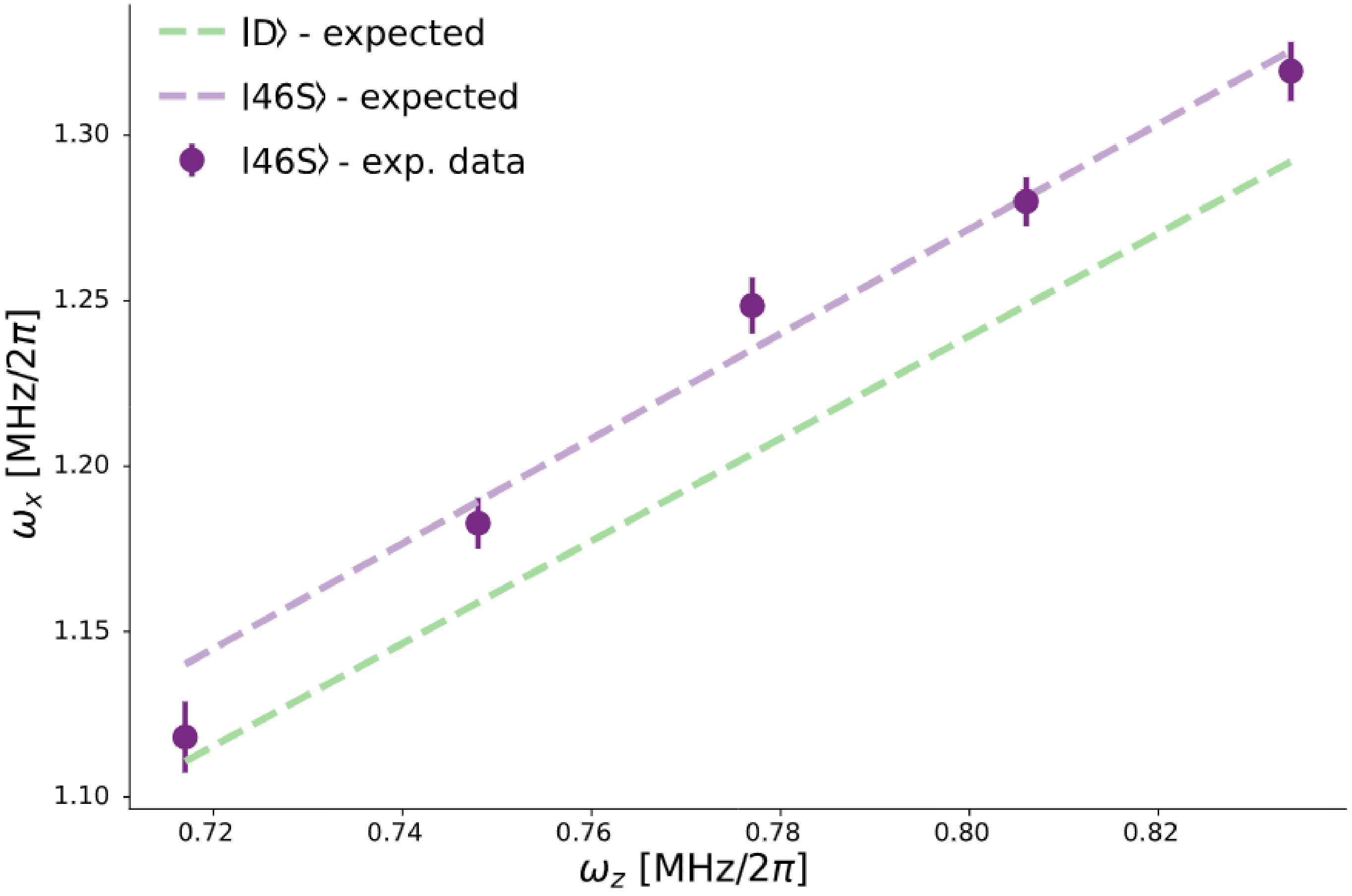

Transition appears at stronger confinement for LLE states:

$$\omega_{x,y} \approx \sqrt{\omega`_{x,y} + \frac{2\rho\alpha^2}{M}}$$

LLE - Lower lying electronic

M. Mallweger et al, arXiv:2507.23631

The structural phase transition is polarisability-dependent.

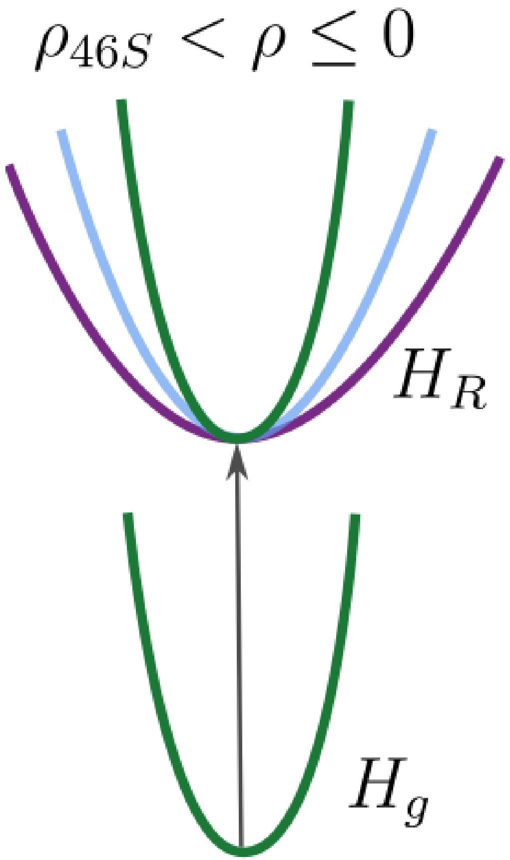

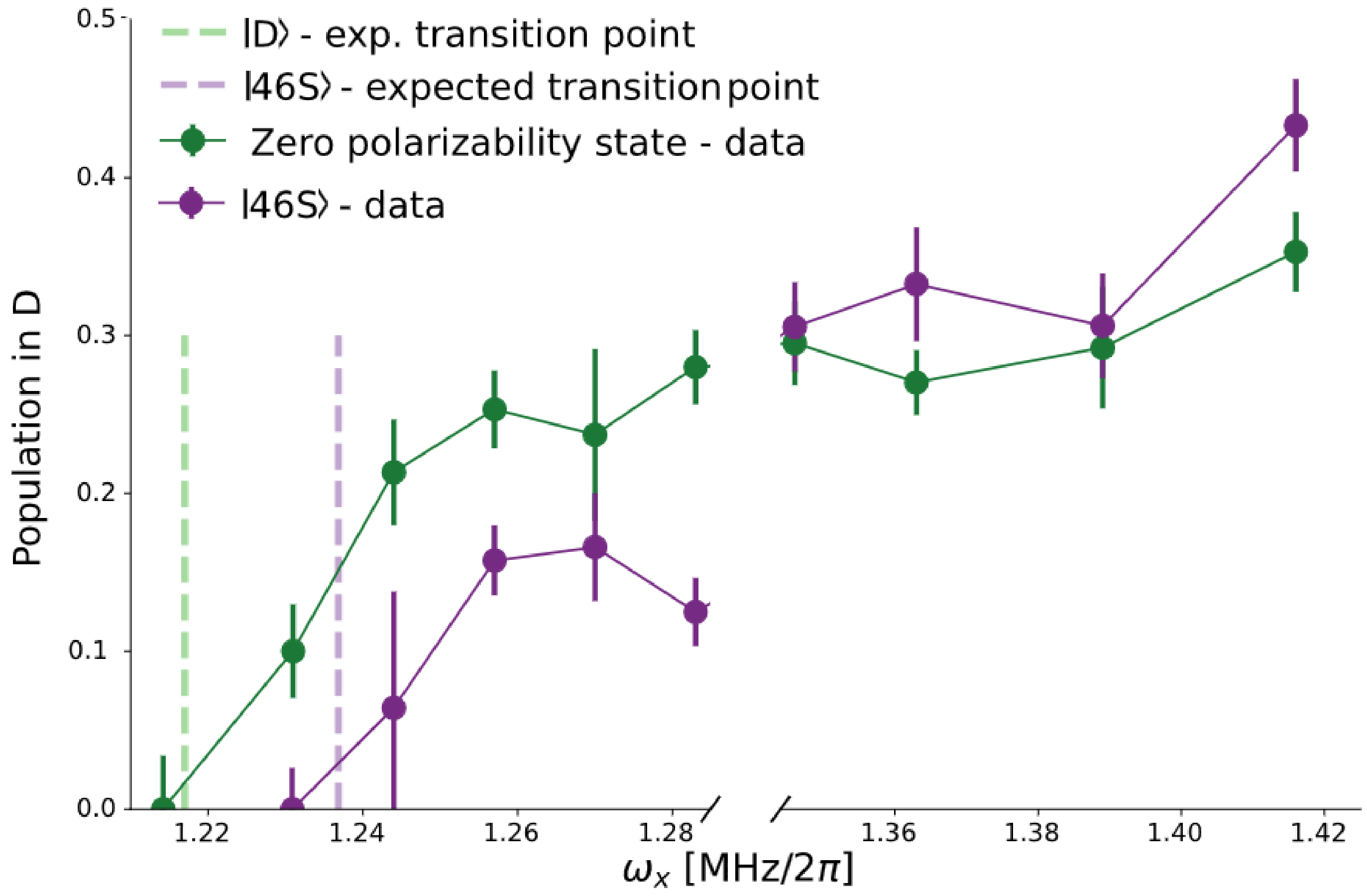

M. Mallweger et al, arXiv:2507.23631

We loose ions due to double ionisation, but it is easy to remove them.

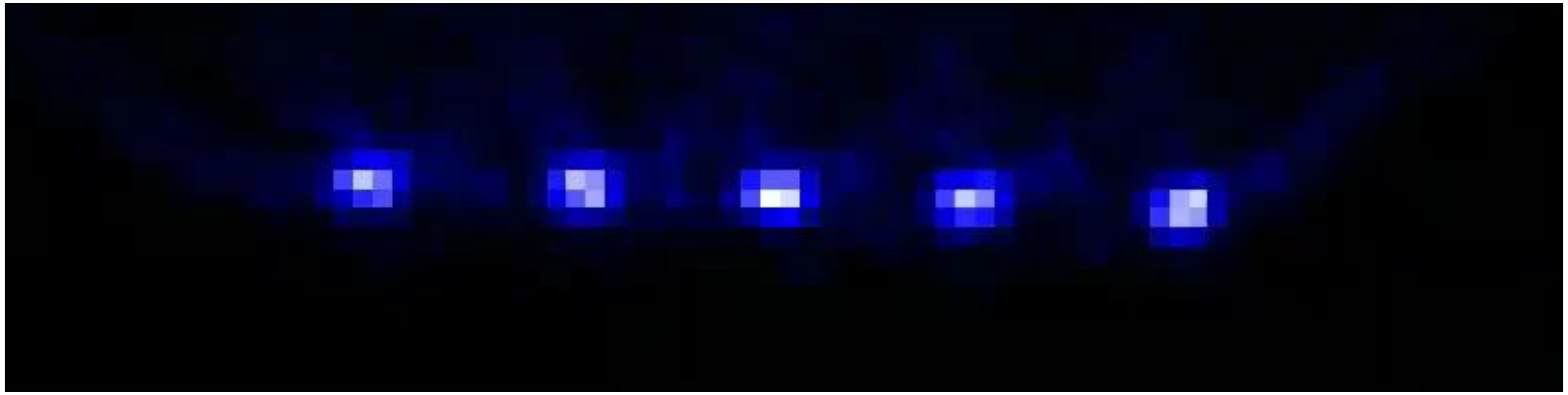

Cryogenic Rydberg ions

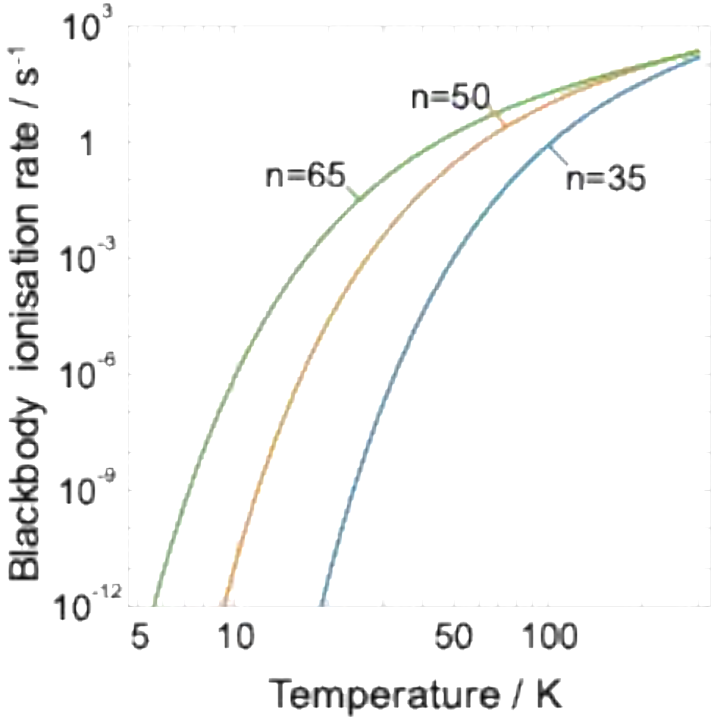

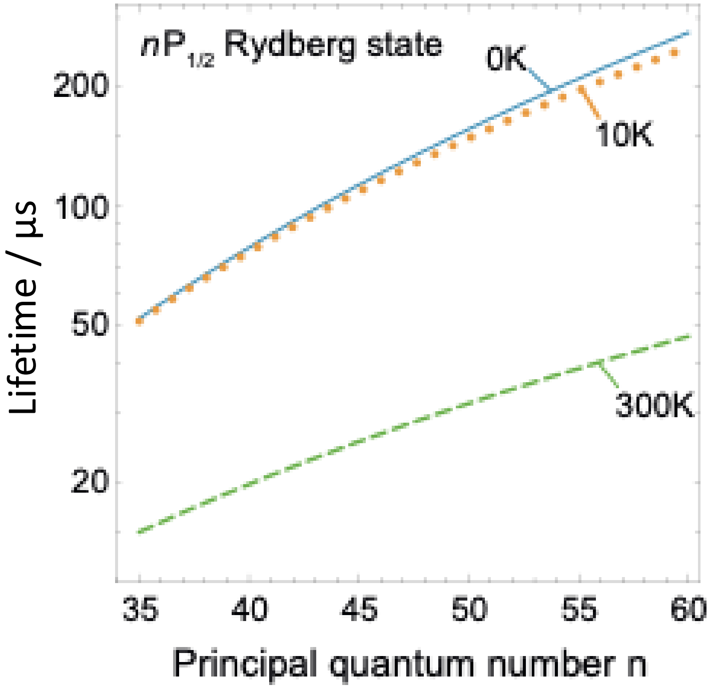

Rydberg ions are rapidly ionized by room-temperature blackbody radiation causing qubit loss.

This loss mechanism can be efficiently suppressed at cryogenic temperatures.
Rydberg state lifetimes will be significantly increased at cryogenic temperatures.

A cryogenic ion trap system is ready for testing.

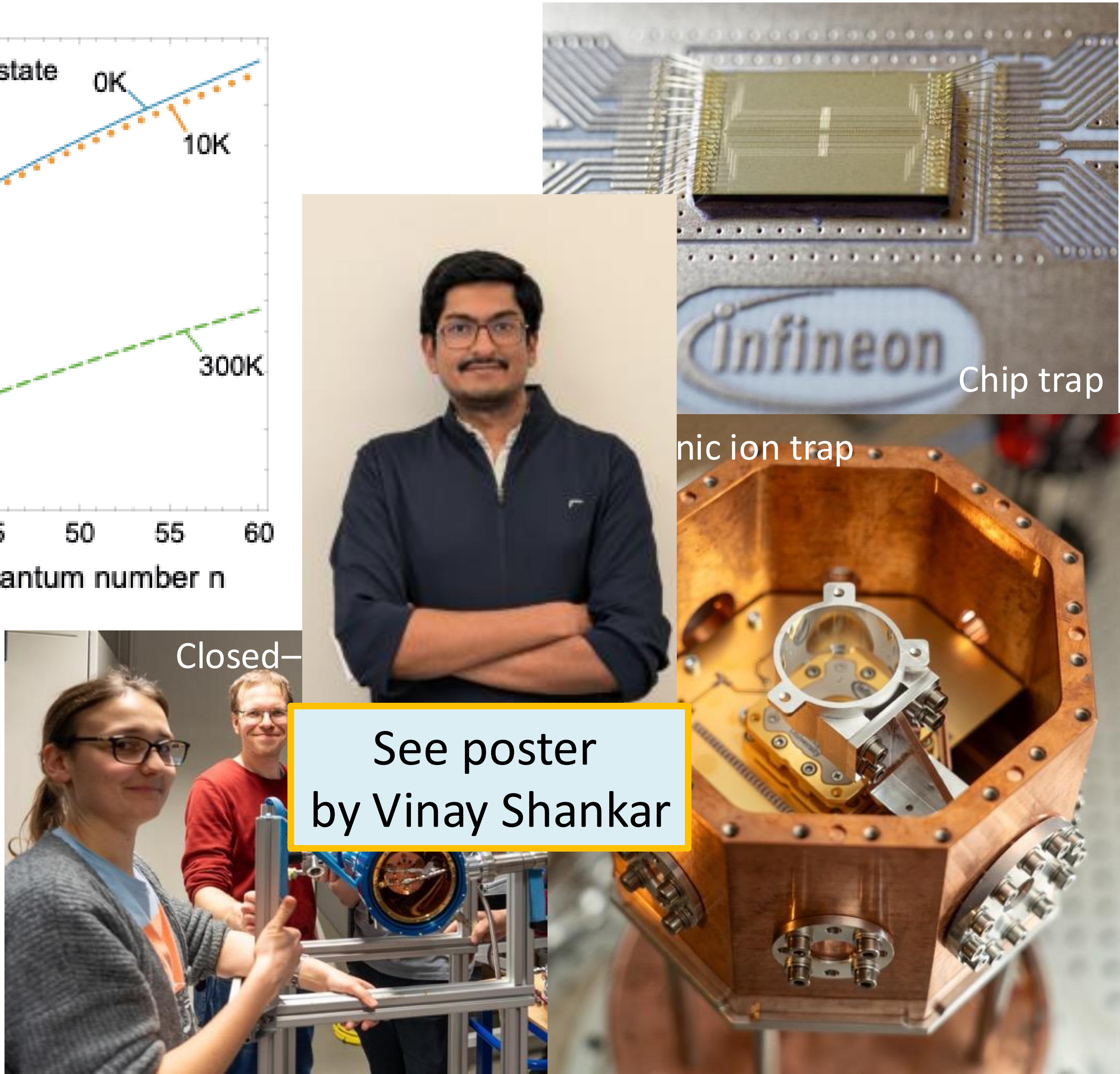

See poster
by Vinay Shankar

Trapped Rydberg ions & applications

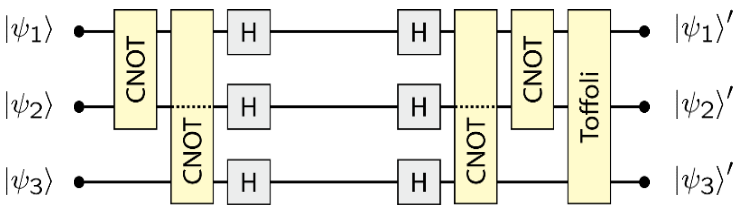

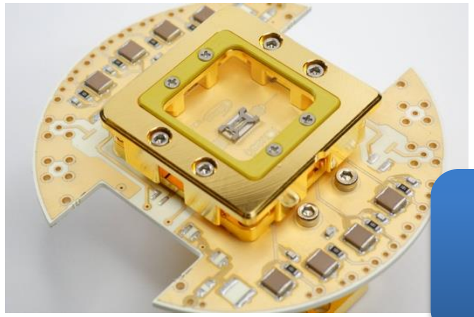

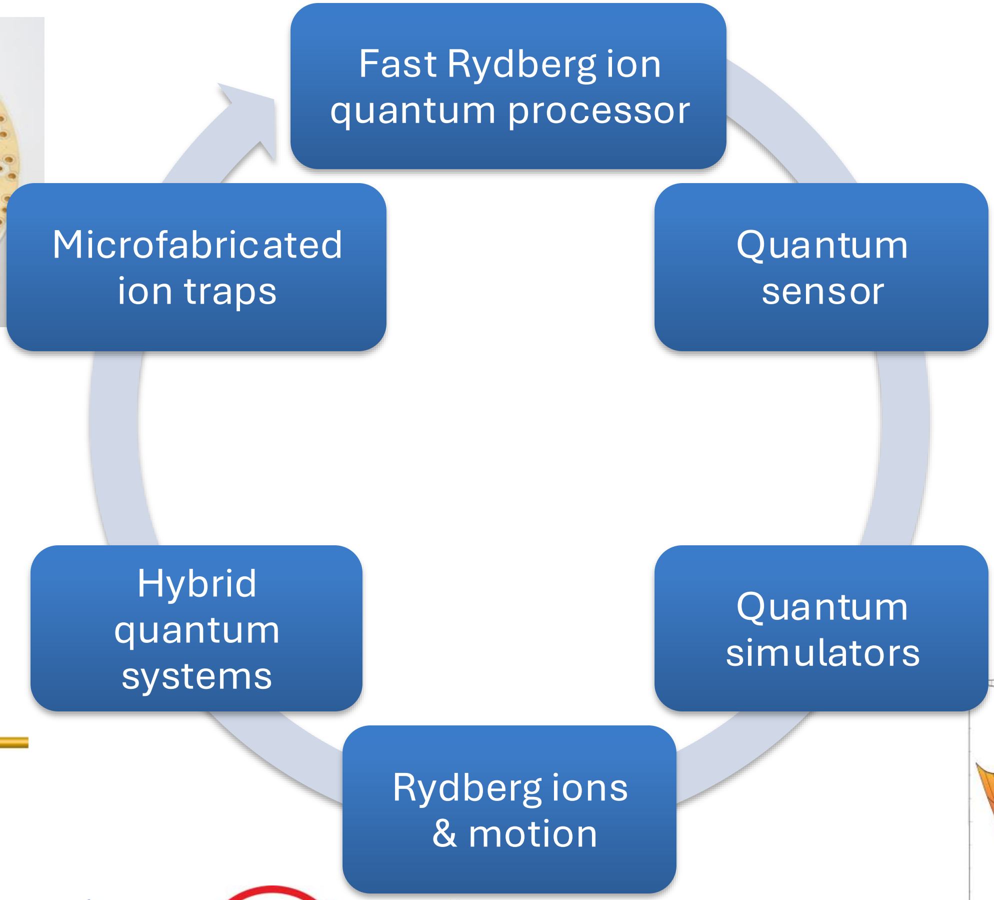

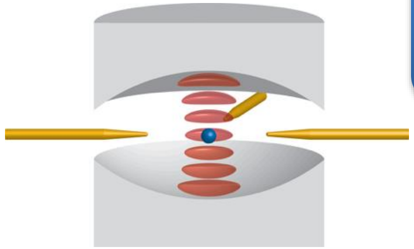

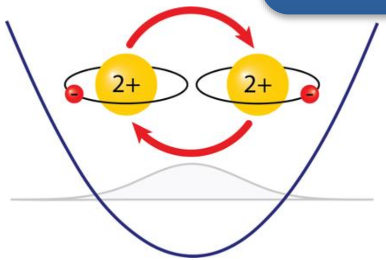

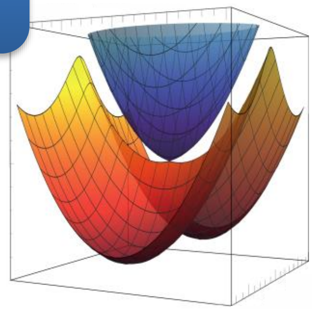

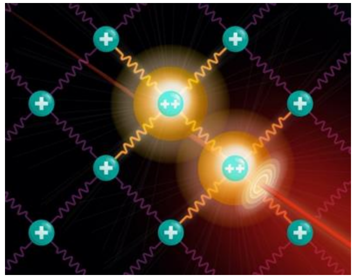

Fabian
Pokorny

Gerard
Higgins

Chi
Zhang

The Team

http://qtech.fysik.su.se/

Theory

Igor
Lesanovsky

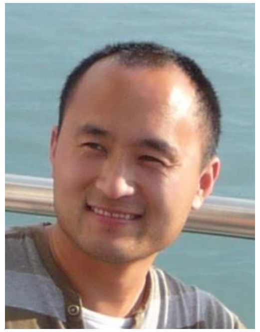

Weibin
Li

Nikolay
Vitanov

Celso
Villas Boas

Romain
Bachelard

Matthias Kleinmann
Adan Cabello

The Team

Fabian Pokorny

Gerard Higgins

Chi Zhang

http://qtech.fysik.su.se/

PhD and postdoc positions available

Funding

European Research Council
Established by the European Commission

cost
EUROPEAN COOPERATION IN SCIENCE & TECHNOLOGY

QUANTERA

European Innovation Council

Vetenskapsrådet

Knut och Alice Wallenbergs Stiftelse

STINT
Stiftelsen för internationalisering av högre utbildning och forskning
The Swedish Foundation for International Cooperation in Research and Higher Education

CAPES

OLLE ENGKVISTS STIFTELSE

Carl Tryggers Stiftelse för Vetenskaplig Forskning